UNIVERSIDADE FEDERAL DO AMAPÁ
PROGRAMA DE PÓS-GRADUAÇÃO EM BIODIVERSIDADE E BIOTECNOLOGIA - REDE BIONORTE

DESENVOLVIMENTO E CARACTERIZAÇÃO DE NANOPARTÍCULAS DE FIBROÍNA DE SEDA COMBINADAS COM ÓLEOS AMAZÔNICOS: UMA PROPOSTA SUSTENTÁVEL CONTRA LARVAS DE *Aedes aegypti* E *Spodoptera frugiperda*

VICTOR HUGO DE SOUZA MARINHO

Macapá-AP

2023

UNIVERSIDADE FEDERAL DO AMAPÁ
PROGRAMA DE PÓS-GRADUAÇÃO EM BIODIVERSIDADE E BIOTECNOLOGIA - REDE BIONORTE

VICTOR HUGO DE SOUZA MARINHO

DESENVOLVIMENTO E CARACTERIZAÇÃO DE NANOPARTÍCULAS DE FIBROÍNA DE SEDA COMBINADAS A ÓLEOS AMAZÔNICOS: UMA PROPOSTA SUSTENTÁVEL CONTRA LARVAS DE *Aedes aegypti* E *Spodoptera frugiperda*

Tese de Doutorado apresentada ao programa de Pós-Graduação em Biodiversidade e Biotecnologia - Rede Bionorte, na Universidade Federal do Amapá, como requisito para a obtenção do Título de Doutor em Biotecnologia.

Orientador: Prof. Dr. Irlon Maciel Ferreira.

Macapá-AP

2023

Dados Internacionais de Catalogação na Publicação (CIP)
Biblioteca Central/UNIFAP-Macapá-AP
Elaborado por Mário das Graças Carvalho Lima Júnior – CRB-2 / 1451

M338 Marinho, Victor Hugo de Souza.
Desenvolvimento e caracterização de nanopartículas de fibroína de seda combinadas a óleos amazônicos: uma proposta sustentável contra larvas de Aedes aegypti e Spodoptera frugiperda / Victor Hugo de Souza Marinho. - Macapá, 2023.
1 recurso eletrônico. 157 folhas.

Tese (Doutorado) - Universidade Federal do Amapá, Programa de Pós-graduação em Biodiversidade e Biotecnologia - Rede Bionorte, Macapá, 2023.
Orientador: Irlon Maciel Ferreira.

Modo de acesso: World Wide Web.
Formato de arquivo: Portable Document Format (PDF).

1. Óleos amazônicos. 2. Casulo do bicho-da-seda. 3. Nanobioinseticida. I. Ferreira, Irlon Maciel, orientador. II. Universidade Federal do Amapá. III. Título.

CDD 23. ed. – 614.571

MARINHO, Victor Hugo de Souza. **Desenvolvimento e caracterização de nanopartículas de fibroína de seda combinadas a óleos amazônicos**: uma proposta sustentável contra larvas de Aedes aegypti e Spodoptera frugiperda . Orientador: Irlon Maciel Ferreira. 2023. 157 f. Tese (Doutorado) - Programa de Pós-graduação em Biodiversidade e Biotecnologia - Rede Bionorte. Universidade Federal do Amapá, Macapá, 2023.

UNIVERSIDADE FEDERAL DO AMAPÁ
PROGRAMA DE PÓS-GRADUAÇÃO EM BIODIVERSIDADE E BIOTECNOLOGIA - REDE BIONORTE

VICTOR HUGO DE SOUZA MARINHO

DESENVOLVIMENTO E CARACTERIZAÇÃO DE NANOPARTÍCULAS DE FIBROÍNA DE SEDA COMBINADAS A ÓLEOS AMAZÔNICOS: UMA PROPOSTA SUSTENTÁVEL CONTRA LARVAS *Aedes aegypti* E *Spodoptera frugiperda*

Tese de Doutorado apresentada ao programa de Pós-Graduação em Biodiversidade e Biotecnologia - Rede Bionorte, na Universidade Federal do Amapá, como requisito para a obtenção do Título de Doutor em Biotecnologia.

Aprovada em: 22 /11/2023

BANCA EXAMINADORA

Documento assinado digitalmente
gov.br IRLON MACIEL FERREIRA
Data: 17/01/2024 14:23:22-0300
Verifique em https://validar.iti.gov.br

Prof. Dr. Irlon Maciel Ferreira (Orientador)
Universidade Federal do Amapá

Documento assinado digitalmente
gov.br ALEX BRUNO LOBATO RODRIGUES
Data: 28/11/2023 15:31:53-0300
Verifique em https://validar.iti.gov.br

Prof. Dr. Alex Bruno Lobato Rodrigues
Universidade Federal do Amapá

Documento assinado digitalmente
gov.br CLEYDSON BRENO RODRIGUES DOS SANTOS
Data: 16/01/2024 16:02:26-0300
Verifique em https://validar.iti.gov.br

Prof. Dr. Cleydson Breno Rodrigues dos Santos
Universidade Federal do Amapá

Documento assinado digitalmente
gov.br MARCOS TAVARES DIAS
Data: 28/11/2023 15:58:17-0300
Verifique em https://validar.iti.gov.br

Prof. Dr. Marcos Tavares Dias
Embrapa

Documento assinado digitalmente
gov.br TIAGO MARCOLINO DE SOUZA
Data: 28/11/2023 16:09:20-0300
Verifique em https://validar.iti.gov.br

Prof. Dr. Tiago Marcolino de Souza
Universidade Estadual do Amapá

TERMO DE AUTORIZAÇÃO PARA PUBLICAÇÃO

Eu, Victor Hugo de Souza Marinho, (x) autorizo ( ) não autorizo a publicação da versão final aprovada de minha Tese de Doutorado intitulada “Desenvolvimento e caracterização de nanopartículas de fibroína de seda combinadas a óleos amazônicos: uma proposta sustentável contra larvas *Aedes aegypti* e *Spodoptera frugiperda*” no Portal do Programa de Pós-Graduação em Biodiversidade e Biotecnologia - Rede BIONORTE (PPG-BIONORTE), bem como no repositório de Teses da CAPES ou junto à biblioteca da Instituição Certificadora.

Macapá-AP, 22 de novembro de 2023.

gov.br
Documento assinado digitalmente
VICTOR HUGO DE SOUZA MARINHO
Data: 11/02/2024 15:54:59-0300
Verifique em https://validar.iti.gov.br

Victor Hugo de Souza Marinho

CPF: 696.240.972-91

RG: 3933988

A minha mãe Zilma Oliveira de Souza (in memoriam) e ao meu pai Altenir da Conceição Gomes, por sempre me incentivarem a buscar por meus objetivos.

AGRADECIMENTOS

A Deus, por ter me acompanhado nesta caminhada com saúde, sabedoria, e por ter gerado oportunidades para atingir meus objetivos.

Aos meus pais Altenir da Conceição Gomes e Zilma Oliveira de Souza (*in memoriam*) pelo apoio, amor, incentivo durante esta fase de minha vida.

Aos meus tios Getúlio Favacho da Silva e Marizete Oliveira de Souza por terem me criado e educado com muito carinho.

Aos meus queridos irmãos e sobrinhos por sempre estarem ao meu lado.

Ao meu amigo/irmão Rogério da Cunha Brito e sua família que mesmo distantes sempre me incentivaram a encarar mais esse desafio, só tenho a agradecer.

Ao Prof. Dr. Irlon Maciel Ferreira pelos ensinamentos, companhia, confiança, sugestões, "paciência" e apoio no desenvolvimento deste trabalho e além de tudo, pela sua amizade.

Ao Prof. Dr. José Carlos Tavares Carvalho pelo apoio ao nos disponibilizar a estrutura, quando necessário, do Laboratório de Pesquisa em Fármacos para a realização de parte deste trabalho.

Aos Professores Dr. Raimundo Nonato Souto e Ricardo Ferreira pelo apoio ao nos oferecer o espaço do Laboratório Arthrolab para a realização de parte deste trabalho.

Aos amigos Noabson Lucas, Sidnei Ribeiro, Marcione Ribeiro, Mayla Ribeiro, Flávio Costa, Elizabeth Santos, Roney Cardoso e tantos outros pela amizade, companheirismo e por viverem comigo tantos momentos bons de lazer.

Aos amigos do Laboratório de Biocatálise e Síntese Orgânica Aplicada: Iracirema Sena, Edmilson Morais, Adriana Maciel, Sônia Oliveira, Inana Fauro, Fabrício Holanda, Fernando Batista, Beatriz Lacerda, Dionísia Pelaes, Swanny Borges, Edmilson Sarmento, Roberto Cardoso, Mateus Matos, Andria Vanessa e tantos outros do nosso grupo de pesquisa, obrigado pelo apoio e amizade de todos.

Aos Professores e Técnico-administrativos do curso de Pós-Graduação da Rede Bionorte pelo suporte técnico e por contribuírem com seus conhecimentos para nossa formação.

A Fundação de Amparo à Pesquisa do Amapá, bem como a Coordenação de Aperfeiçoamento de Pessoal de Nível Superior pelo fomento da pesquisa e fornecimento de bolsas.

E se nesta vida uma pessoa, por sua diligência e obediência, adquirir mais conhecimento e inteligência do que outra, ela terá tanto mais vantagens no mundo futuro (Doutrina e Convênios 130:19).

MARINHO, Victor Hugo de Souza. **Desenvolvimento e caracterização de nanopartículas de fibroína de seda combinadas a óleos amazônicos: Uma proposta sustentável contra larvas de *Aedes aegypti* e *Spodoptera frugiperda***. 2023. 157 f. Tese (Doutorado em Biodiversidade e Biotecnologia, Rede BIONORTE) – Universidade Federal do Amapá, Macapá, 2023.

RESUMO

Nanopartículas poliméricas (NPs) estão sendo usadas como alternativa viável aos inseticidas convencionais para o controle de diversos insetos-praga. Entre os inseticidas de base biológica, os inseticidas contendo compostos bioativos botânicos são bem eficazes na melhoria da toxicidade para as larvas desses insetos. Deste modo, o objetivo do presente trabalho foi o desenvolvimento e a caraterização de nanopartículas poliméricas de fibroína de seda combinadas a ésteres butílicos semissintetizados a partir de óleos amazônicos (*Astrocaryum murumuru* Mart, *Bertholletia excelsa e Carapa guianensis* Aublet), e avaliação do potencial inseticida contra larvas de *Aedes aegypti* e *Spodoptera* f*rugiperda*. As nanopartículas tiveram sua estabilidade temporal avaliadas por até 50 dias em 4 ºC e 32 ºC, apresentando tamanhos de partículas que variaram de 187.6 (±0.8) nm a 540.8 (±23.8) nm, índice de polidispersidade entre 0.238 a 0.560 e potencial zeta variando de -39.7 (±1.4) mV a -62.9 (±0.7) mV. As análises por microscopia eletrônica de transmissão mostraram que as nanopartículas exibiram distribuição uniforme e formato esférico. Além disso, as nanopartículas de fibroína de seda apresentaram perfil de liberação lento e controlado induzindo assim uma elevada taxa de mortalidade nas larvas de 3º estágio de *Ae. aegypti* e *S. frugiperda*. As nanopartículas ainda foram capazes de inibir a oviposição de fêmeas do *Ae. aegypti*, e apresentou atividade ovicida contra *S. frugiperda*. Contudo, as nanopartículas não exibiram efeitos teratogênicos em embriões do peixe zebrafish (*Danio rerio*) até 72 h pós-fertilização, sugerindo que podem ser utilizadas sem causar danos ao meio-ambiente. Em conjunto, esses dados indicam que as nanopartículas de fibroína de seda combinadas a ésteres butílicos de óleos amazônicos podem tornar-se um biometrial promissor para o controle desses insetos.

Palavras-chave: Óleos amazônicos; Casulo do bicho-da-seda; Fibroína de seda; Nanobioinseticida.

MARINHO, Victor Hugo de Souza**. Development and characterization of silk fibroin nanoparticles combined with Amazonian oils: A sustainable proposal against *Aedes aegypti* and *Spodoptera frugiperda* larvae.** 2023. 157 f. Thesis (Doctorate in Biodiversity and Biotechnology, BIONORTE) - Federal University of Amapá, Macapá, 2023.

ABSTRACT

Polymeric nanoparticles (NPs) are being used as a viable alternative to conventional insecticides for the control of various insect pests. Among biologically-based insecticides, insecticides containing botanical bioactive compounds are very effective in improving the toxicity of the larvae of these insects. The aim of this study was to develop and characterize polymeric silk fibroin nanoparticles combined with butyl esters semi-synthesized from Amazonian oils (*Astrocaryum murumuru* Mart, *Bertholletia excelsa and Carapa guianensis* Aublet), and to evaluate their insecticidal potential against *Aedes aegypti* and *Spodoptera frugiperda* larvae. The nanoparticles had their temporal stability assessed for up to 50 days at 4 ºC and 32 ºC, with particle sizes ranging from 187.6 (±0.8) nm to 540.8 (±23.8) nm, polydispersity index between 0.238 and 0.560 and zeta potential ranging from -39.7 (±1.4) mV to -62.9 (±0.7) mV. Transmission electron microscopy analysis showed that the nanoparticles were uniformly distributed and spherical in shape. In addition, the silk fibroin nanoparticles showed a slow and controlled release profile, thus inducing a high mortality rate in the third-stage larvae of *Ae. aegypti* and *S. frugiperda*. The nanoparticles were also able to inhibit the oviposition of *Ae. aegypti* females, and showed ovicidal activity against *S. frugiperda*. However, the nanoparticles showed no teratogenic effects on zebrafish (*Danio rerio*) embryos up to 72 h post-fertilization, suggesting that they can be used without causing harm to the environment. Taken together, these data indicate that silk fibroin nanoparticles combined with butyl esters from Amazonian oils could become a promising biomaterial for controlling these insects.

Keywords: Amazonian oils; Silkworm cocoon; Silk fibroin; Nanobioinsecticide.

LISTA DE FIGURAS

*As figuras do Capitulo 2, 3 e 4 aparecem aqui com o prefixo 2, 3 e 4, respectivamente.

LISTA DE TABELAS

*As figuras do Capitulo 2, 3 e 4 aparecem aqui com o prefixo 2, 3 e 4, respectivamente.

SUMÁRIO

INTRODUÇÃO

Nas últimas duas décadas, o interesse por inseticidas oriundos ou à base de produtos naturais tem crescido, sobretudo, pelos problemas ocasionados pelo uso dos inseticidas sintéticos, como o mecanismo de resistência, ressurgência e erupção de pragas, além do uso indiscriminados desses inseticidas causando danos ao meio ambiente e a animais não-alvos. Adicionado a isto, tem-se o rápido aumento do custo de síntese de novas sustâncias bioativas e a crescente dificuldade de se descobrir novas classes de compostos com efetiva ação inseticida [1].

Diante desse contexto, a nanotecnologia surge como uma das principais tecnologias do século XXI. Biomateriais de pequenos tamanhos são capazes de mudar suas propriedades físico-químicas e podem ser aplicados na agricultura no setor alimentar, no ramo farmacêutico auxiliando na entrega de fármacos, na indústria de inseticidas na busca por inseticidas ambientalmente seguros, entre outros [2,3]. Destarte, é uma das maiores promessas para melhorar a estabilidade, eficácia e o padrão de segurança de nanomateriais, entre esses os inseticidas [4,5].

O Brasil, país detentor da maior biodiversidade do planeta, possui cerca de 10 a 20%, do total de 1 milhão e meio de espécies já catalogadas no mundo. Essa enorme biodiversidade, sobretudo da região amazônica, tem incentivado a estruturação de cadeias produtivas e a expansão de centros de pesquisa biotecnológica direcionada a bioprospecção de novos produtos na região. Haja vista que nessa parte do território brasileiro existem inúmeras espécies vegetais produtoras de sementes oleaginosas, das quais se extraem óleos vegetais de composição química e propriedades físicas diversas [6,7].

A exploração de insumos oriundos da floresta amazônica já é realizada por povos nativos há muito tempo, tendo foco no uso de frutas, amêndoas, folhas e espécies oleaginosas, em geral como plantas medicinais para o tratamento empírico de doenças [8,9]. Atualmente, a castanha-da-Amazônia (*Bertholletia excelsa*), o murumuru (*Astrocaryum murumuru* Mart.) e a andiroba (*Carapa guianensis* Aublet) estão entre as espécies vegetais que fornecem produtos florestais não madeireiros de alto valor agregado, esses produtos florestais são utilizados em diversos setores industriais como na indústria alimentícia, de cosméticos, farmacêutica, biocombustíveis entre outras [10].

Nos últimos anos tem se utilizado várias espécies vegetais produtoras de bioativos medicinais que apresentam potencial inseticida. Dentre essas, as oleaginosas despontam como alternativa para a obtenção de bioprodutos com ação inseticida mais seletivas e menos

prejudicial ao meio ambiente [11]. Isso tem ocorrido principalmente em decorrência das exigências do mercado consumidor, tornando-se importante a busca por novos compostos que auxiliem no controle de insetos-praga, com menor contaminação ambiental e maior seletividade [12].

A utilização de inseticidas sintéticos, principalmente os não seletivos, ainda é a forma mais comum de controle de insetos-praga. Apesar da grande contribuição econômica desses inseticidas, muitos problemas decorrem do seu uso incorreto e desordenado. Como a presença de resíduos tóxicos em alimentos, intoxicação de produtos rurais e consumidores, contaminação do solo e da água, seleção de pragas resistentes e prejuízos a populações de organismos não-alvo [13].

O *Aedes aegypti* é um vetor de doenças de grande relevância para a saúde pública nas regiões dos trópicos e subtrópicos e em praticamente todo continente americano. As principais arboviroses transmitidas por esse vetor são: febre amarela, dengue, Chikungunya e Zika vírus. Essas arboviroses são causa de preocupação para a saúde pública, com impactos clínicos, econômicos e sociais. Seu controle representa um desafio, principalmente no Brasil [14]. Em 2022, o Brasil registrou 1.450,270 casos de dengue com taxa de incidência de 679,9 casos por 100 mil habitantes [15].

A *Spodoptera frugiperda* (lagarta-do-cartucho) é um inseto lepidóptero que em sua fase larval tem preferência alimentar por folhas e brotos de diversas culturas agrícolas e cultivares, como o milho, a soja, o algodão, entre outras. Seus hábitos alimentares a torna uma praga polífaga, migratória e destrutiva de diversas plantações no hemisfério ocidental. A manutenção populacional da espécie se mantém constante por quase todo o ano, causando danos a agricultura alimentar gerando consequentemente perdas econômicas [16]. Logo, todas essas características levaram os pesquisadores a considerá-la uma praga de importância econômica [17]. Dados os problemas decorrentes do uso de inseticidas sintéticos, há a necessidade de se encontrar um manejo ecologicamente correto para o controle de inseto-pragas que ofereça um mecanismo de ação menos tóxico e econômico [18].

Em vista do exposto, o presente trabalho buscou coletar informações dos constituintes químicos majoritários de óleos amazônicos e as ações biológicas das nanopartículas de fibroína de seda combinadas com ésteres graxos obtidos da gordura de *A. murumuru* e dos óleos de *C. guianensis e B. excelsa*, com o intuito de se conhecer as potencialidades das espécies vegetais oleaginosas da região amazônica, atrelando o conhecimento tradicional ao cientifico para contribuir de maneira sustentável com a biodiversidade da Amazônia, com perspectivas para o crescimento cientifico e econômico da região.

Nesse sentido, o presente trabalho buscou responder a seguinte pergunta: as nanopartículas de fibroína de seda associadas a ésteres graxos da gordura de *A. murumuru* e dos óleos de *C. guianensis e B. excelsa* são bioinseticidas eficazes frente ao *Ae. aegypti* e a *S. frugiperda*?

O estudo se caracteriza de natureza experimental e quanti-qualitativo e apresenta como hipótese de nulidade (H0): as nanopartículas de fibroína de seda associadas a ésteres graxos da gordura de *A. murumuru* e dos óleos de *C. guianensis e B. excelsa* não são bioinseticidas eficazes frente ao *Ae. aegypti* e a *S. frugiperda;* e como hipótese alternativa (H1): as nanopartículas de fibroína de seda associadas a ésteres graxos da gordura de *A. murumuru* e dos óleos de *C. guianensis e B. excelsa* são bioinseticidas eficazes frente ao *Ae. aegypti* e a *S. frugiperda.*

Diante disso, o presente trabalho avaliou a atividade larvicida e de oviposição de nanopartículas de fibroína de seda associadas a óleos amazônicos frente às larvas de 3º instar de *Ae. aegypti*, bem como a atividade larvicida e ovicida dessas nanopartículas frente às larvas de 3º instar de *S. frugiperda*, como alternativa aos inseticidas sintéticos convencionais.

OBJETIVOS

Objetivo geral

Desenvolver e caracterizar nanopartículas de fibroína de seda combinadas a ésteres graxos semissintetizados a partir da gordura de *Astrocaryum murumuru* Mart. e dos óleos de *Carapa guianensis* Aublet e *Bertholletia excelsa* e avaliar seu potencial larvicida contra larvas de *Aedes aegypti* e *Spodoptera frugiperda*.

Objetivos específicos

- ✓ Caracterizar o perfil físico-químico (densidade, teor de peróxido, grau de acidez e saponificação) dos óleos de *C. guianensis* e *B. excelsa;*
- ✓ Identificar e quantificar os principais ácidos graxos presentes na gordura de *A. murumuru* e dos óleos de *C. guianensis* e *B. excelsa;*
- ✓ Caracterizar por Ressonância Magnética Nuclear de hidrogênio (^{1}H) e carbono (^{13}C), Espectroscopia de infravermelho - FTIR e Cromatografia Gasosa Acoplada a Espectrômetro de Massas, a gordura de *A. murumuru*, os óleos de *C. guianensis* e *B. excelsa* e seus respectivos ésteres graxos;
- ✓ Desenvolver nanopartículas de fibroína de seda combinadas com ésteres graxos semissintetizados a partir da gordura de *A. murumuru* e dos óleos de *C. guianensis* e *B. excelsa;*
- ✓ Caracterizar as nanopartículas quanto aos seus aspectos físico-químicos através das técnicas de dispersão dinâmica da luz, calorimetria de varredura diferencial e microscopia de transmissão;
- ✓ Comparar o perfil da atividade larvicida e de oviposição das nanopartículas de *A. murumuru, B. excelsa* e *C. guianensis* frente às larvas de 3º instar de *Ae. aegypti;*
- ✓ Comparar o perfil da atividade larvicida e ovicida das nanopartículas de *A. murumuru, B. excelsa* e *C. guianensis* frente às larvas de 3º instar de *S. frugiperda;*
- ✓ Avaliar o grau de toxicidade das nanopartículas de *B. excelsa* e *C. guianensis* em embriões do modelo animal zebrafish (*Danio rerio*).

A partir dos objetivos apresentados, esta tese foi estruturada em quatro capítulos, nos quais são abordados os seguintes conteúdos:

- ✓ Capítulo 1: A contextualização do problema através da fundamentação teórica da temática abordada.
- ✓ Capítulo 2: Development of an environmentally friendly formulation of silk fibroin combined from *Astrocaryum murumuru* Mart. effective against *Aedes aegypti* larvae.
- ✓ Capítulo 3: Nanoparticles from silk fibroin and amazon oils: Potential larvicidal activity and oviposition deterrence against *Aedes aegypti*.
- ✓ Capítulo 4: Potencial controle ecológico de nanopartículas de fibroína de seda e óleos amazônicos contra *Spodoptera frugiperda.*

REFERÊNCIAS

[1] B. Adelino de Melo, S. Ramos de Oliveira, D. Teles Leite, C. Ferreira Barreto, H. de Souza Silva, Revista verde de agroecologia e desenvolvimento sustentável, grupo verde de agricultura alternativa (Gvaa) Issn 1981-8203. Inseticidas botânicos no controle de pragas de produtos armazenados botanical insecticides to pest control in stores, (2011) 1–10.

[2] M. García, T. Forbe, E. Gonzalez, Potenciais aplicações de nanotecnologia no setor agro-alimentar, Cienc. e Tecnol. Aliment. 30 (2010) 573–581.

[3] S. Mesci-Haftaci, H. Ankarali, M. Caglar, A. Yavuzcan, Reliability of colposcopy in Turkey: Correlation with pap smear and 1-year follow up, Asian Pacific J. Cancer Prev. 15 (2014) 7317–7320.

[4] G. Benelli, Plant-mediated biosynthesis of nanoparticles as an emerging tool against mosquitoes of medical and veterinary importance: a review, Parasitol. Res. 115 (2016) 23–34.

[5] R. Pavela, K. Murugan, A. Canale, G. Benelli, *Saponaria officinalis*-synthesized silver nanocrystals as effective biopesticides and oviposition inhibitors against *Tetranychus urticae* Koch, Ind. Crops Prod. 97 (2017) 338–344.

[6] P.G. Kevan, B.F. Viana, The global decline of pollination services, Biodiversity. 4 (2003) 3–8.

[7] E.S. Priorit, R. Para, D.O.S. Benef, Avaliação e identificação de ações prioritárias para a conservação , utilização sustentável e repartição dos benefícios da biodiversidade na amazônia brasileira, (n.d.).

[8] I. Ottobelli, V.A. Facundo, J. Zuliani, C.C. Luz, H.O.B. Brasil, J.S.L.T. Militão, R. Braz-

Filho, Estudo químico de duas plantas medicinais da Amazônia: *Philodendron scabrum* K. Krause (Araceae) e *Vatairea guianensis* aubl. (Fabaceae), Acta Amaz. 41 (2011) 393–400.

[9] D.L. Santos, J.S. Moraes, Z.T. de S. Araujo, I.R. da Silva, Saberes tradicionais sobre plantas medicinais na conservação da biodiversidade amazônica resumo, Ciências Em Foco. 12 (2019) 86–95.

[10] O.F. Giatti, P.H. Mariosa, S.S. Alfaia, S.C.P. da Silva, H.D.S. Pereira, Socioeconomic potential of non-timber forest products in the sustainable development reserve of Uatuma, Amazonas, Rev. Econ. e Sociol. Rural. 59 (2021) 1–19.

[11] R.M. da Silva, N.P. Ribeiro, C. da S. Rodrigues, R.A. Pelvine, J.N. Rondon, M.P. Cereda, Behavioral characterization and alternative control methods of the bamboo borer [*Dinoderus minutus* Fabricius (Coleoptera: Bostrichidae)], Idesia. 37 (2019) 5–12.

[12] A.G. Spletozer, C.R. Dos Santos, L.A. Sanches, J. Garlet, Plants with insecticide potential: Focus on amazon species, Cienc. Florest. 31 (2021) 974–997.

[13] D. Šunjka, Š. Mechora, An alternative source of biopesticides and improvement in their formulation—Recent Advances, Plants. 11 (2022) 1–13.

[14] M. das G.M. Freire, V. Mussi-Dias, A.F. dos S. Neto, C.M. Dos Santos, A.T.M. Figueiredo Silva, Zero *Aedes*: Fora Dengue, Fora Zika, Fora Chikungunya, Biológicas & Saúde. 7 (2017) 23–31.

[15] R. Preto, Boletim_epidemiologico_SVS_47, 53 (2022).

[16] H. He, X. Qin, F. Dong, J. Ye, C. Xu, H. Zhang, Z. Liu, X. Lv, Y. Wu, X. Jiang, X. Cheng, Synthesis, characterization of two matrine derivatives and their cytotoxic effect on Sf 9 cell of *Spodoptera frugiperda*, Sci. Rep. 10 (2020) 1–10.

[17] F.A. Paredes-Sánchez, G. Rivera, V. Bocanegra-García, H.Y. Martínez-Padrón, M. Berrones-Morales, N. Niño-García, V. Herrera-Mayorga, Advances in control strategies against *Spodoptera frugiperda*. A review, Molecules. 26 (2021).

[18] A. Priyanca Devi, A. Alsulimani, J.R. Hidalgo, A. Neske, R.Z. Sayyed, M. Hassan, K.L. Ameta, H. Elshazly, Bis- and mono-substituted chalcones exert anti-feedant and toxic effects on fall armyworm *Spodoptera frugiperda*, Saudi J. Biol. Sci. 28 (2021).

CAPÍTULO 1 - REFERENCIAL TEÓRICO

1.1 ÓLEOS E GORDURAS DE ORIGEM VEGETAL

Óleos e gorduras derivados de espécies vegetais são compostos por fosfolipídeos, diésteres, manoésteres e triésteres de cadeias alquílicas longas. Este último, formado a partir de uma molécula de glicerol com três moléculas de ácidos graxos, podendo os ácidos graxos possuírem cadeias de 3 a 24 carbonos [1,2]. Esses triésteres são bem utilizados como matéria-prima em diversos setores como o de alimentação, da indústria médica, da cosmética e da farmacologia. São componentes essenciais na produção de alimentos industrializados por suas diversas propriedades nutricionais [3].

Os óleos e gorduras vegetais são nutrientes importantes na dieta do homem, desempenhando um importante papel no fornecimento de ácidos graxos essenciais e energia. Os ácidos graxos essenciais são aqueles que não podem ser produzidos pelo homem em seu organismo através de seu metabolismo, devendo ser ingeridos diariamente por meio de alimentos, como sementes de oleaginosas, peixes, algas e outros [4].

As diferentes propriedades físicas e químicas que os lipídios possuem está intrinsicamente ligada ao tamanho da sua cadeia carbônica, número da posição das duplas ligações e linearidade (estereoespecificidade, *cis-tras*). Os ácidos graxos possuem diferentes tamanhos de cadeia (3 a 24 átomos de carbono) e são classificados como saturados e insaturados. Os ácidos graxos insaturados possuem duplas ligações e são considerados quimicamente mais instáveis, são denominados monoinsaturados quando sua cadeia carbônica possui apenas uma dupla ligação e poliinsaturados quando possuem duas ou mais duplas ligações [5]. Os ácidos graxos saturados são menos reativos em comparação aos insaturados, e apresentam ponto de fusão superior em relação ao ácido graxo correspondente de mesmo tamanho de cadeia com uma ou mais dupla ligação [6].

Segundo Rose e Connoly (1999) [7] a nomenclatura dos ácidos graxos se inicia pela numeração dos átomos de carbonos do grupo carboxila terminal, os átomos de carbono de número 2 e 3 adjacentes ao grupo carboxila são nomeados de carbonos α e β, respectivamente, e o último é o ω ou *n*-carbono. A posição da dupla ligação é indicada pelo símbolo Δ, acompanhado por um número, a exemplo: Δ^9 referindo-se a dupla ligação entre os átomos 9 e 10 numerados a partir do grupo carboxila.

O ácido oleico é um ácido graxo que pode ser sintetizado por todos os mamíferos, inclusive o homem. Este ácido possui uma dupla ligação entre os carbonos 9 e 10 do grupo

metila final, sendo designado como ácido graxo monoinsaturado ω9 ou *n*-9. Os ácidos graxos poliinsaturados ω3 (*n*-3) e ω6 (*n*-6) não podem ser sintetizados por mamíferos por não possuírem a enzima Δ9-dessaturase, enzima responsável por introduzir a dupla ligação (*cis*) entre os átomos de carbono 9 e 10, devendo deste modo ser obtidos através da dieta e são denominados de ácidos graxos essenciais [7,8].

Existem dois tipos de ácidos graxos essenciais, os ácidos graxos *n*-6 derivados do ácido *cis*-linoleico (C18:2), e os ácidos graxos *n*-3 derivados do ácido α-linolênico (C18:3) [9] (Figura 1.1). São chamados de essenciais por possuírem funções celulares normais, e atuarem como precursores na síntese de ácidos graxos poliinsaturados de cadeia longa como os ácidos araquidônico, eicosapentanóico e docosahexaenoico, que desempenham importantes funções celulares como a integridade e fluidez das membranas, atividade das enzimas de membrana, interações lipídio-proteína e síntese de eicosanoides como as prostaglandinas, leucotrienos e tromboxanos [10].

Figura 1.1 – Estruturas químicas do ácido oleico (ω9), ácido linoleico (ω6) e do ácido α-linolênico (ω3).

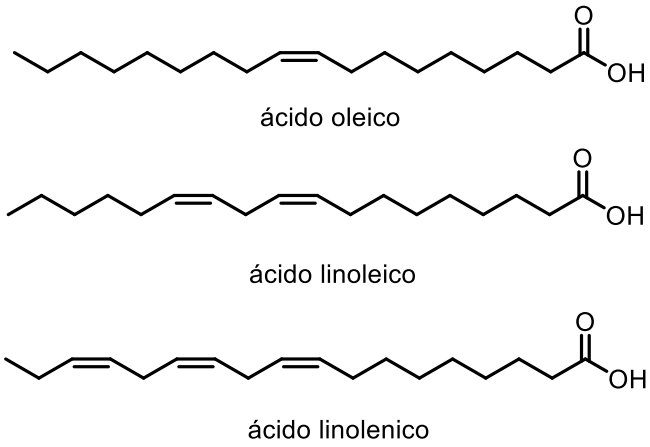

Fonte: Adaptado de Rose e Connely (1999).

A região amazônica possui a maior diversidade genética de espécies vegetais produtoras de óleos do planeta. São de grande importância pois possuem propriedades funcionais importante capazes de produzir efeitos metabólicos ou fisiológicos úteis para manter uma boa saúde e ajudar na redução de doenças [3,11]. A diversidade de aplicações dos óleos vegetais revela sua importância para a obtenção de novos produtos, por serem de fácil acesso, baixo custo e envolvidos em combinações químicas estruturantes para diversos setores industriais [12].

1.1.1 A gordura de *Astrocaryum murumuru* Mart (murumuru)

A espécie *Astrocaryum murumuru* Mart., é nativa da Amazônia e do norte da América do Sul, pertence à família Aracaceae. Esta palmeira é conhecida popularmente como murumuruzeiro [13].

A espécie representa cerca de 15% das espécies de palmeiras nas áreas de várzeas da Amazônia e está entre as cinco espécies com maior índice de importância econômica [14]. O fruto de murumuru contém cerca de 42% de gordura sólida de cor amarela e não apresenta sabor ou odor pronunciado. A gordura é rica em ácidos graxos de cadeia média e longa, como o ácido láurico, mirístico e palmítico, sendo esses ácidos graxos largamente utilizados industrialmente [15]. Na indústria de cosméticos a gordura é utilizada para a fabricação de sabonetes, cremes e xampus, e na indústria alimentícia é muito utilizada na produção de margarina e derivados [16].

A gordura ainda é usada como alternativa na geração de energia, através da produção de biocombustível [17] (Figura 1.2). Para a indústria farmacêutica a gordura torna-se uma excelente alternativa na veiculação de formulações, por possuir propriedades importantes como biodegradabilidade, biocompatibilidade demostrando que este bioproduto têm elevado potencial para a produção de nanopartículas lipídicas sólidas efetivas para o transporte de medicamentos hidrossolúveis e lipossolúveis [18].

Figura 1.2 – Gordura e sementes de *Astrocaryum murumuru*.

Fonte: Amazon oil.

1.1.2 Óleo de *Bertholletia excelsa* (castanha-da-Amazônia)

A castanha-da-Amazônia é uma árvore nativa da região amazônica, pertence à família Lecythidaceae e do gênero *Bertholletia*, espécie *excelsa*. A denominação botânica *Bertholletia excelsa* H.B.K ocorreu quando a espécie foi descrita em 1808, por Humboldt, Bompland e Kunth, em homenagem aos pesquisadores [19]. O fruto da castanheira é um ouriço que mede cerca de 20 cm de diâmetro, contendo em seu interior cerca de 12 a 24 sementes ou castanhas as quais envolve as amêndoas, parte comestível do fruto [19,20].

As amêndoas da castanha-da-Amazônia são fontes de importantes constituintes com ação antioxidante e elevado teor de vitamina E, possuindo ainda percentuais de α, β, γ tocoferóis que estão diretamente relacionados à compostos fenólicos e vem sendo relatados como constituintes funcionais [21]. O óleo da castanha-da-Amazônia possui alto teor de selênio, um importante antioxidante que está relacionado à redução de alguns tipos de câncer e outras patologias [22,23].

O óleo extraído das amêndoas da castanha-da-Amazônia apresenta elevado valor funcional, seu perfil de ácidos graxos é constituído por monoglicerídeos, diglicerídeos e poliglicerídeos, em menor quantidade (Figura 1.3). A grande relevância encontra-se nos ácidos graxos insaturados, principalmente, o linoleico, oleico e o linolênico que estão relacionados a atividades farmacológicas apresentando eficácia no combate às dermatites de contato irritativa, dermatite de contato alérgica e dermatite atópica. Esses ácidos graxos possuem também características antimicrobianas que melhoram a capacidade de defesa imunológica nata [19,23].

Figura 1.3 – Óleo e sementes da *Bertholletia excelsa*.

Fonte: Autor

1.1.3 Óleo de *Carapa guianensis* Aublet (andiroba)

A andiroba é amplamente distribuída na Amazônia, pertence à família Meliaceae, espécie *Carapa guianensis.* Esta espécie vegetal tem grande potencial quando retratado seus componentes medicinais e funcionais [24]. Possui frutos redondos, sementes grandes e angulares de onde se extraí seu óleo com propriedades fitoterápicas [25]. A andiroba foi relatada pela primeira vez pelo farmacêutico Jean Baptiste Christophe Fusée-Aublet, no ano de 1775.

O óleo fixo da andiroba, bem como de outras espécies vegetais apresentam em sua composição principalmente triglicerídeos, ácidos livres, monoacilgliceróis e diacilgliceróis, além de uma pequena quantidade de fosfolipídeos, esteróis livres e esterificado, álcoois triterpênicos, tocoferóis e tocotrienóis, compostos fenólicos, carotenos entre outros [26] (Figura 1.4). Dentre os ácidos graxos presente no óleo da andiroba destacam-se o ácido oleico, o ácido palmítico e o ácido linoleico.

O uso etnofarmacológico deste óleo inclui o tratamento de dores artríticas, infecções do ouvido, doenças de pele, entre outros [27]. Outro notável potencial do óleo da andiroba está associado à sua atividade larvicida contra *Ae. aegypti*, o vetor da dengue e várias outras doenças, até hoje negligenciadas ou emergentes. A ampla gama de atividades biológicas e propriedades etnofarmacológicas faz do óleo de andiroba uma valiosa matéria-prima para diferentes setores industriais, destacando-se a indústria farmacêutica e a de cosméticos [28].

Figura 1.4 – Óleo e sementes da *Carapa guianensis*.

Fonte: Autor.

1.2 FIBROÍNA DE SEDA E SUAS APLICAÇÕES

Os biopolímeros estão cada vez mais presentes no setor industrial e nas pesquisas científicas, por suas diversas propriedades e vantagens exclusivamente sobre alguns materiais sintéticos. Esses biomateriais são desenvolvidos para servir a uma ampla gama de usos na natureza, pois possuem propriedades químicas e mecânicas vantajosas para muitas aplicações, especialmente ambiental e farmacológica [29]. Vários polímeros naturais têm sido utilizados como matriz para a administração de fármaco, como os polissacarídeos, incluindo a celulose, a quitosana, o ácido hialurônico, o alginato dextrano e amido, além de proteínas, como o colágeno, a elastina, a albumina e a fibroína de seda [30].

Os biopolímeros podem advir de várias fontes, como plantas, microrganismos e animais. Alguns dos principais biopolímeros naturais estudados ou em uso incluem quitosana, queratina, elastina e fibroína de seda [31]. A seda é produzida por diferentes larvas da ordem Lepidoptera, incluindo bichos-da-seda, escorpião, aranhas, entre outros animais [32]. A maioria da produção mundial de seda utilizada na indústria têxtil e em outras aplicações é produzida pelo bicho-da-seda domesticado *Bombyx mori*. A seda proveniente do bicho-da-seda consiste de duas principais proteínas a fibroína e a sericina [29]. A fibroína é a proteína do tipo folha pregueada, anti-paralela e que conferem o caráter fibroso ao casulo do bicho-da-seda, enquanto a sericina é uma proteína que fornece um tipo de liga que mantém o casulo unido e, tanto uma quanto a outra podem ser utilizadas sozinhas ou em conjunto para a produção de filmes com propriedades químicas e físicas únicas [33].

A principal estrutura da fibroína de seda é uma sequência de repetição de três aminoácidos (Ser-Gly-Ala), formando uma estrutura secundária homogênea em uma conformação β-folha antiparalela [34]. A região β-folha antiparalela cristalina da fibroína compreende dois terços da proteína e a região amorfa das fibras representa um terço e, juntas essas regiões conferem a fibroína de seda propriedades mecânicas únicas [35]. Além disso, a fibroína de seda é um copolímero natural que contém blocos hidrofílicos e hidrofóbicos, que faz dela um potencial material para sistemas emulsificantes. Os blocos hidrofóbicos são os responsáveis pela conformação β-folha através de ligações de hidrogênio entre os blocos e ambas as regiões conferem alta resistência, insolubilidade e estabilidade térmica à fibroína de seda [36].

A biodegradação é a capacidade que um material tem de ser decomposto em componentes mais simples e fáceis de tratar. Este fenômeno ocorre por processos biológicos diferentes, tais como metabolismo bacteriano ou ação de enzimas. No organismo, materiais

estranhos são biodegradados através de interações complexas entre fatores biológicos, químicos e físicos. O processo de biodegradação de um biomaterial em compostos não nocivos é importante para muitas aplicações, como na engenharia de materiais e na liberação controlada de fármacos [32].

Constatou-se que produtos ativos contendo pequenos tamanhos de poros e altas concentrações de fibroína degradam-se lentamente e, este achado é importante tanto para a engenharia de tecido quanto para a liberação controlada de fármacos utilizando a fibroína de seda como veículo. Na engenharia de tecidos, compostos contendo fibroína podem ser modificados para degradar em taxas mais lentas ou mais baixa, dependendo da taxa de crescimento do tecido, enquanto que para liberação controlada, a fibroína pode ser modificada para degradar em diferentes taxas, dependendo do tempo e a cinética de liberação necessária para a entrega do fármaco [29].

A biocompatibilidade é a capacidade que um material tem de não provocar rejeição imunológica em uma aplicação especifica no interior do hospedeiro. A partir desta definição, a biocompatibilidade de um material não é uma propriedade intrínseca do material, mas ela depende da resposta imunológica do hospedeiro. Algumas dessas respostas incluem, citotoxicidade celular do material ou dos produtos de degradação, resposta enzimática e resposta trombogênica [32,37,38]. Portanto, os indicadores de um material biocompatível são a baixa capacidade inflamatória, baixa toxicidade celular e baixa formação de trombose [29].

A citotoxicidade celular de um biomaterial ou produto químico é a toxicidade que eles podem causar quando estão em contato com as células. Materiais citotóxicos podem causar uma série de danos prejudiciais as células do hospedeiro, incluindo necrose e eventual lise celular ou apoptose, ou diminuição do crescimento e viabilidade celular. A microscopia pode ser utilizada para inspecionar a morfologia celular, e as diferenças na membrana celular e organelas podem ser indicativos de efeitos citotóxicos [38].

A fibroína de seda, por ser um biopolímero natural que exibe excelente biocompatibilidade e biodegradabilidade, é um material vantajoso para os sistemas de liberação controlada de fármacos. Filmes produzidos a partir da fibroína de seda conseguem encapsular e estabilizar proteínas e enzimas por forças intermoleculares entre a seda e as biomoléculas, liberando em seguida as proteínas não-desnaturadas e as enzimas em plena atividade [39]. A fibroína de seda pode ainda ser utilizada como esferas para imobilizar enzimas, afim de catalisar reações de transesterificação para a produção de biodiesel, na obtenção de epóxidos precursores da síntese de azóis com finalidades antifúngicas [40,41], bem como nanopartículas com a finalidade de liberar princípios ativos de extratos vegetais, óleos vegetais e compostos

biologicamente ativos com ampla atividade farmacológica, como atividades anti-inflamatória, anti-helmíntica, inibidor de lipo-oxigenase [42–44], além de atuar como agente larvicida contra vetores de doenças, como o mosquito *Ae. aegypti* [45–48] (Figura 1.5).

Figura 1.5 – Biomateriais produzidos a partir de casulos de seda.

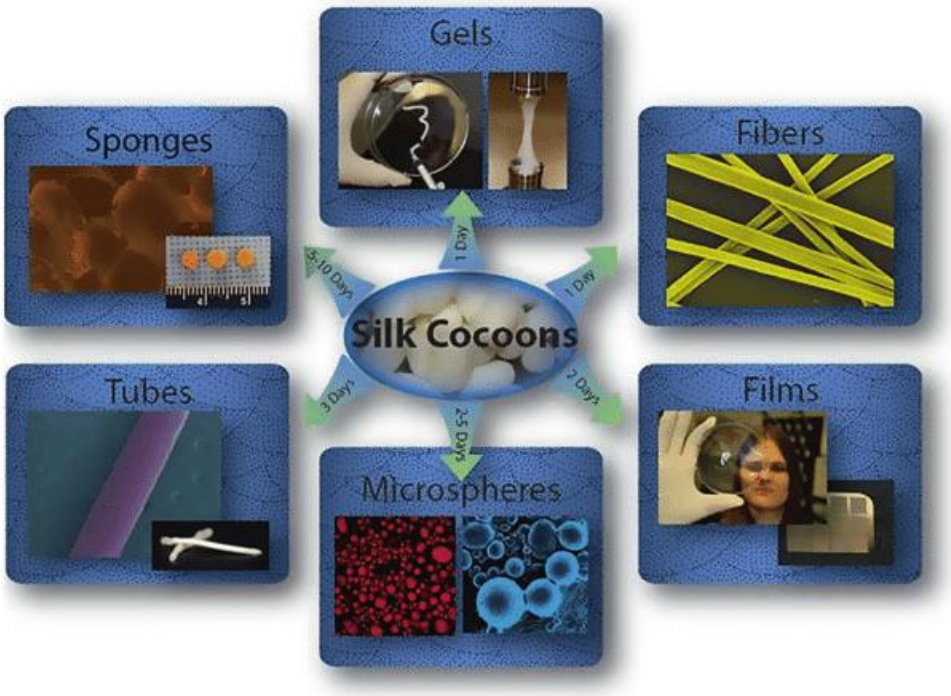

Fonte: Nature (2011).

Devido à coexistência de regiões hidrofóbicas e hidrofílicas distintas, a fibroína de seda pode residir nas interfaces de um fluído e estabilizar de forma eficaz sistemas dispersos, reduzindo de forma eficiente a tensão interfacial e formando um filme estérico e altamente viscoelásticos na interface [49,50]. A redução da tensão interfacial facilita a formação de gotas menores durante o processo de homogeneização da nanodispersão, reduzindo assim o risco do fenômeno de coalescência durante o processo de emulsificação e armazenamento a longo prazo [51].

1.3 NANOTECNOLOGIA E SUAS APLICAÇÕES

A nanotecnologia é considerada uma das tecnologias chaves do século XXI. Materiais nanométricos são partículas coloidais de tamanho que variam de 10 a 1000 nm alterando suas propriedades físicas e químicas. Uma variedade de produtos industriais, farmacêuticos e

médicos foram inovados através da nanotecnologia [52,53]. A nanotecnologia tem sido aplicada no ramo farmacêutico para a entrega de ativos farmacêuticos para uma variedade de doenças e distúrbios [54]. Na agricultura, no setor alimentar e de inseticidas a sua inserção é relativamente recente [55] (Figura 1.5). No geral, materiais nanométricos são esféricos por natureza, e sua superfície é lipofílica e amorfa apresentando geralmente carga negativa, e devido ao seu tamanho são translucidas [56].

O desenvolvimento de biopesticidas tornou-se um componente importante no sistema de gestão integrada de pragas [57,58]. Apesar dos biopesticidas apresentarem um caráter ecológico, eles sofrem uma série de problemas, como métodos de produção dispendiosos, fraca capacidade de armazenamento, suscetibilidade às condições ambientais, eficácia seletiva no controle de pragas e vetores, o que dificulta o seu rápido progresso e utilização. Assim, a situação atual é comparável à dos pesticidas comerciais sintéticos [59]. O desenvolvimento de novos biopesticidas eficazes, seguros e comprovados que convençam as instituições reguladoras, é também um grande desafio.

Do mercado global de pesticidas, apenas 5% é composto por biopesticidas, pois é importante garantir a estabilidade e a eficácia destes no controle de pragas. Os novos compostos bioativos, as novas formulações de pesticidas, a sua produção e as suas melhorias no sistema de distribuição, são campos de investigação sempre atuante e estão sempre apoiados pelos avanços e inovações tecnológicas [59].

Nesse contexto, nos último 50 anos, os sistemas de distribuição de pesticidas foram aprimorados através da preparação promissoras de formulações de liberação controlada. Inicialmente, as formulações de liberação controlada foram preparadas a partir do revestimento de compostos bioativos em uma matriz polimérica, através das quais os compostos bioativos são liberados de forma controlada para o ambiente durante um período de tempo definido [60]. A principal vantagem das formulações com liberação controlada é o fato de reduzir substancialmente a quantidade de pesticida a níveis inferiores aos exigidos para os pesticidas convencionais, atuando durante um período de tempo semelhante [61].

O modelo de liberação de um composto bioativo está relacionado com a natureza química da formulação e pode ocorrer através da difusão e desmontagens das nanomatrizes poliméricas contendo o composto bioativo após contato com a água e uma subsequente liberação do composto [62]. Nas nanoformulações, em que ocorrem ligações polímero-pesticida, é necessária uma reação de hidrólise para a liberação do composto bioativo, e esta liberação é afetada pela força destas ligações químicas, pelas propriedades químicas de ambas as moléculas e pelo tamanho e estrutura da macromolécula. A tecnologia de encapsulação tem

sido muito utilizada no ramo farmacêutico, porque esta tecnologia protege o fármaco, mantêm sua concentração dentro de um intervalo ótimo, ajustando a liberação dos componentes ativos proporcionando a sustentabilidade do efeito [63].

Nanoformulações à base de polímeros naturais conseguem encapsular uma ampla variedade de moléculas hidrofóbicas [64], e um exemplo desse biomaterial é a fibroína de seda que tem ganhado cada vez mais atenção nos últimos anos na área biomédica, farmacêutica e industrial [63,64]. A fibroína de seda possui uma ampla gama de plataformas de distribuição de drogas tais como hidrogéis, filmes, micropartículas, nanopartículas entre outros [64]. Dispositivos de entrega de fármacos feitos à base de fibroína de seda podem ser fabricados por uma variedade de técnicas, e sua escolha depende do modo de aplicação, cinética de liberação desejada e estabilidade do fármaco [65]. A liberação de fármacos a uma taxa definida ao longo de um período específico só é possível por sintonizar propriedades do polímero como sua estrutura, morfologia, composição, orientação da fibra e porosidade da teia fibrosa [66,67].

Diante disso, a nanotecnologia apresenta-se como alternativa para diferentes áreas como por exemplo, materiais têxteis, alimentos, fertilizantes, pesticidas, proteção de plantas, biocombustíveis, biocompostos e indústrias agroquímicas para criar novos produtos com uma vasta gama de aplicações. Nesse contexto, as nanopartículas poliméricas por possuírem propriedades físicas únicas como uniformidade e condutância, tornam-se materiais desejáveis na ciência dos materiais e em outras áreas como as de biopesticidas [68], por serem possíveis substitutos frente aos inseticidas e pesticidas sintéticos, reduzindo deste modo os impactos ambientais sem perder sua eficiência [69].

1.4 *Aedes aegypti*

O mosquito *Ae. aegypti* pertence à família Culicidae, ordem Diptera e gênero Aedes. O *Ae. aegypti* é oriundo do continente africano, entretanto, acompanhou o homem ao longo de sua ininterrupta migração pelo mundo e permaneceu onde as alterações antrópicas propiciaram sua proliferação [70]. Deste modo, o mosquito se estabeleceu nos países da América latina, dentre eles o Brasil, acredita-se que foi inserido nesses países no período colonial por meio dos navios negreiros [71,72].

Várias espécies de mosquitos do gênero Aedes podem servir como transmissores de diversas arboviroses como: Dengue, Zika vírus, Chikungunia e Febre amarela, no Brasil duas delas estão hoje inseridas o *Ae. aegypti* e o *Aedes albopictus* [73]. A sua alimentação tem como base a seiva de plantas e sangue, porém somente o mosquito macho se alimenta de seiva. O

repasto sanguíneo é realizado pela fêmea, geralmente durante o dia para oferecer proteínas para a maturação dos ovos [71]. Ao ser fecundada, a fêmea é atraída para reservatórios escuros ou sombreados, com superfícies ásperas, onde possa depositar seus ovos, de preferência em água limpa ao invés de água que contenha matéria orgânica [71,74].

A metamorfose do mosquito ocorre de forma completa, e o ciclo de vida do *Ae. aegypti* compreende quatro fases: ovo, larva (quatro estágios larvários), pupa e mosquito [74] (Figura 1.6). O seu ciclo de desenvolvimento tem duração de 10 dias, o inseto adulto pode resistir por um período de 30 a 35 dias [75]. O mosquito é encontrado principalmente no meio urbano, por possuir hábitos domésticos e diurnos. Entretanto, o *Ae. aegypti* tem demonstrado adaptações em diferentes condições ambientais. Tem sua densidade populacional diretamente influenciada pela presença de chuvas [70].

Figura 1.6 – Ciclo de vida do mosquito *Aedes aegypti*.

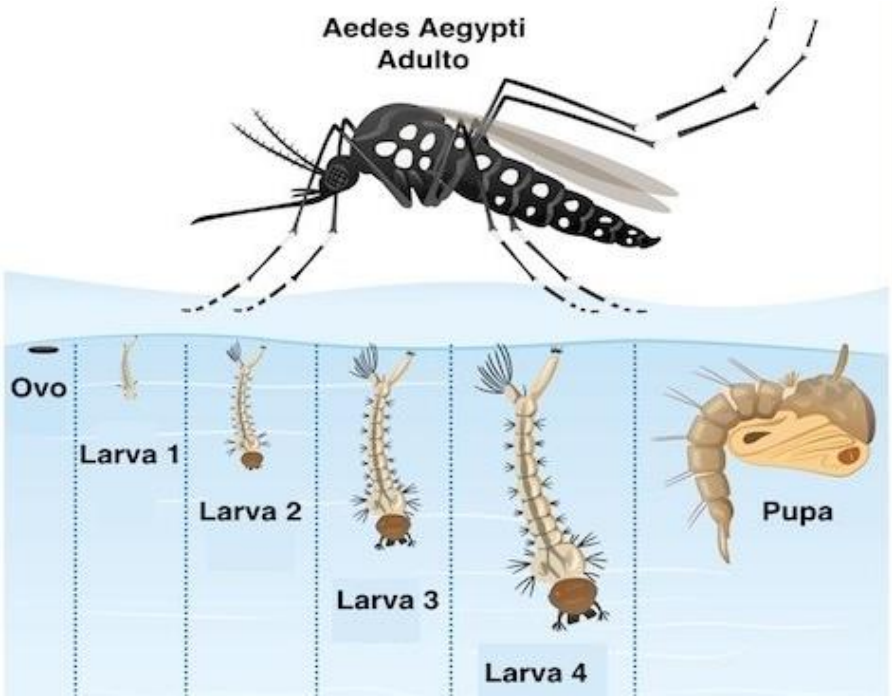

Fonte: Grupo Rede D'or.

No Brasil, as arboviroses como a dengue, febre amarela, Chikungunya e mais recente a Zika, estão associadas a grandes epidemias. Estas são doenças infecciosas febris de caráter inespecífico, sendo vinculadas pelos mesmos vetores: *Ae. aegypti* e *Ae. albopictus* [76]. Os arbovírus possuem uma ampla variação de hospedeiros vertebrados e invertebrados; podendo infectar mamíferos, aves, répteis e insetos [77].

O ciclo de transmissão da doença se inicia quando a fêmea do mosquito se alimenta do sangue de um hospedeiro infectado. O vírus presente no sangue entra em contato com as células epiteliais do intestino médio do mosquito e se replica infectando outros tecidos como as glândulas salivares do mosquito, e este ao se alimentar de sangue novamente transmite o vírus a um novo hospedeiro através da sua saliva infectada [78].

Umas das principais formas de controlar ou reduzir doenças infecciosas está embasada no controle e manejo de vetores, através de métodos ambientais, biológicos e químicos [73]. A literatura já relata o uso de inseticidas bioativos que visam erradicar ou controlar vetores. Inseticidas à base de produtos naturais já são bastante utilizados na prevenção ou controle de pragas, além desse objetivo busca-se também que esses inseticidas não sejam tóxicos ao meio ambiente e a animais não-alvo. Tais compostos enfatizam atuar em um alvo molecular especifico do vetor [79].

1.5 *Spodoptera frugiperda*

A *Spodoptera furgiperda* foi classificada em 1797 por J. E. Smith, como pertencente ao filo Arthropoda, ordem Lepidoptera e família Noctuidae. A espécie conhecida como lagarta-do-cartucho é uma das principais pragas de diversas gramíneas de importância agronômica (milho, arroz, trigo e etc) [80,81] e de dicotiledôneas como as solanáceas, leguminosas e outras [82,83]. A espécie é originária das zonas tropicais e subtropicais das Américas, sendo facilmente encontrada no continente sul-americano [84].

O Brasil possui características favoráveis para o desenvolvimento da lagarta-do-cartucho como temperatura para reprodução, além de uma grande gama de plantas hospedeiras. O habito alimentar generalista e a disponibilidade de plantas hospedeiras pelo cultivo simultâneo, ou em sucessão, favorecem a ocorrência de lagartas da espécie *Spodoptera* spp [85]. Quando adulta a fêmea é capaz de atingir uma média de 2000 ovos durante seu ciclo de vida, com postura de cerca de 50 a 300 ovos [86]. Segundo Ruiz (2015) [87], o estágio larval da espécie é composto por 4 a 7 instares, dependendo da disponibilidade de alimentação, temperatura e herança genética. A espécie apresenta desenvolvimento completo com quatro fases distintas: ovos, lagartas, pulpas e adultos (Figura 1.7).

Figura 1.7 – Ciclo de vida da *Spodoptera frugiperda*.

Fonte: Promip.

A principal forma de controle para a lagarta-do-cartucho ainda é o uso de inseticidas sintéticos com um amplo número de moléculas já registradas frente a *S. frugiperda* [88]. Esses inseticidas possuem vários mecanismos de ação como os neurotóxicos, inibidores de quitina e receptores de rionodina. Entretanto, são eficazes somente quando aplicados de maneira correta. Cerca de 30 a 70% dos produtos aplicados para o controle de *S. frugiperda* não possuem uma eficácia elevada por utilização de técnicas inadequadas o que ocasiona perdas na produtividade estimadas em torno de 15 a 34% causadas pela ação do inseto ao longo do desenvolvimento da planta [80,89].

No Brasil há relatos de dificuldades para o controle de *S. frugiperda* em diversas culturas, pois já foram registrados casos de populações resistentes para alguns defensivos como o lambda-cialotrina, clorpirifós e outros. A resistência pode estar ligada ao fato de a espécie atacar diversas culturas em qualquer período do ano, fazendo com que haja uma frequência e uma intensificação maior no uso desses inseticidas para o controle da lagarta [88,89]. Diante do exposto, há a necessidade de inseticidas à base de bioprodutos com características importantes que vão além da sua eficácia, ou seja, devem ser produtos seletivos de longo período residual que atuem nas partes das plantas que são mais atacadas pela lagarta, diminuindo desse modo o número de aplicações e os custos operacionais [90].

1.6 REFERÊNCIAS

[1] M.M. Conceição, V.J. Fernandes, A.F. Bezerra, M.C.D. Silva, I.M.G. Santos, F.C. Silva, A.G. Souza, Dynamic kinetic calculation of castor oil biodiesel, J. Therm. Anal. Calorim. 87 (2007) 865–869.

[2] S. Vecchio, L. Campanella, A. Nuccilli, M. Tomassetti, Kinetic study of thermal breakdown of triglycerides contained in extra-virgin olive oil, J. Therm. Anal. Calorim. 91 (2008) 51–56.

[3] H.F. de Castro, A.A. Mendes, J.C. dos Santos, C.L. de Aguiar, Modificação de óleos e gorduras por biotransformação, Quim. Nova. 27 (2004) 146–156.

[4] T. Costa, N. Jorge, Compostos Bioativos Benéficos Presentes em Castanhas e Nozes, Cient. Ciênc. Biol. Saúde. 13 (2011) 195.

[5] S.J. Bell, D. Bradley, R.A. Forse, B.R. Bistrian, The new dietary fats in health and disease, J. Am. Diet. Assoc. 97 (1997) 280–286.

[6] A.P.B. Ribeiro, J.M.L.N. de Moura, R. Grimaldi, L.A.G. Gonçalves, Interesterificação química: alternativa para obtenção de gorduras zero trans, Quim. Nova. 30 (2007) 1295–1300.

[7] D.P. Rose, J.M. Connolly, Omega-3 fatty acids as cancer chemopreventive agents, Pharmacol. Ther. 83 (1999) 217–244.

[8] J.E. Teitelbaum, W. Allan Walker, Review: The role of omega 3 fatty acids in intestinal inflammation, J. Nutr. Biochem. 12 (2001) 21–32.

[9] U.N. Das, Essential fatty acids: Biochemistry, physiology and pathology, Biotechnol. J. 1 (2006) 420–439.

[10] K.A. Youdim, A. Martin, J.A. Joseph, Essential fatty acids and the brain: Possible health implications, Int. J. Dev. Neurosci. 18 (2000) 383–399.

[11] J. Neves Rodrigues, C. Anton, L.A. Gioielli, Cristalização de lipídios estruturados obtidos a partir de gordura do leite e óleo de milho, Rev. Bras. Ciencias Farm. J. Pharm. Sci. 39 (2003) 93–103.

[12] G.H.R. Cavalcante, Estudo de óleos nativos da Amazônia (Babaçu e andiroba): modificação química, caracterização e avaliação como biolubrificante, (2016) 82.

[13] C. Pesce, Oleaginosas da Amazônia, 2º, Belém, 2009.

[14] S.S. de Almeida, D.D. do Amaral, A.S.L. da Silva, Análise florística e estrutura de florestas de várzea no estuário amazônico, Acta Amaz. 34 (2004) 513–524.

[15] V.S. Bezerra, Considerações sobre a palmeira murumuruzeiro (*Astrocaryum murumuru*

Mart.), Comun. Técnico, 130. (2012) 1–6.

[16] C.B.R. Rocha, R.C. de V. Potiguara, Morfometria das fibras das folhas de *Astrocaryum murumuru* var. murumuru Mart. (ARECACEAE), Acta Amaz. 37 (2007) 511–516.

[17] J.E. Kim, Book of Abstracts, (2019) 930.

[18] Centro de Gestão e Estudos Estratégicos - CGEE, Sub-rede de Dermocosméticos na Amazônia a partir do Uso Sustentável de sua Biodiversidade com enfoques para as Cadeias Produtivas da: Castanha-do-pará e dos Óleos de Andiróba e Copaíba, (2007) 209.

[19] J. Yang, Brazil nuts and associated health benefits: A review, Lwt. 42 (2009) 1573–1580.

[20] K.M. Phillips, D.M. Ruggio, M. Ashraf-Khorassani, Phytosterol composition of nuts and seeds commonly consumed in the United States, J. Agric. Food Chem. 53 (2005) 9436–9445.

[21] T. Chunhieng, K. Pétritis, C. Elfakir, J. Brochier, T. Goli, D. Montet, Study of selenium distribution in the protein fractions of the Brazil nut, *Bertholletia excelsa*, J. Agric. Food Chem. 52 (2004) 4318–4322.

[22] H.E. Seifried, D.E. Anderson, E.I. Fisher, J.A. Milner, A review of the interaction among dietary antioxidants and reactive oxygen species, J. Nutr. Biochem. 18 (2007) 567–579.

[23] M. Venkatachalan, S.K. Sathe, Chemical composition of selected edible nut seeds, J. Agric. Food Chem. 54 (2006) 4705–4714.

[24] M.W. dos S. Lima, D. Pauletto, Andiroba (*Carapa guianensis* Aubl): análise bibliométrica de publicações nas ciências agrárias no período de 2009 a 2019, Rev. Ibero-Americana Ciências Ambient. 12 (2021) 98–110.

[25] I.D.K. Ferraz, J.L.C. Camargo, P. de T.B. Sampaio, Sementes e plântulas de andiroba (*Carapa guianensis* Aubl . e *Carapa procera* D. C.): Aspecto s botânicos, ecológicos e tecnológicos, Acta Amaz. 4 (2002) 16.

[26] C.F. Araujo-Lima, A.S. Fernandes, E.M. Gomes, L.L. Oliveira, A.F. Macedo, R. Antoniassi, A.E. Wilhelm, C.A.F. Aiub, I. Felzenszwalb, Antioxidant activity and genotoxic assessment of crabwood (andiroba, *Carapa guianensis* Aublet) seed oils, Oxid. Med. Cell. Longev. 2018 (2018).

[27] B.S. Nayak, J. Kanhai, D.M. Milne, L.P. Pereira, W.H. Swanston, Experimental evaluation of ethanolic extract of carapa guianensis L. leaf for its wound healing activity using three wound models, Evidence-Based Complement. Altern. Med. (2011) 2011.

[28] J.S. Prophiro, M.A.N. Da Silva, L.A. Kanis, B.M. Da Silva, J.E. Duque-Luna, O.S. Da Silva, Evaluation of time toxicity, residual effect, and growth-inhibiting property of

Carapa guianensis and *Copaifer*a sp. in *Aedes aegypti*, Parasitol. Res. 110 (2012) 713–719.

[29] K. Bailey, Potential applications of silk fibroin as a biomaterial, (2013) 137.

[30] Z. Zhao, A. Chen, Y. Li, J. Hu, X. Liu, J. Li, Y. Zhang, G. Li, Z. Zheng, Fabrication of silk fibroin nanoparticles for controlled drug delivery, J. Nanoparticle Res. 14 (2012).

[31] A. Sionkowska, Current research on the blends of natural and synthetic polymers as new biomaterials: Review, Prog. Polym. Sci. 36 (2011) 1254–1276.

[32] L. Meinel, O. Betz, R. Fajardo, S. Hofmann, A. Nazarian, E. Cory, M. Hilbe, J. McCool, R. Langer, G. Vunjak-Novakovic, H.P. Merkle, B. Rechenberg, D.L. Kaplan, C. Kirker-Head, Silk based biomaterials to heal critical sized femur defects, Bone. 39 (2006) 922–931.

[33] M.L. Gimenes, L. Liu, X. Feng, Sericin/poly(vinyl alcohol) blend membranes for pervaporation separation of ethanol/water mixtures, J. Memb. Sci. 295 (2007) 71–79.

[34] A. Motta, L. Fambri, C. Migliaresi, Regenerated silk fibroin films: Thermal and dynamic mechanical analysis, Macromol. Chem. Phys. 203 (2002) 1658–1665.

[35] Y. Cao, B. Wang, Biodegradation of silk biomaterials, Int. J. Mol. Sci. 10 (2009) 1514–1524.

[36] E. Bini, D.P. Knight, D.L. Kaplan, Mapping domain structures in silks from insects and spiders related to protein assembly, J. Mol. Biol. 335 (2004) 27–40.

[37] W.H. Park, W.S. Ha, H. Ito, T. Miyamoto, H. Inagaki, Y. Noishiki, Relationships between antithrombogenicity and surface free energy of regenerated silk fibroin films, Fibers Polym. 2 (2001) 58–63.

[38] X. Tang, F. Ding, Y. Yang, N. Hu, H. Wu, X. Gu, Evaluation on in vitro biocompatibility of silk fibroin-based biomaterials with primarily cultured hippocampal neurons, J. Biomed. Mater. Res. - Part A. 91 (2009) 166–174.

[39] Q. Lu, X. Wang, X. Hu, P. Cebe, F. Omenetto, D.L. Kaplan, Stabilization and release of enzymes from silk films, Macromol. Biosci. 10 (2010) 359–368.

[40] I.M. Ferreira, S.A. Yoshioka, J. V. Comasseto, A.L.M. Porto, Immobilization of Amano lipase from *Pseudomonas fluorescens* on silk fibroin spheres: an alternative protocol for the enantioselective synthesis of halohydrins, RSC Adv. 7 (2017) 12650–12658.

[41] I.M. Ferreira, L.D.S. Ganzeli, I.G. Rosset, S.A. Yoshioka, Ethylic biodiesel production using lipase immobilized in silk fibroin-alginate spheres by encapsulation, Catal. Letters. 147 (2017) 269–280.

[42] M. Tavares-Dias, L.R. Neves, C.M.G. Alves, J.N. Nogueira, F.B. Neves, A.V.P. Pinto,

J.C.T. Carvalho, I.M. Ferreira, In vitro anthelminthic activity of *Lippia alba* essential oil combined with silk fibroin against monogeneans of *Colossoma macropomum* (Serrasalmidae), Aquac. Res. 52 (2021) 5099–5104.

[43] F.H. Holanda, R.R. Pereira, V.H.S. Marinho, D.E.Q. Jimenez, L.M.M. Costa Ferreira, R.M. Ribeiro-Costa, F.F.O. de Sousa, I.M. Ferreira, Development of nanostructured formulation from naringenin and silk fibroin and application for inhibition of lipoxygenase (LOX), RSC Adv. 13 (2023) 23063–23075.

[44] F.H. Holanda, A.N. Ribeiro, B.L. Sánchez-Ortiz, G.C. de Souza, S.F. Borges, A.M. Ferreira, A.C. Florentino, S.A. Yoshioka, L.S. Moraes, J.C.T. Carvalho, I.M. Ferreira, Anti-inflammatory potential of baicalein combined with silk fibroin protein in a zebrafish model (*Danio rerio*), Biotechnol. Lett. 45 (2022) 235–253.

[45] V.H.S. Marinho, F.H. Holanda, I.F. Araújo, D.E.Q. Jimenez, R.R. Pereira, A.L.M. Porto, A.M. Ferreira, J.C.T. Carvalho, A.C.G. Albuquerque de Freitas, C.P. Fernandes, R.N.P. Souto, I.M. Ferreira, Nanoparticles from silk fibroin and Amazon oils: Potential larvicidal activity and oviposition deterrence against *Aedes aegypti*, Ind. Crops Prod. 203 (2023).

[46] V.H.S. Marinho, F.B. Neves, D.E.Q. Jimenez, F.R. Oliveira, A.V.T.L.T. Santos, R.M.A. Ferreira, R.N.P. Souto, J.C.T. Carvalho, S.A. Yoshioka, I.M. Ferreira, Development of an environmentally friendly formulation of silk fibroin combined with fatty acid from *Astrocaryum murumuru* Mart. effective against *Aedes aegypti* larvae, J. Drug Deliv. Sci. Technol. 75 (2022).

[47] S.F.R. Sarquis, V.H.S. Marinho, F.B. Neves, I.R. Sarquis, I.F. Araújo, L.F. Damasceno, R.M.A. Ferreira, R.N.P. Souto, C.T. Carvalho, I.M. Ferreira, *Carapa guianensis* Aubl . (Meliaceae) oil associated with silk fibroin , as alternative to traditional surfactants , and active against larvae of the vector *Aedes aegypti*, 157 (2020).

[48] I.F. Araújo, H.A. Loureiro, V.H.S. Marinho, F.B. Neves, R.S.F. Sarquis, S.M.M. Faustino, S.A. Yoshioka, R.M.A. Ferreira, R.N.P. Souto, I.M. Ferreira, Larvicidal activity of the methanolic, hydroethanolic and hexanic extracts from *Acmella oleracea*, solubilized with silk fibroin, against *Aedes aegypti*, Biocatal. Agric. Biotechnol. 24 (2020) 101550.

[49] A.R. Mackie, M.J. Ridout, G. Moates, F.A. Husband, P.J. Wilde, Effect of the interfacial layer composition on the properties of emulsion creams, J. Agric. Food Chem. 55 (2007) 5611–5619.

[50] A. Prins, M.A. Bos, F.J.G. Boerboom, H.K.A.I. van Kalsbeek, Relation between surface

rheology and foaming behaviour of aqueous protein solutions, Stud. Interface Sci. 7 (1998) 221–265.

[51] J.S. Li, H.T. Cheng, Studying on preperation and emulsifying properties of silk protein calcium salt made from waste silk, Adv. Mater. Res. 197–198 (2011) 60–64.

[52] E. Fröhlich, Cellular targets and mechanisms in the cytotoxic action of non-biodegradable engineered nanoparticles, Curr. Drug Metab. 14 (2013) 976–988.

[53] J.B. Unsworth, C. Corsi, J.M. Van Emon, A. Farenhorst, D.J. Hamilton, C.J. Howard, R. Hunter, J.J. Jenkins, G.A. Kleter, R.S. Kookana, J.O. Lalah, M. Leggett, K.S.B. Miglioranza, H. Miyagawa, N. Peranginangin, B. Rubin, B. Saha, N.A. Shakil, Developing global leaders for research, regulation, and stewardship of crop protection chemistry in the 21st century, J. Agric. Food Chem. 64 (2016) 52–60.

[54] J. Safari, Z. Zarnegar, Advanced drug delivery systems: Nanotechnology of health design A review, J. Saudi Chem. Soc. 18 (2014) 85–99.

[55] M. García, T. Forbe, E. Gonzalez, Potenciais aplicações de nanotecnologia no setor agro-alimentar, Cienc. e Tecnol. Aliment. 30 (2010) 573–581.

[56] Y. Singh, J.G. Meher, K. Raval, F.A. Khan, M. Chaurasia, N.K. Jain, M.K. Chourasia, Nanoemulsion: Concepts, development and applications in drug delivery, J. Control. Release. 252 (2017) 28–49.

[57] S.K. Archana Singh, Biopesticides for integrated crop management: Environmental and regulatory aspects, J. Biofertilizers Biopestic. 05 (2014) 1–3.

[58] J. Pretty, Z.P. Bharucha, Integrated pest management for sustainable intensification of agriculture in Asia and Africa, Insects. 6 (2015) 152–182.

[59] S. Gasic, B. Tanovic, Biopesticide formulations, possibility of application and future trends, Pestic. i Fitomedicina. 28 (2013) 97–102.

[60] Z.Z. Li, S.A. Xu, L.X. Wen, F. Liu, A.Q. Liu, Q. Wang, H.Y. Sun, W. Yu, J.F. Chen, Controlled release of avermectin from porous hollow silica nanoparticles: Influence of shell thickness on loading efficiency, Uv-shielding property and release, J. Control. Release. 111 (2006) 81–88.

[61] A. Ferraz, J.A. Souza, F.T. Silva, A.R. Gonçalves, R.E. Bruns, A.R. Cotrim, R.M. Wilkins, Controlled release of 2,4-d from granule matrix formulations based on six lignins, J. Agric. Food Chem. 45 (1997) 1001–1005.

[62] D. Yoo, D. Lee, Oligochitosan-stabilized photoluminescent gold nanoconstructs for optical bioimaging, Biomater. Res. 21 (2017) 1–7.

[63] S. Hofmann, C.T. Wong Po Foo, F. Rossetti, M. Textor, G. Vunjak-Novakovic, D.L.

Kaplan, H.P. Merkle, L. Meinel, Silk fibroin as an organic polymer for controlled drug delivery, J. Control. Release. 111 (2006) 219–227.

[64] E. Wenk, H.P. Merkle, L. Meinel, Silk fibroin as a vehicle for drug delivery applications, J. Control. Release. 150 (2011) 128–141.

[65] M.G. Montalbán, S. Chakraborty, J. Peña-García, H. Verli, G. Villora, H. Pérez-Sánchez, F.G. Díaz-Baños, Molecular insight into silk fibroin based delivery vehicle for amphiphilic drugs: Synthesis, characterization and molecular dynamics studies, J. Mol. Liq. 299 (2020) 112156.

[66] M.S.M. Al-Nimer, H.G. Hameed, M.M. Mahmood, Antiproliferative effects of aspirin and diclofenac against the growth of cancer and fibroblast cells: *In vitro* comparative study, Saudi Pharm. J. 23 (2015) 483–486.

[67] D.B. Khadka, D.T. Haynie, Protein- and peptide-based electrospun nanofibers in medical biomaterials, Nanomedicine Nanotechnology, Biol. Med. 8 (2012) 1242–1262.

[68] S.T. Thul, B.K. Sarangi, R.A. Pandey, Expert opinion on environmental biology nanotechnology in agroecosystem: Implications on plant productivity and its soil environment, (2013).

[69] P. Version, International Journal of Scientific and Research Publications april 2012 Edition, 2 (2012).

[70] R.L. De Oliveira, Principais mosquitos de importância sanitária no Brasil, 1994.

[71] J.B. Azevedo, Análise do ciclo biológico do *Aedes aegypti* (Diptera: Culicidae) exposto a cenários de mudanças climáticas previstas pelo IPCC (Intergovernmental panel on climate change), 2015.

[72] V.A.R. Cardoso, T.A.G. Andrade, A guerra contra um mosquito: A relação entre mídia, *Aedes aegypti* e os problemas ambientais, in: 5º Simpósio Gestão ambient. e biodiversidade, 2016.

[73] S.B. França, Síntese e avaliação da atividade larvicida de derivados do ácido cinâmico no combate ao *Aedes aegypti*, 2019.

[74] Ministério da saúde, Dengue instruções para pessoal de combate ao vetor: manual de normas técnicas, Ministério da saúde: Fundação Nacional de Saúde, 3º ed, Brasília, 2001.

[75] R.C. Catão, Dengue no Brasil: Abordagem geográfica na escala nacional, Cultura acadêmica, São Paulo, 2012.

[76] T.N. Lima-Camara, Emerging arboviruses and public health challenges in Brazil, Rev. Saude Publica. 50 (2016) 1–7.

[77] N. Lopes, C. Nozawa, R.E.C. Linhares, Características gerais e epidemiologia dos

arbovírus emergentes no Brasil, Rev. Pan-Amazônica Saúde. 5 (2014) 55–64.

[78] C. V. Tikhe, G. Dimopoulos, Mosquito antiviral immune pathways, Dev. Comp. Immunol. 116 (2021) 103964.

[79] M.A. Esmeraldo, Bioprodutos derivados de biomassa vegetal no combate ao mosquito transmissor da dengue - *Aedes aegypti*, 2016.

[80] J.E. Smith, L. Noctuidae, E.M. Duas, G.R. Busato, A.D. Grützmacher, M.S. Garcia, F.P. Giolo, S.D. Nörnberg, Consumo e utilização de alimento por *Spodoptera frugiperda*, Neotrop. Entomol. 31 (1995).

[81] E. Brasileira, P. Agropecuiiria -Embrapa, V. Ministério Da Agricultura, I Circular técnica a lagarta-do-cartucho na cultura do milho, (1995).

[82] I. Zepeda-Jazo, Sustainable management of agricultural pest in México, Agric. Soc. y Desarro. 15 (2017) 99–108.

[83] G.M. Pogue, A world revision of the genus *Spodoptera* (Guenée) Lepidoptera: Noctuidae. Memoirs of the American Entomological Society, 43: 1-201, 2002.

[84] J.L. Capinera, Southern armyworm, eridania (Cramer) (Insecta: Lepidoptera: Noctuidae). Florida: University of Florida, (1999).

[85] R.G. Luttrell, J.S. Mink, Damage to Cotton Fruiting Structures by the Fall Armyworm, *Spodoptera frugiperda* (Lepidoptera: Noctuidae), 44 (1999) 35–44.

[86] I. Cruz, M.A.R. Monteiro, Controle biológico da lagarta do cartucho do milho *Spodoptera frugiperda* utilizando o parasitóide de ovos *Trichogramma pretiosum*. Sete Lagoas: Embrapa Milho e Sorgo, 2004.

[87] L.M.Q. Ruiz, Uso de baculovirus como alternativa de control biologico de *Spodoptera frugiperda* en el cultivo del maiz: una revisión conceptual y de avnces en su aplicación. Tese (Mestrado) - Universidad Abierta y a Distancia, 2015.

[88] R.A. Carvalho, C. Omoto, L.M. Field, M.S. Williamson, C. Bass, Investigating the molecular mechanisms of organophosphate and pyrethroid resistance in the fall Armyworm *Spodoptera frugiperda*, 8 (2013).

[89] P. Roberto, S. Pereira, Pragas da lavoura de trigo, (2009).

[90] J.C.L. Barboza, Controle de *Helicoverpa armigera* (Hübner) (Lepidoptera: Noctuidae) na cultura da soja com diferentes inseticidas, volumes e pontas de pulverização. Dissertação (Mestrado) – Faculdade de Engenharia de Santa Maria, Universidade Federal de Santa Maria, 2015.

Artigo 1

Artigo publicado no periódico **Journal of Drug Delivery Science and Technology** (ISSN 2588-8943) Qualis A3 em biotecnologia, segundo a classificação do quadriênio 2017-2020 da plataforma Sucupira – CAPES

Development of an environmentally friendly formulation of silk fibroin combined with fatty acid from *Astrocaryum murumuru* Mart. effective against *Aedes aegypti* larvae

Victor H. S. Marinho[a], Fernando B. Neves [a], David E. Q. Jimenez[a], Fabio R. Oliveira[b], Abrahão Victor T. L. T. Santos[c], Ricardo M. A. Ferreira[d], Raimundo N. P. Souto[d], José C. T. Carvalho[c], Sérgio A. Yoshioka[e], Irlon M. Ferreira[a,*]

[a]Biocatalysis and Applied Organic Synthesis Laboratory, Federal University of Amapá, Campus Universitário Marco Zero do Equador, Rodovia Juscelino Kubitschek de Oliveira Km 02, Bairro Zerão, 68902-280, Macapá, AP, Brazil.

[b]Laboratory of Quality Control and Bromatology, Federal University of Amapá, Campus Universitário Marco Zero do Equador, Rodovia Juscelino Kubitschek de Oliveira Km 02, Bairro Zerão, 68902-280, Macapá, AP, Brazil.

[c]Drug Research Laboratory, Federal University of Amapá, Campus Universitário Marco Zero do Equador, Rodovia Juscelino Kubitschek de Oliveira Km 02, Bairro Zerão, 68902-280, Macapá, AP, Brazil.

[d]Artropod Laboratory, Federal University of Amapá, Campus Universitário Marco Zero do Equador, Rodovia Juscelino Kubitschek de Oliveira Km 02, Bairro Zerão, 68902-280, Macapá, AP, Brazil.

[e]Biochemistry and Biomaterials Laboratory, Institute of Chemistry of São Carlos, University of São Paulo, Universidade de São Paulo, Av. Trabalhador São-Carlense 400, 13560-970, São Carlos, SP, Brazil.

*Corresponding author: irlon.ferreira@gmail.com / orcid.org/0000-0002-4517-0105

Abstract

The *Aedes aegypti* mosquito is a vector of several diseases, including dengue, yellow fever and the Zika virus. Synthetic insecticides such as chlorpyrifos and chlorothalonil have been used to control this vector, despite causing damage to both the environment and humans. Research into natural active compounds with a low environmental impact is therefore required. The present study developed an environmentally friendly formulation of silk fibroin (SF) combined with fatty acid esters [ethyl (FAEE-SF), propyl (FAPE-SF) and butyl (FABE-SF)] from *A. murumuru* fat, which was effective against larvae of the *Ae. aegypti* vector. The FABE-SF nanoparticle induced a higher mortality rate in *Ae. aegypti* larvae after 48 h (LC_{50} = 21.35 μg.mL^{-1}). The stability of the nano was monitored for 21 days, and FABE-SF exhibited greater stability throughout this period, with average particle, zeta and PDI values of around 217.5 ± 0.85 nm, -25.6 ± 3.24 mV and 0.338 ± 0.01, respectively. This is the first work of its type to identify the larvicidal activity of fatty acid esters from *A. murumuru*, combined with silk fibroin, against *Ae. aegypti*.

Keywords: Nanoparticles; Silkworm cocoon; Larvicidal activity; Biomaterial; Biopesticide; Fatty acid esters.

2.1 INTRODUCTION

The effective and sustainable control of mosquito population vectors of diseases is a challenging task [1,2]. For many years, the control of such populations has involved the use of various synthetic insecticides, such as organochlorines, organophosphates and pyrethroids [3]. However, the indiscriminate and frequent use of such substances has caused selected populations of mosquitoes to become more resistant, as well as resulting in environmental pollution from their non-selective inhibitory enzymatic actions [4], putting humans and other non-target populations at risk [5]. An effective low-cost insecticide with a lower environmental risk is therefore required [1,2].

There is a growing demand for biopesticides, since certain plant species contain a variety of bioactive compounds with insecticidal properties [1]. Fat extracted from the fruits of *A. murumuru*, for example, is a potentially effective biopesticide for vector control. *A. murumuru* fat is easily obtained, as the species is widely distributed around the Amazon estuary. Its natural fat is used as a raw material in the cosmetics and food industries, as its composition contains saturated fatty acids such as lauric and myristic acid [6]. Although the larvicidal, insecticidal, and repellent action of fatty acids against mosquitoes has been widely reported in literature [7–9], there are few studies on the effects of natural products used as larvicidal agents against insects [10].

Nanoparticles are widely used drug delivery systems, nanoparticles formulated from copolymers and proteins have become a viable alternative to improve the dispersion of essential or fixed oils in aqueous vehicles, as mosquitoes and other disease vectors require an aqueous environment for their life cycle [11]. There is a growing interest in the production of protein-based nanoparticulate systems due to their unique functionalities, protein-based carriers are biodegradable, non-antigenic and have excellent biocompatibility [12]. The different functional groups of proteins can trigger a biological response to cells, as the surface of nanoparticles can be modified by the covalent binding of drugs and ligands to increase therapeutic efficiency [13].

Silk fibroin is a natural polymer produced by insects and spiders, and therefore offers highly diverse sequences, structures, and properties [14]. The study of silks started from the cocoon of the domesticated silkworm *Bombyx mori* and the spider *Nephila clavipes* [15]. Silk fibroin is a natural amphiphilic block of hydrophobic and hydrophilic co-polymers that mix together, giving it flexibility and robustness [14,16]. Furthermore, fibroin is used in tissue engineering, and in the delivery system of bioactive compounds, such as drugs, peptides and

proteins [17,18], and in a variety of biomaterials, such as nanoparticles, nanospheres, hydrogels and films [19].

In the last decade, nanotechnology has been applied in a wide range of different areas such as medicine, electronics, catalysis and agriculture [20]. Nanopesticides or nanoformulations involving thin films or encapsulation of the active ingredient of the pesticide in nanostructures have emerged, the main advantage of which is the slow and controlled release of their active ingredients [21], which makes them environmentally safer and non-hazardous in comparison with chemical pesticides [22]. In this context, researchers have developed different types of nanopesticides, such as nanoencapsulated formulations, nanoemulsions, nanogels, and nanospheres [23]. In this way, nanoparticles can help in the production of new pesticides, insecticides and repellents [24]. With this, nanotechnology can revolutionize insect management, providing innovative tools for the controlled and safe delivery of pesticides [25].

Our research group has been investigating biopesticides using silk fibroin as a vehicle for drug delivery. Araújo [26] evaluated the larvicidal action of the hydroethanolic, methanolic, and hexane extracts of *Acmella oleracea* leaves solubilized in silk fibroin (2%), while Sarquis [27] reported the activity of free fatty acids from *Carapa guianensis* Aubl oil combined with silk fibroin against *Ae. aegypti* larvae, and found an LC_{50} of 16.7 $\mu g.mL^{-1}$ after 48 h.

Therefore, continuing the study about silk protein as a vehicle for active larvicides, the present study aimed to evaluate the preparation of potentially sustainable, stable, and low-cost larvicidal nanoparticles containing fatty esters from *A. murumuru* fat combined with silk fibroin solution.

2.2 MATERIAL AND METHODS

2.2.1 Reagents and solvents

The fat of *A. murumuru* Mart. was purchased from Aspacs (Amazonas, Brazil). Ethanol (99.5%) was purchased from Solven (São Paulo, Brazil), and isopropanol (99.5%) and butanol (99.5%) were purchased from Quimex (São Paulo, Brazil). The solvents *n*-hexane (98.5%) and ethyl acetate (98%), used in the purification of the esters by column chromatography, were obtained from Synth (São Paulo, Brazil). The Amano AK Lipase from *Pseudomonas fluorescens* (20.000 U/g) was purchased from Sigma-Aldrich (São Paulo, Brazil) and fatty acid standards (Lauric, Myristic, Oleic and Stearic) were purchased from Sigma-Aldrich (São Paulo, Brazil).

2.2.2 Synthesis of ethyl, isopropyl and butyl esters of *A. murumuru* Mart. fat catalyzed by Amano AK lipase from *Pseudomonas fluorescens*

The enzymatic transesterification of the fat was performed separately for the ethyl, isopropyl and *n*-butyl alcohols to generate the respective esters (FAEE, FAPE and FABE), as described by Ferreira [28] with some modifications.

Transesterification was performed in a 50 mL reaction flask containing 1.0 g of fat, 3 mL of respective alcohol and 0.1 g (10%) of Lipase from *Pseudomonas fluorescens*. The reaction mixtures were magnetically stirred for 24 h at room temperature. Afterwards, the reaction solutions were filtered, the organic phases were dried with anhydrous sodium sulfate and filtered, and the solvents were removed by vacuum under reduced pressure. The products were purified by silica gel column chromatography, with the mobile phase involving a mixture of *n*-hexane and ethyl acetate (9:1). The isolated products were characterized by their spectroscopic data (GC-MS and FTIR).

2.2.3 Preparation of ethyl ester of lauric, myristic, oleic and stearic acids

First, the esters of oleic, myristic, stearic and lauric acids were prepared by enzymatic catalysis to be employed as standards in GC-MS. Transesterification was performed in a 25 mL reaction flask containing 1.0 g of respective acids, 3 mL of ethanol and 0.1 g (10%) of Lipase from Pseudomonas fluorescens. The reaction remained under agitation for 48h and the reaction was monitored by thin-layer chromatography (TLC). The mixture was dried with anhydrous Na_2SO_4 and purified by flash chromatography with silica gel as the stationary phase, and n-hexane:ethyl acetate (9:1) as the eluent. The products were characterized by CG-MS analysis and retention time was compared with the chromatographic profile of the fatty ethyl esters by the transesterification of *A. murumuru* fat (Supplementary Information).

2.2.4 Gas chromatography-mass espectrometry (GC-MS)

The samples (FAEE, FAPE and FABE) were analyzed by gas chromatography mass spectrometry (GC-MS). These analyses were performed in a Shimadzu GC2010 system with a mass selective detector (Shimadzu MS2010plus) in electron ionization mode (EI, 70 eV) and equipped with a 30m×0.25mm×0.25µm RTX-5MS column. The GC–MS conditions were: an oven temperature starting at 130 °C and remaining at this temperature for 2 min, increasing to 290 °C at 5 °C min^{-1}, and maintained for 2 min. The total analysis time was 36 min. The injector

and detector temperature were maintained at 210 ºC; 1 µL of sample was injected with 1:15 split, and helium was used as the carrier gas at a 1.0 mL min^{-1} flow rate. The ions were monitored from 3 to 36 min in the *m*/*z* 40–500. The components present in the samples were identified through comparison of spectral data with those in the Wiley library.

2.2.5 Infrared spectroscopy analysis

A Fourier transform infrared spectrophotometer (Shimadzu FTIR IRTracer-100) recorded the FAT (*A. murumuru*), FAEE, FAPE and FABE spectra using a potassium bromide beam splitter. The KBr pellet method was employed and the background spectrum was collected. The range was set from 400 to 4000 cm^{-1} with 16-cm^{-1} resolution.

2.2.6 Diferential scanning calorimetry (DSC)

Differential scanning calorimetry was performed using DSC-60 plus equipment (Shimadzu, Kyoto, Japan). Sample (5 mg) was placed in a closed aluminum pan and subjected to heating rate of 10 °C min^{-1} to a temperature of 100 °C with nitrogen atmosphere at 50 cm^3 min^{-1} as described by Gabbay [29].

2.2.7 Preparation of the silk fibroin solution

The silk fibroin solution was prepared based on the method developed by Maciel [30]. Silkworm cocoons (3.0 g, from Bratac, Brazil) were degummed in a boiling (2%) (w/v) Na_2CO_3 solution for 30 min. The resultant fibers were filtrated and washed with distilled water (3 x 500 mL). Subsequently, silk fiber were dissolved in a ternary solution (50 mL) of H_2O:EtOH:$CaCl_2$ (8:2:1 molar proportions) at 30 ºC for 4 h. This mixture was then dialyzed (cellulose tube with an exclusion limit of 16 kDa, from Viskase, Brazil) for 3 days at room temperature, and the water was changed every 24 h. The fibroin solution was centrifuged (6000 rpm for 10 min) to remove impurities and larger particles. The concentration of the silk fibroin solution was adjusted to 2% (w/w).

2.2.8 Preparation of ester/silk fibroin nanoparticles

The nanoparticles (FAEE-SF, FAPE-SF and FABE-SF) were produced by the emulsification process. In summary, deionized water was added to esters (FAEE, FAPE or FABE) and the silk fibroin solution (2%). The 10 mL solution contained 94% silk fibroin

solution (2%), 1% active compounds and 5% of a mixture of ethanol and isopropanol (1:1). The nanoparticles were prepared based on Sarquis [27] with slight modifications.

Initially, a mixture of ethanol and isopropanol was added to the esters (FAEE, FAPE or FABE) under constant magnetic agitation (300 rpm) for 30 min. Next, the aqueous phase containing a silk fibroin solution was added with continuous agitation for 5 min in a vortex.

Nanoparticles were stored at refrigerator temperature (4 °C) and drying oven (32 °C) evaluated from 1 to 21 days after preparation. The droplet size, polydispersity index and zeta potential of the nanoparticles were determined using a ZS zetasizer (Malvern, United Kingdom). Each sample was diluted with distilled water (1:10) to avoid multiple scattering effects, in accordance with Anarjan and Tan [31]. Measurements were taken in triplicate. The average droplet size was expressed in mean diameter. All analyzes were performed at 25 ºC.

2.2.9 Larvicidal activity

Nanoparticles of silk fibroin combined with esters (FAEE-SF, FAPE-SF and FABE-SF) were prepared at different concentrations (7.5, 15, 25, 50 and 75 µg.mL^{-1} from a stock solution of 10.000 µg.mL^{-1}) for the larvicidal tests in *Ae. aegypti*. Five replicates with 10 larvae each were performed. The negative control consisted of the silk fibroin solution without the asset, and a dichlorvos solution (6.25 ng.mL^{-1}) was used as the positive control. The larval mortality rate was determined after 24 h and 48 h of incubation at a temperature of 25 ºC and a humidity of 75%. The larvae were considered dead when they did not respond to any stimulus or did not move on the surface of the solution, in comparison with those observed in the control. The bioassay was conducted according to WHOPES [32].

2.2.10 Morphological analysis on larvae

After treatment, the larvae were fixed in 10% formalin. Their external morphology was then analyzed under an optical microscope and photographed using a digital camera (MDCE - SC USB 2.0) with the ScopeImage 9.0 software package.

2.2.11 Statistical analysis

Probit analysis was performed with a 95% confidence interval to determine the lethal concentrations (LC_{50} and LC_{90}), and the Chi-squared test was performed using the Statgraphics Centurion XV version 15.2.11 software package (Statpoint Technologies, Inc., Warrenton, VA). If the control mortality of the treated groups was between 5% and 20%, the analysis was

corrected in accordance with the formula *mortality (%)* = $X - Y/X \times 100$, where X = percentage survival in the untreated control group and Y = percentage survival in the treated sample [32].

2.3 RESULTS AND DISCUSSION

2.3.1 Composition profile of fatty acid of *A. murumuru* fat

The transesterification reaction of *A. murumuru* fat with ethanol, isopropanol and *n*-butanol using Amano AK lipase from *P. fluorescens* provided a fatty acid ethyl ester (FAEE) percentage of 78.4%, a fatty acid propyl ester (FAPE) percentage of 75.1% and a fatty acid butyl ester (FABE) percentage of 63.5%, after purification in a chromatographic column with silica gel.

The gas chromatographic analysis of FAEE from *A. murumuru* revealed a composition formed of saturated, monounsaturated, and polyunsaturated fatty acids (Table 2.1 and Fig. 2.1). However, the highest saturated fatty acid percentage in *A. murumuru* fat from the present study was 95.5%, with the predominant presence of lauric acid (C12:0) and myristic acid (C14:0), at 53.5% and 25.8%, respectively. Other saturated fatty acids, such as stearic (C18:0), capric (C10:0) and caprylic (C8:0) acids, were also present in *A. murumuru* fat, in smaller proportions (Table 2.1). From the unsaturated fatty acid, oleic (C18:1) and linoleic (C18:2) acid were identified, at 3.8% and 0.7%, respectively. Due to a high short-chain fatty acid content, this fat is used in the food industry to make margarine [33]. The chromatographic profile of the compounds found in the samples were compared with the spectral data of those presented in the Wiley library, and exhibited high levels of similarity.

The proportion of polyunsaturated/saturated fatty acids (P/S) of the *A. murumuru* fat used was 0.007. Other studies have indicated higher P/S indexes for *A. murumuru* fat. Pereira [34] identified the fatty acid composition of *A. murumuru* and found lauric acid as the main constituent with a relative abundance of (47.6%) and a P/S index of 0.04.

Table 2.1. Fatty acid composition (%) of *A. murumuru* fat by GC-MS analysis.

Fatty acid	Peak	Time (min)	Relative Concentration (%)[c]
Caproic (C6:0)	1	3.63	1.73
Caprylic (C8:0)	2	6.54	2.40
Lauric (C12:0)	3	10.11	53.51
Myristic (C14:0)	4	13.63	25.79
Palmitic (C16:0)	5	16.92	8.59
Linoleic (C18:2)	6	19.51	0.66
Oleic (C18:1)	7	19.59	3.88
Stearic (C18:0)	8	19.96	3.45
Total Saturated	-	-	95.47
Total Monounsaturated	-	-	3.88
Total Polyunsaturated	-	-	0.66

*Percentage of FAEE corresponding fatty acid; [b]MS database (NIST 5.0).

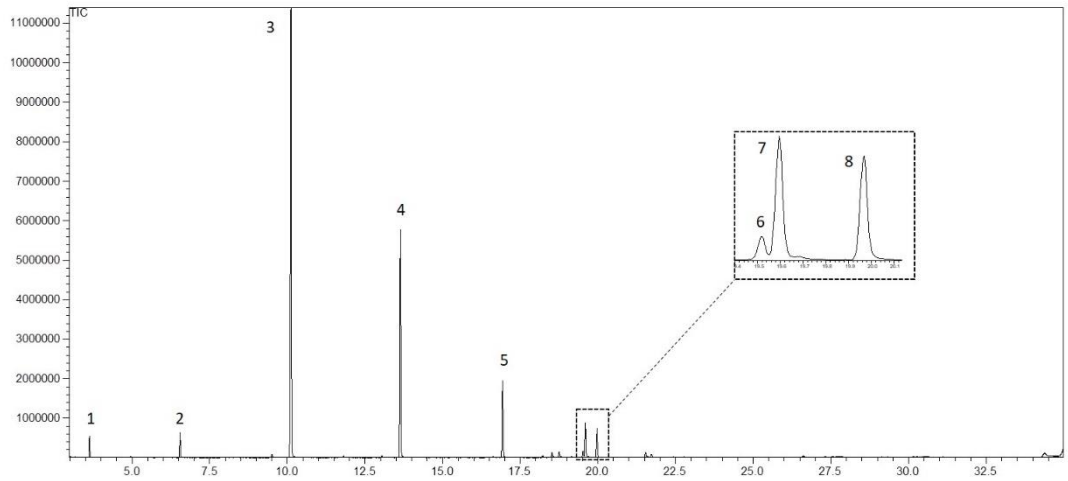

Fig. 2.1. Fatty ethyl ester compositions of *A. murumuru* fat, determined by GC-MS analysis. Caproic (1); Caprylic (2); Lauric (3); Myristic (4); Palmitic (5); Linoleic (6); Oleic (7); Stearic (8) acid.

The FTIR spectra (Fig. 2.2) for the three esters obtained from *A. murumuru* revealed evidence of the formation of esters, including a C–H stretching vibration in the 2950-2853 cm^{-1} region for the presence of unsaturated and saturated carbons. Stretching bands C=O at 1740 cm^{-1} are related to carbonyl group vibration, and bands characteristic of unsaturated esters were

observed, such as C–C–O at 1164 cm^{-1} [35]. A stretching vibration C=C in the region of 1655-1686 cm^{-1} provided evidence of the presence of unsaturated carbons. C–H asymmetric angular stretching bands were observed at 1466-1371 cm^{-1} and O–C–C stretching bands in the region of 1113-1111 cm^{-1}.

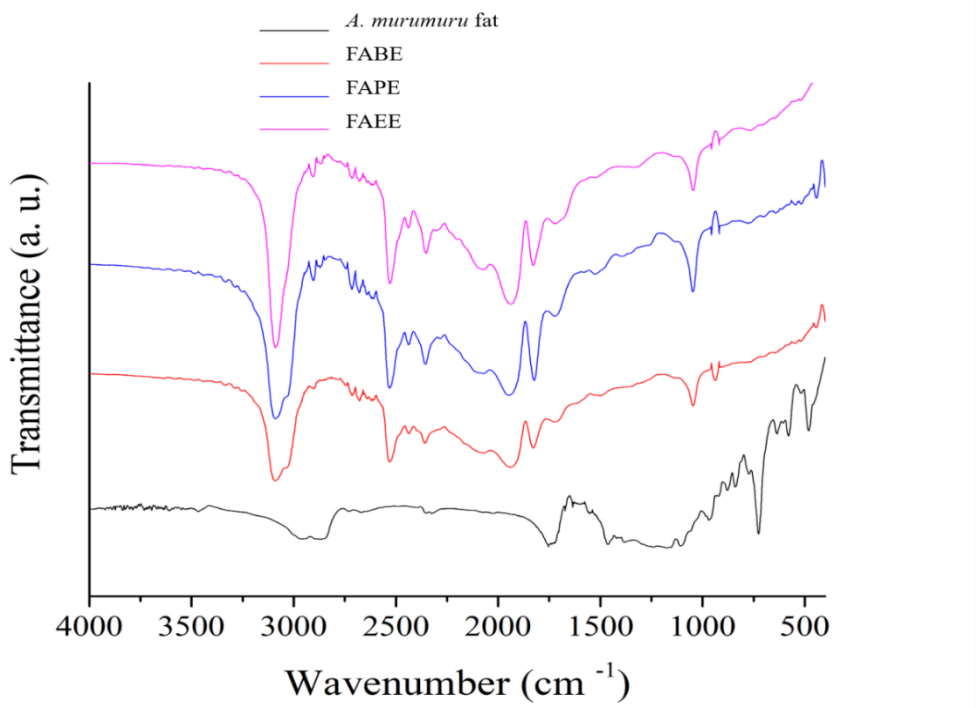

Fig. 2.2. FTIR spectra of *A. murumuru* fat and derivatives esters (FAEE, FAPE and FABE).

2.3.2 Preparation and study of silk fibroin/esters nanoparticles

Dynamic light scattering (DLS) analysis to verify the particle size distribution of formulations (FAEE-SF, FAPE-SF and FABE-SF) were recorded at the beginning of the experiment and every 7 days during storage (Table 2.2). The size of all the nanoparticles prepared was satisfactory (Fig. 2.3), and no phase separation was observed in the formulation during storage at 4 ºC for 21 days, showing that silk protein can play an important role in the stability of the lipid particles from the conjunct of fatty acid esters.

The stability of the nanoparticles of silk fibroin combined with esters is based on a number of factors, including: 1) the fact that silk fibroin is an amphiphilic polymer with large hydrophobic domains, interrupted by small hydrophilic spacers, and the N and C-termini of the chains are also highly hydrophilic [36]. Therefore, the amphiphilicity of the chain organization is likely to play a significant role in the stability of the nanoparticles; and 2) the viscosity of the aqueous phase increases with the addition of the silk fibroin solution, which may have inhibited

droplet aggregation and gravitational separation [37]. This favors Brownian motion and inhibits flocculating and coalescing [38,39].

2.3.3 Short-term stability study

The results of the present study revealed that the stability of the mixture depended on the fatty acid ester type present in the sample. For FABE-SF, the particle diameter was smaller (215.5 ± 1.57 nm and 217.5 ± 0.85 at 0 days on the 21st day, respectively) than the particle size of nanoparticles formed from fatty acid esters with propanol and ethanol [274.06 ± 2.41 nm (0 days) and 702.5 ± 92.43 nm (0 days), respectively] (Table 2.2). Alcohols, like ethanol, induce fibroin to transform into a Silk II crystalline [40]. However, a reduction in the particle size was observed, which was significant in the case of the FAEE-SF nanoparticle, starting at 702.5 (± 92.43) nm (0 day) and reducing to 229.4 (± 8.31) nm (21st day). It is therefore believed that the relationship between the ester structures can influence the particle diameter in the case of a nanoparticle formed by ethanol, propanol, and butanol fatty acid esters from *A. murumuru* fat (fatty acid mixture).

The polydispersity index (PDI) indicates the homogeneity and stability of the size of the particles distributed in the nanoparticles. PDI values of around 0.3 or below indicate a more homogeneous size distribution of the particles dispersed in the nanoparticles [41]. FABE-SF had a good PDI value, ranging from 0.320 (± 0.03) to 0.338 (± 0.01), while FAPE-SF had a PDI value ranging from 0.452 (± 0.02) to 0.415 (± 0.04), and FAEE-SF a PDI value of 0.709 (± 0.08) to 0.396 (± 0.03). One notable finding was the reduction in the PDI values of the FAEE-SF and FAPE-SF nanoparticles on the 21st day, to 0.396 and 0.415, respectively (Table 2.2). The results of the present study indicate that the elongation of the ester carbon chain (-Ethyl; -Isopropyl and -*n*-Buthyl) influenced the thermodynamic balance of the phases. Factors such as the spontaneous diffusion and evaporation of volatile material from the internal phase have been observed as a mechanism for reducing particles size [42].

Zeta potential is the electrostatic potential at the slipping plane a few molecules away from the surface [43]. For the nanoparticles to be considered stable by electrostatic repulsion alone, a zeta potential value ± 20 is required [44]. The nanoparticles exhibited zeta potential values between -53.9 mV (±4.50) and -25.6 mV (±3.24) on all 21 days of monitoring. The FAEE-SF nanoparticle exhibited zeta values between -53.9 mV (±4.50) and -33.3 mV (±0.65), while FAPE-SF obtained values between -46.4 mV (±5.31) and -34.9 mV (±3.84) and FABE-SF exhibited zeta values between -43.6 mV (±5.42) and -25.6 mV (±3.24) (Table 2.2). The

stability of a polymer is important for the storage of a drug delivery device. The stability of these nanoparticles may be related to the improved balance between the dissociation of the propyl and butyl esters with the carboxylic and amino groups present in silk fibroin, resulting in a slight variation in the zeta potential of these nanoparticles, making them more stable. Electrophoretic mobility experiments have demonstrated that SF was positively charged below pH 3.9 and negatively charged above pH 3.9 [45], which is its pI (isoelectric point = 3.9).

Table 2.2. Particle size distribution, PDI and Zeta of nanoparticles prepared with silk fibroin and esters.

Fatty acid ester	Time (days)	Size (nm)	PDI	Zeta (mV)
 FAEE-SF	0	702.5 (±92.43)	0.709 (±0.08)	-53.9 (±4.50)
	7	512.9 (±152.35)	0.528 (±0.15)	-40.4 (±0.76)
	14	315.7 (±5.96)	0.415 (±0.01)	-33.6 (±6.20)
	21	229.4 (±8.31)	0.396 (±0.03)	-33.3 (±0.65)
 FAPE-SF	0	274.06 (±2.41)	0.452 (±0.02)	-46.4 (±5.31)
	7	293.3 (±20.43)	0.419 (±0.02)	-38.4 (±0.78)
	14	293.5 (±11.50)	0.439 (±0.02)	-30.7 (±2.94)
	21	280.5 (±14.16)	0.415 (±0.04)	-34.9 (±3.84)
 FABE-SF	0	215.5 (±1.57)	0.320 (±0.03)	-43.6 (±5.42)
	7	248.9 (±6.25)	0.419 (±0.02)	-46.0 (±2.21)
	14	235.3 (±8.73)	0.366 (±0.02)	-29.5 (±1.85)
	21	217.5 (±0.85)	0.338 (±0.01)	-25.6 (±3.24)

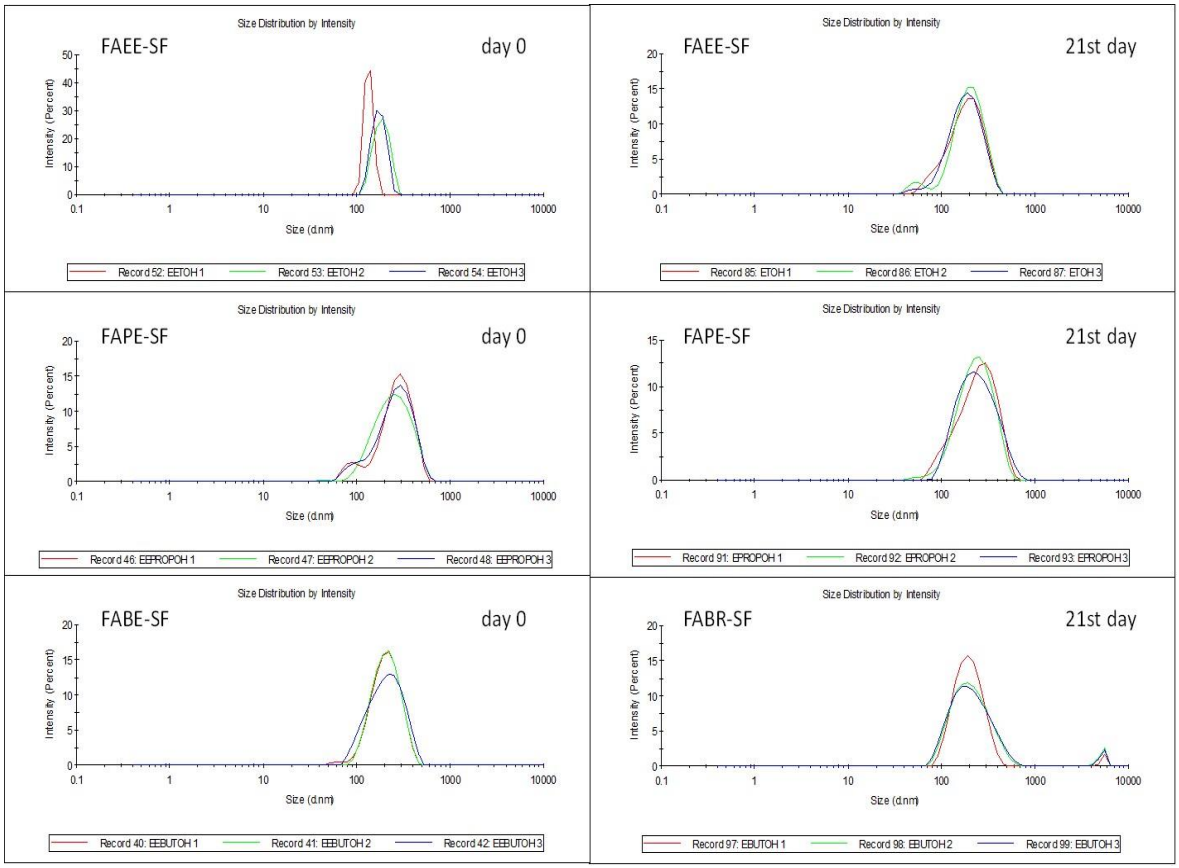

Fig. 2.3. Average particle size – FAEE-SF; Day 0: 702.5 ± 92.43 nm; Day 21: 229.4 ± 8.31 nm; FAPE-SF; Day 0: 274.06 ± 2.41 nm; Day 21: 280.5 ± 4.16 nm; FABE-SF; Day 0: 215.5 ± 1.57 nm; Day 21: 217.5 ± 0,85 nm.

In the present study, the storage stability of the FABE-SF nanoparticle was determined by comparing the zeta size, PDI and zeta potential values at 4 °C and 32 ºC. As shown in Fig. 2.4, were no significant changes in the particle size, PDI, zeta potential and visual appearance of the FABE-SF after 21 days of testing at 4 °C and 32 ºC. Thus, the optimized formulation FABE-SF can also be considered a stable system at the temperatures studied.

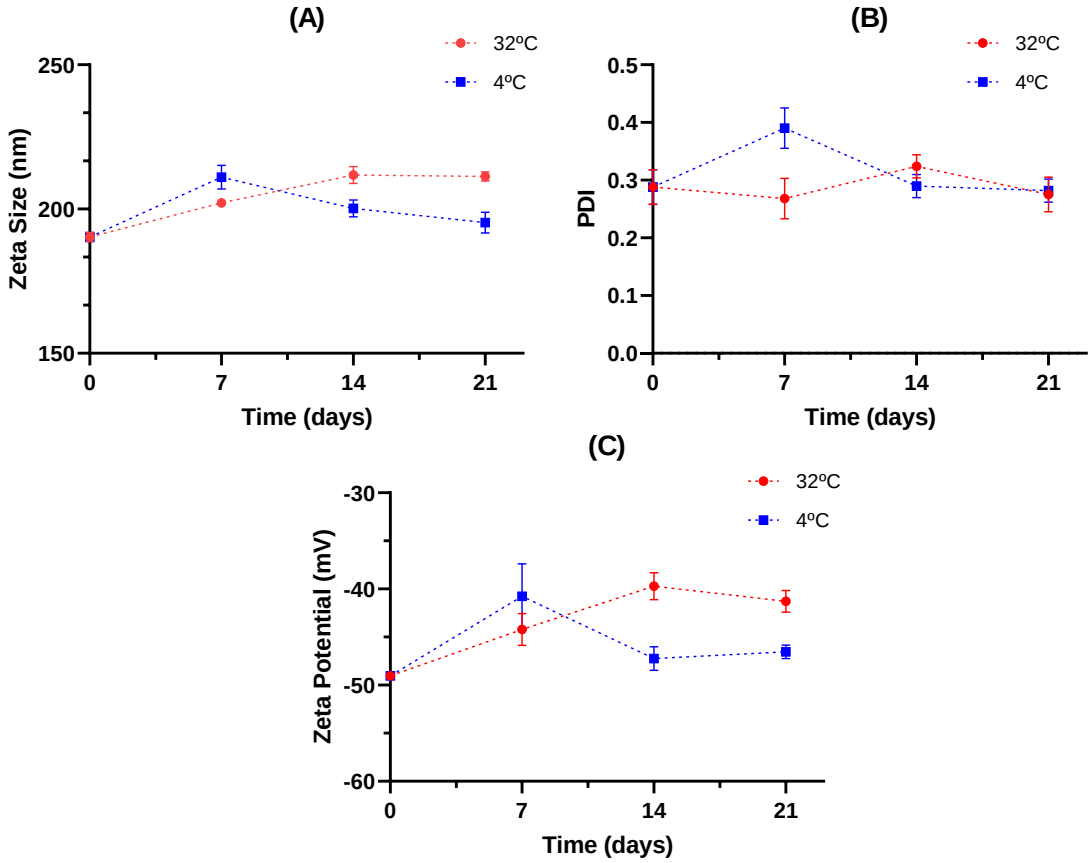

Fig. 2.4. (A) Particle size (nm); (B) polydispersity index (PDI); and (C) zeta potential (mV) of the nanoparticles from the first to the 21th day of preparation for FABE-SF at 4 °C and 32ºC.

2.3.4 Analysis of differential scanning calorimetry (DSC)

The DSC analysis showed that the prepared nanoformulations are silk fibroin nanoparticles combined with fatty acid esters. Analysis of the DSC curve for the FABE-SF nanoformulation exhibited a prominent peak at 185 °C, a steep slope and an exothermic peak at 230 °C indicating a thermal transformation from silk I to silk II. Furthermore, a small shift is perceived at 274 °C indicating the thermal stability of the silk II conformation in the nanoparticles (Fig. 2.5).

Pham [46] found similar results when developing crosslinked silk fibroin nanoparticles, the DSC curves of the formulations showed the silk II conformation, with the absence of the peak at 230 ºC, as well as a slight displacement of decomposition of the peak at 285 ºC indicating the thermal stability of the silk II conformation in the nanoparticles.

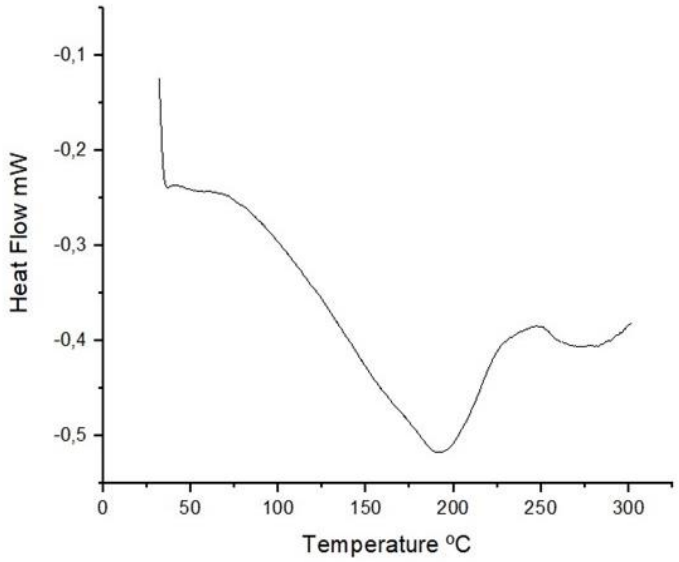

Fig. 2.5. DSC curve of silk fibroin nanoparticle combined with *A. murumuru* butyl ester (FABE-SF).

2.3.5 Larvicidal activity from nanoparticles of silk fibroin combined with esters

The choice of solvents of a formulation is essential for determining larvicidal activity in an aqueous medium. Initially, we evaluated the effect of the fatty esters solubilized in DMSO (5%), and the nanoparticles of silk fibroin combined with fatty esters, at concentrations of 25 and 75 µg.mL^{-1} (Table 2.3). The results were then obtained after 24 h against *Ae. aegypti* III instar larvae.

At the concentrations of 25 and 75 µg.mL^{-1} tested, the results showed that all the fatty acid esters (FAEE, FAPE and FABE) from *A. murumuru* fat combined with silk fibroin had greater larvicidal activity against the mosquitoes than fatty acid esters in DMSO (Table 2.3). The FAPE-SF and FABE-SF nanoparticles, for example, exhibited 92% mortality at a concentration of 75 µg.mL^{-1}, while the FAEE-SF nanoparticle yielded a mortality rate of 68% at the same concentration. This result highlights the loading capacity of the fibroin formulation and its positive impact on biological activity. It is likely that nanoparticles interact inside the larva cells, leading to more rapid death than with the DMSO solution, due to changes in active release kinetics (Table 2.4). Additionally, hydrophobic interactions were found to be the main cause of interactions between SF and the fatty acid esters from *A. murumuru* fat. Similarly, Sarquis [27] reported that a nanoemulsion containing 75% silk fibroin solution 2%, 5% fatty acid from *C. guianensis* Aubl. and 24% ethanol was effective against *Ae. aegypti* (III instar larvae) with LC_{50} values of 94.45 µg.mL^{-1} at 24 h and 16.79 µg.mL^{-1} at 48 h.

The use of silk fibroin in the nanoparticles system has a number of advantages, including the biodegradation process, which occurs via enzymatic degradation, the production of non-

toxic by-products, and the controllable degradation rate, which set it apart from other synthetic or natural polymers [47].

Table 2.3. Comparison of the larvicidal activity of the nanoparticles (FAEE-SF, FAPE-SF and FABE-SF) and in 5% DMSO.

Larvicidal active agent	Time (hours)	% Mortality 75 µg/mL	% Mortality 25 µg/mL
FAEE-SF	24 h	68 (±2.19)	54 (±1.09)
FAPE-SF		92 (±0.89)	28 (±0.89)
FABE-SF		92 (±0.89)	52 (±0.89)
FAEE-DMSO		28 (±0.83)	6 (±0.54)
FAPE-DMSO		70 (±2)	6 (±1.09)
FABE-DMSO		70 (±2)	6 (±1.09)
FAEE-SF	48 h	98 (±0.89)	78 (±0.89)
FAPE-SF		94 (±1.09)	52 (±0.89)
FABE-SF		100 (±0)	66 (±1.09)
FAEE-DMSO		34 (±1.09)	6 (±1.09)
FAPE-DMSO		70 (±2)	8 (±0.89)
FABE-DMSO		76 (±3.03)	8 (±1.09)

In view of the preliminary results, other concentrations were tested to determine the LC_{50} and LC_{90} values of nanoparticles against *Ae. aegypti* larvae at 24 and 48 h.

Among the nanoparticles, FABE-SF exhibited the highest mortality rate after 24 h, of 92% at 75 µg.mL^{-1} and 4% at 7.5 µg.mL^{-1}, the lowest concentration tested. At 48 h, the mortality rate was 100% at 75 µg.mL^{-1} and 20% at 7.5 µg.mL^{-1} (Fig. 2.6A and 2.6B). In contrast, a negative control consisting solely of fibroin solution exhibited no larvicidal action. This result demonstrates the lack of toxicity of the fibroin solution against *Ae. aegypti*.

Table 2.4. LC_{50} and LC_{90} values for *Ae. aegypti* in contact with the nanoparticles (FAEE, FAPE and FABE) and in 5% DMSO.

	24 hours				48 hours			
	LC_{50} (µg.mL^{-1}) (LCL-UCL)	LC_{90} (µg.mL^{-1}) (LCL-UCL)	X^2 (df=4)	P	LC_{50} (µg.mL^{-1}) (LCL-UCL)	LC_{90} (µg.mL^{-1}) (LCL-UCL)	X^2 (df=4)	P
FAEE-SF	45.42 (40.25 – 51.48)	83.56 (74.15 – 97.11)	48.9534	0.000	21.28 (18.33 – 24.53)	41.26 (36.44 – 48.14)	85.0352	0.000
FAPE-SF	40.29 (36.41 – 44.61)	64.69 (58.76 – 72.65)	8.7489	0.068	31.28 (27.58 – 35.39)	57.02 (51.03 – 65.25)	15.7390	0.003
FABE-SF	32.00 (27.62 – 36.80)	65.61 (58.00 – 76.43)	32.7666	0.000	21.35 (17.99 – 24.94)	45.52 (39.87 – 53.81)	20.0456	0.000
FAEE-DMSO	94.96 (80.31 – 122.95)	142.08 (116.35 – 196.57)	2.74536	0.253	87.63 (75.65 – 108.17)	130.49 (109.53 – 171.37)	2.34280	0.310
FAPE-DMSO	63.01 (56.45 – 70.42)	91.16 (82.08 – 10.66)	0.90610	0.636	62.25 (55.63 – 69.91)	91.64 (82.19 – 105.53)	1.55002	0.461
FABE-DMSO	63.01 (56.45 – 70.42)	91.16 (82.08 – 104.66)	0.90610	0.636	60.08 (53.75 – 66.93)	86.39 (78.15 – 98.23)	0.74155	0.690

*LC – lethal concentration (50% and 90%); LCL – lower confidence limit; UCL – upper confidence limit; X^2 – chi-square; df – degree of freedom; significant at $P < 0.05$.

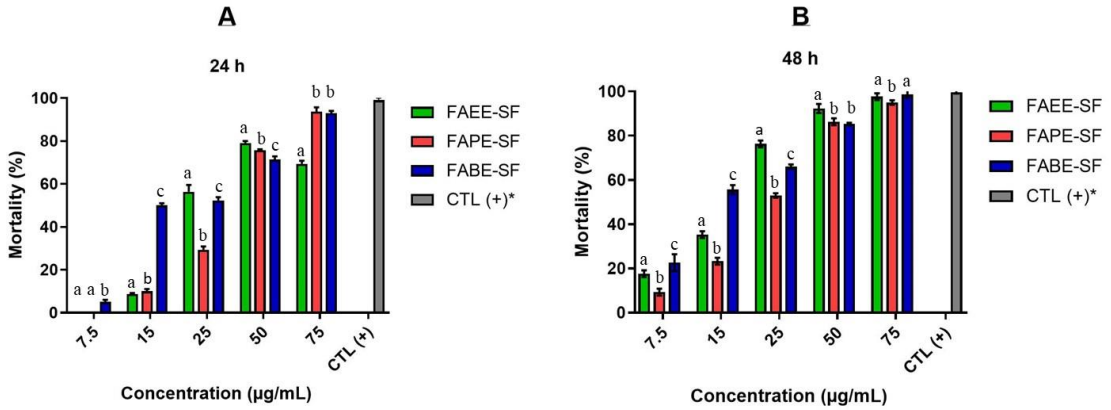

Fig. 2.6. Percentage mortality of *Ae. aegypti* after 24 h (A) and 48 h (B) of exposure to the nanoparticles (FAEE-SF, FAPE-SF and FABE-SF) in different concentration; CLT (+): Dichlorvos solution (*6.25 ng.mL^{-1}). Each value in the column chart is the average of five repetitions ± standard deviation and represents the mortality rate of the three emulsions. Statistical significance is shown by the different lowercase letters, based on the ANOVA test ($p < 0.05$).

Values for the LC_{50} and LC_{90} lethal concentrations (Table 2.4) using Probit analysis were also established. The silk fibroin nanoparticles with fatty acids esters from *A. murumuru* fat tested herein were effective against III instar *Ae. aegypti* larvae, with LC_{50} values ranging from 32 to 45.42 $\mu g.mL^{-1}$ at 24 h, and from 21.35 to 21.28 $\mu g.mL^{-1}$ at 48 h (Table 2.4). FAEE-SF had an LC_{50} of 45.42 $\mu g.mL^{-1}$, while FAPE-SF and FABE-SF had LC_{50} values of 40.29 $\mu g.mL^{-1}$ and 32 $\mu g.mL^{-1}$, respectively, at 24 h. When the larvae of *Ae. aegypti* were exposed to the FABE-SF nanoparticle for 48 h, the LC_{50} value was 21.35 $\mu g.mL^{-1}$ and the LC_{90} value was 45.52 $\mu g.mL^{-1}$.

The present study found that around 78% mortality was observed at a concentration lower than 75 $\mu g.mL^{-1}$ for the FAEE-SF and FAPE-SF nanoparticles, after 24 h of larvae exposure. The FABE-SF nanoparticle at 24 h exhibited mortality of 92% at a concentration of 75 $\mu g.mL^{-1}$, and 100% mortality at 48 h. These results make it clear that nanoparticles of different esters with silk fibroin represent promising larvicidal agents against *Ae. aegypti*.

Although the toxicity mechanism of these nanoparticles is not well known, we suggest that the larvicidal properties of the nanoparticle, especially FABE-SF, come from the interaction between their hydrophobic character and the silk protein, enhanced by the increased alkyl chain of the fatty acid.

Our results are corroborated by the findings of Kannathasan [48], who obtained good larvicidal activity against *Culex quinquefasciatus* using long-chain saturated methyl esters extracted from *Vitex trifolia* leaves, with LC_{50} and LC_{90} values of 9.26 and 21.28 $\mu g.mL^{-1}$, respectively, after 24 h of treatment. It should be noted that this plant species has a fatty acid composition similar to that of *A. murumuru* fat.

De Melo [49] performed larvicidal tests on *C. quinquefasciatus* using different fatty acids, such as oleic acid, palmitic acid, stearic acid, linoleic acid and linolenic acid and their respective methyl esters. In this study, saturated fatty acids, such as stearic acid and palmitic acid, demonstrated moderate larvicidal activity. In the present study it can be suggested that lauric acid, the saturated fatty acid present in greatest quantities in the *A. murumuru* fat, is responsible for larvicidal action against *Ae. aegypti*.

Tibúrcio [50] observed that methyl esters from different vegetable oils can result in potentially larvicidal bioproducts. The different methyl esters used in this study had LC_{50} values ranging from 42.32 to 196.27 $\mu g.mL^{-1}$, with the lowest LC_{50} value observed for the methyl ester obtained from sunflower oil. These findings suggest that esters obtained from different vegetable oils may represent a promising class of new larvicide compounds.

Optical microscopy images of the *Ae. aegypti* larvae after 48 h of exposure in the nanoparticles (FAEE-SF, FAPE-SF and FABE-SF) revealed precipitated of the nanoparticles in the larvae, which caused lesions in the cuticles of their initial segments, such as the head and thorax. In addition to adhering to the lateral bristles, darkening and twisting was also observed on the body of the larvae (Fig. 2.7B). These morphological alterations in the larvae are the lethality effect of the nanoparticles. Sarquis [27] observed similar changes when using a nanoemulsion with free fatty acid from *C. guianensis* and silk fibroin, which caused changes in the anal papilla and in the digestive and respiratory systems of *Ae. aegypti* larvae. Araújo [26] observed morphological alterations in the respiratory siphon and anal papilla in *Ae. aegypti* larvae when using a hexanic extract from the leaves of *Ac. oleracea* solubilized in silk fibroin. Together, these results indicate that precipitation and the penetration of silk fibroin particles into the larval cuticle are crucial for larvicidal activity and may be recognized as a possible mechanism of insecticidal action. There were no changes in the structures of the larvae exposed to the control (Fig. 2.7A).

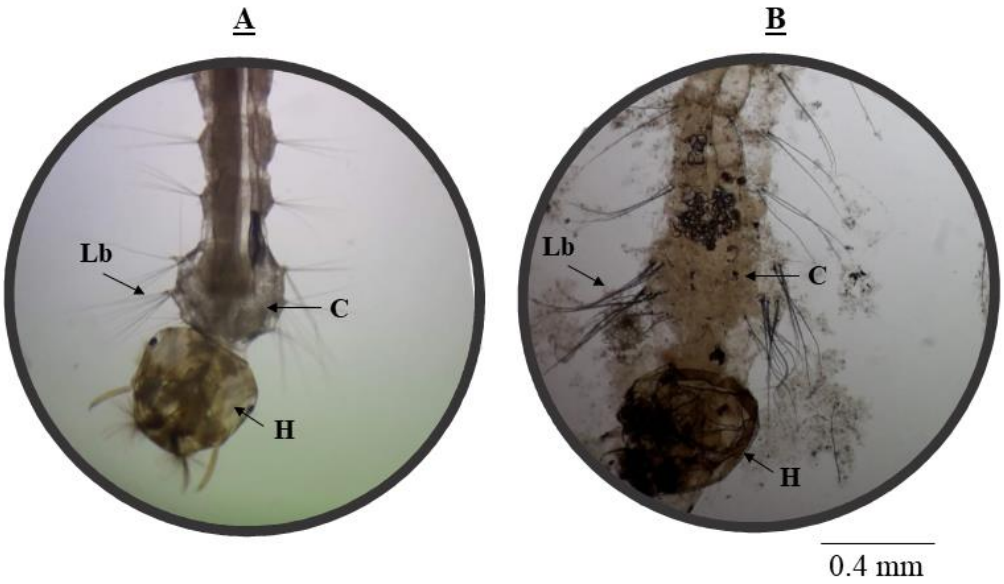

Fig. 2.7. Optical microscopy image of the initial segment of the *Ae. aegypti* (0.4 mm). (A) Larva exposed to negative control (silk fibroin solution 2%) with intact head, chest, and lateral bristles. (B) Larvae treated with nanoparticle (FABE-SF 50 µg/mL) showing deformation and darkening of the head and chest, as well as adherence of the biomaterial to the lateral bristles. **H:** head; **Lb:** lateral bristles; **C:** chest.

The use of FABE-SF nanoparticle is based on global trends towards sustainable development and the growing use of renewable and biodegradable raw materials, such as esters of murumuru, which demonstrate better biological performance than synthetic-based vehicles (in this case DMSO) for mosquito larval control drug-delivery systems.

2.4 CONCLUSION

This is the first study to use different esters combined with silk fibroin as larvicidal agents. The esters (FAEE, FAPE and FABE) combined with the silk fibroin solution exhibited strong larvicidal activity, especially the FABE-SF nanoparticle, which presented a CL_{50} value of 21.35 $\mu g.mL^{-1}$, after 48 h of larvae exposure, and displayed greater temporal stability throughout all 21 days of monitoring, with an average particle value of 217.5 (± 0.85) nm, a zeta potential of -25.6 (± 3.24) mV and a PDI of 0.338 (± 0.01). The FABE-SF exhibited both a hydrophobic and hydrophilic character, increasing the biodistribution and bioavailability control of the fatty acid esters in the aqueous medium. It was also observed that the nanoparticles caused structural changes in the larvae, affecting their development and survival. This mortality rate shows that the formulations can be used as biopesticides.

CRediT authorship contribution statement

Victor H. Marinho, Fábio R. Oliveira and Irlon M. Ferreira: Conceptualization, Methodology, Validation, Software, Formal analysis, Investigation, Data curation, Writing – original draft. **Sergio A. Yoshioka, Ricardo M. A. Ferreira**, D**avid E. J. Quintero, Abrahão V. T. L. Santos:** Methodology, Investigation, Writing – original draft, Writing – review & editing, Visualization. **Irlon M. Ferreira, Raimundo N. P. Souto and José C. T. Carvalho:** Conceptualization, Supervision, Project administration, Funding acquisition.

Declaration of Competing Interest

The authors declare that they have no known competing financial interests or personal relationships that could have influenced the present study.

Acknowledgements

The authors would like to acknowledge the Research Support Foundation of the State of Amapá (Fundação de Amparo à Pesquisa do Estado do Amapá, FAPEAP; grant no.

34568.515.22257.28052017), the Coordination for the Improvement of Higher Education Personnel - Brazil (CAPES), for the financing in part of the present work, and the Graduate Program in Biodiversity and Biotechnology of the BIONORTE Network (PPG-BIONORTE) for financial support.

Supplementary data to this article can be found online at https://doi.org/10.1016/j.jddst.2022.103626.

2.5 REFERENCES

[1] G. Benelli, H. Mehlhorn, Declining malaria, rising of dengue and Zika virus: Insights for mosquito vector control, Parasitol. Res. 115 (2016) 1747–1754.

[2] F. Baldacchino, B. Caputo, F. Chandre, A. Drago, A. della Torre, F. Montarsi, A. Rizzoli, Control methods against invasive *Aedes* mosquitoes in Europe: A review, Pest Manag. Sci. 71 (2015) 1471–1485.

[3] A.M. Rodrigues, C. de G. Sampaio, J.S.N. de Souza, A.R. Campos, A.B.R. da Silva, S.M. de Morais, V.E.P. Martins, Different susceptibilities of *Aedes aegypti* and *Aedes albopictus* larvae to plant-derived products, Rev. Soc. Bras. Med. Trop. 52 (2019) 0–2.

[4] R.J. Gilliom, P.A. Hamilton, Pesticides in the nation's streams and groundwater, 1992–2001: a summary, United States Geol. Surv. Fact Sheet 2006-3028. (2006).

[5] M. Sarwar, N. Ahmad, M. Toufiq, Host plant resistance relationshiphs in chickpea (*Cicer arietinum* L.) against gram pod borer (*Helicoverpa armigera* Hubner), Pakistan J. Bot. 41 (2009) 3047–3052.

[6] V.S. Bezerra, Considerações sobre a palmeira murumuruzeiro (*Astrocaryum murumuru* Mart.), Comun. Técnico, 130. (2012) 1–6.

[7] P.A.Z. Suarez, S.M. Plentz Meneghetti, M.R. Meneghetti, C.R. Wolf, Transformation of triglycerides into fuels, polymers and chemicals: Some applications of catalysis in oleochemistry, Quim. Nova. 30 (2007) 667–676.

[8] H. Perumalsamy, M.J. Jang, J.R. Kim, M. Kadarkarai, Y.J. Ahn, Larvicidal activity and possible mode of action of four flavonoids and two fatty acids identified in *Millettia pinnata* seed toward three mosquito species, Parasites and Vectors. 8 (2015) 1–14.

[9] O.J. Bosch, M. Geier, J. Boeckh, Contribution of fatty acids to olfactory host finding of female *Aedes aegypti*, Chem. Senses. 25 (2000) 323–330.

[10] P. Sharma, L. Mohan, K.K. Dua, C.N. Srivastava, Status of carbohydrate, protein and lipid profile in the mosquito larvae treated with certain phytoextracts, Asian Pac. J. Trop.

Med. 4 (2011) 301–304.

[11] J. Echeverría, R. Albuquerque, Nanoemulsions of Essential Oils: New tool for control of vector-borne diseases and *in Vitro* effects on some parasitic agents, Medicines. 6 (2019) 42.

[12] Z. Zhao, Y. Li, M. Bin Xie, Silk fibroin-based nanoparticles for drug delivery, Int. J. Mol. Sci. 16 (2015) 4880–4903.

[13] M. Jahanshahi, Z. Babaei, Protein nanoparticle: A unique system as drug delivery vehicles, African J. Biotechnol. 7 (2008) 4926–4934.

[14] Y.Q. Zhang, W. De Shen, R.L. Xiang, L.J. Zhuge, W.J. Gao, W.B. Wang, Formation of silk fibroin nanoparticles in water-miscible organic solvent and their characterization, J. Nanoparticle Res. 9 (2007) 885–900.

[15] R. Noufi, L 0 1995, 3 (1995) 235–238.

[16] K. Tanaka, S. Inoue, S. Mizuno, Hydrophobic interaction of P25, containing Asn-linked oligosaccharide chains, with the H-L complex of silk fibroin produced by *Bombyx mori*, Insect Biochem. Mol. Biol. 29 (1999) 269–276.

[17] L.D. Koh, Y. Cheng, C.P. Teng, Y.W. Khin, X.J. Loh, S.Y. Tee, M. Low, E. Ye, H.D. Yu, Y.W. Zhang, M.Y. Han, Structures, mechanical properties and applications of silk fibroin materials, Prog. Polym. Sci. 46 (2015) 86–110.

[18] J. Kundu, Y. Il Chung, Y.H. Kim, G. Tae, S.C. Kundu, Silk fibroin nanoparticles for cellular uptake and control release, Int. J. Pharm. 388 (2010) 242–250.

[19] Q. Cheng, B. Zhang, Y. He, Q. Lu, D.L. Kaplan, Silk nanofibers as robust and versatile emulsifiers, ACS Appl. Mater. Interfaces. 9 (2017) 35693–35700.

[20] L. Pavoni, G. Benelli, F. Maggi, G. Bonacucina, Green nanoemulsion interventions for biopesticide formulations, Elsevier Inc., 2019.

[21] A.R. Bilia, C. Guccione, B. Isacchi, C. Righeschi, F. Firenzuoli, M.C. Bergonzi, Essential oils loaded in nanosystems: A developing strategy for a successful therapeutic approach, Evidence-Based Complement. Altern. Med. 2014 (2014).

[22] H. Mehlhorn, Volume 8 Series editor, n.d. http://www.springer.com/series/8816.

[23] M. Kah, T. Hofmann, Nanopesticide research: Current trends and future priorities, Environ. Int. 63 (2014) 224–235.

[24] C.G. Athanassiou, N.G. Kavallieratos, G. Benelli, D. Losic, P. Usha Rani, N. Desneux, Nanoparticles for pest control: current status and future perspectives, J. Pest Sci. (2004). 91 (2018) 1–15.

[25] M. Rai, A. Ingle, Role of nanotechnology in agriculture with special reference to

management of insect pests, Appl. Microbiol. Biotechnol. 94 (2012) 287–293.

[26] I.F. Araújo, H.A. Loureiro, V.H.S. Marinho, F.B. Neves, R.S.F. Sarquis, S.M.M. Faustino, S.A. Yoshioka, R.M.A. Ferreira, R.N.P. Souto, I.M. Ferreira, Larvicidal activity of the methanolic, hydroethanolic and hexanic extracts from *Acmella oleracea*, solubilized with silk fibroin, against *Aedes aegypti*, Biocatal. Agric. Biotechnol. 24 (2020) 101550.

[27] S.F.R. Sarquis, V.H.S. Marinho, F.B. Neves, I.R. Sarquis, I.F. Araújo, L.F. Damasceno, R.M.A. Ferreira, R.N.P. Souto, C.T. Carvalho, I.M. Ferreira, Industrial Crops & Products *Carapa guianensis* Aubl. (*Meliaceae*) oil associated with silk fibroin , as alternative to traditional surfactants , and active against larvae of the vector *Aedes aegypti*, 157 (2020).

[28] I.M. Ferreira, L.D.S. Ganzeli, I.G. Rosset, S.A. Yoshioka, Ethylic biodiesel production using lipase immobilized in silk fibroin-alginate spheres by encapsulation, Catal. Letters. 147 (2017) 269–280.

[29] T.V. Gabbay Alves, R. Silva da Costa, A.T. Aguiar Gomes, C.E. Ferreira da Costa, P. Perego, J.O. Carréra Silva Júnior, A. Converti, R.M. Ribeiro Costa, Quality control of Amazonian cocoa (*Theobroma cacao* L.) by-products and microencapsulated extract by thermal analysis, J. Therm. Anal. Calorim. 134 (2018) 993–1000.

[30] I. Maciel, L. Coutinho, S. Akinobo, M. Nitschke, A. Haroldo, L. Pizzuti, M. Helena, R. Seleghim, A. Luiz, M. Porto, Chemoselective reduction of chalcones by whole hyphae of marine fungus *Penicillium citrinum* CBMAI 1186 , free and immobilized on biopolymers, Biocatal. Agric. Biotechnol. (2014) 1–7.

[31] N. Anarjan, C.P. Tan, Developing a three component stabilizer system for producing astaxanthin nanodispersions, Food Hydrocoll. 30 (2013) 437–447.

[32] WHOPES, Guidelines for laboratory and field testing of mosquito larvicides, World Heal. Organ. (2005) 1–41.

[33] V. Kostik, S. Memeti, B. Bauer, Fatty acid composition of edible oils and fats, J. Hyg. Eng. Des. 4 (2013) 112–116.

[34] E. Pereira, M.C. Ferreira, K.A. Sampaio, R. Grimaldi, A.J. de A. Meirelles, G.J. Maximo, Physical properties of Amazonian fats and oils and their blends, Food Chem. 278 (2019) 208–215.

[35] A. Enumo, I.P. Gross, R.H. Saatkamp, A.T.N. Pires, A.L. Parize, Evaluation of mechanical, thermal and morphological properties of PLA films plasticized with maleic acid and its propyl ester derivatives, Polym. Test. 88 (2020) 106552.

[36] S. Lu, J. Li, S. Zhang, Z. Yin, T. Xing, D.L. Kaplan, The influence of the hydrophilic-

lipophilic environment on the structure of silk fibroin protein, J. Mater. Chem. B. 3 (2015) 2599–2606.

[37] J. Feng, Q. Chen, X. Wu, S.M. Jafari, D.J. McClements, Formulation of oil-in-water emulsions for pesticide applications: impact of surfactant type and concentration on physical stability, Environ. Sci. Pollut. Res. 25 (2018) 21742–21751.

[38] A.M. Al-Sabagh, M.M. Emara, M.R. Noor El-Din, W.R. Aly, Preparation of water-in-diesel fuel nanoemulsions using high-energy emulsification method and a study of some of their surface active properties, J. Dispers. Sci. Technol. 33 (2012) 970–976.

[39] P. Khuwijitjaru, Y. Kimura, R. Matsuno, S. Adachi, Preparation of finely dispersed O/W emulsion from fatty acid solubilized in subcritical water, J. Colloid Interface Sci. 278 (2004) 192–197.

[40] M. Tsukada, G. Freddi, P. Monti, A. Bertoluzza, N. Kasai, Structure and molecular conformation of tussah silk fibroin films: Effect of methanol, J. Polym. Sci. Part B Polym. Phys. 33 (1995) 1995–2001.

[41] C. Lemarchand, P. Couvreur, C. Vauthier, D. Costantini, R. Gref, Study of emulsion stabilization by graft copolymers using the optical analyzer Turbiscan, Int. J. Pharm. 254 (2003) 77–82.

[42] H.D. Silva, M.A. Cerqueira, B.W.S. Souza, C. Ribeiro, M.C. Avides, M.A.C. Quintas, J.S.R. Coimbra, M.G. Carneiro-Da-Cunha, A.A. Vicente, Nanoemulsions of β-carotene using a high-energy emulsification-evaporation technique, J. Food Eng. 102 (2011) 130–135.

[43] D.G. Dalgleish, Adsorption of protein and the stability of emulsions, Trends Food Sci. Technol. 8 (1997) 1–6.

[44] S. Honary, F. Zahir, Effect of zeta potential on the properties of nano-drug delivery systems - A Review (Part 2), 12 (2013) 265–273.

[45] Ö. Malay, D. Yalçin, A. BatIgün, O. Bayraktar, Characterization of silk fibroin/hyaluronic acid polyelectrolyte complex (PEC) films, J. Therm. Anal. Calorim. 94 (2008) 749–755.

[46] D.T. Pham, N. Saelim, W. Tiyaboonchai, Crosslinked fibroin nanoparticles using EDC or PEI for drug delivery: physicochemical properties, crystallinity and structure, J. Mater. Sci. 53 (2018) 14087–14103.

[47] T.P. Nguyen, Q.V. Nguyen, V. Nguyen, T. Le, Q. Van Le, Silk fibroin-based biomaterials for biomedical, (2019) 1–25.

[48] K. Kannathasan, A. Senthilkumar, V. Venkatesalu, M. Chandrasekaran, Larvicidal

activity of fatty acid methyl esters of *Vitex* species against *Culex quinquefasciatus*, Parasitol. Res. 103 (2008) 999–1001.

[49] A.R. de Melo, I.J. Pereira Garcia, J.E. Serrão, H.L. Santos, L.A. Rodrigues dos Santos Lima, S.N. Alves, Toxicity of different fatty acids and methyl esters on *Culex quinquefasciatus* larvae, Ecotoxicol. Environ. Saf. 154 (2018) 1–5.

[50] J.D. Tibúrcio , F.P. Varotti, D.O. Azevedo, E.P. Siqueira-filho, J.E. Serrão, Larvicidal activity of vegetable oils and esterified compounds against *Culex quinquefasciatus* (Diptera_ Culicidae), Ecotoxicol. Environ. Saf. 143 (2017) 57–61.

Artigo 2

Artigo publicado no periódico **Journal Industrial Crops and Products** (ISSN 1872-633X) Qualis A1 em biotecnologia, segundo a classificação do quadriênio 2017-2020 da plataforma Sucupira – CAPES

Polymeric Nanoparticles from Silk Fibroin and Amazon Oils: Potential Larvicidal Activity and Oviposition Deterrence Against *Aedes aegypti*

Victor H. S. Marinho[a], Fabrício H. Holanda[a], Inana F. Araújo[a], David E. Q. Jimenez[a], Rayanne R. Pereira[b], André L.M. Porto[c], Adriana M. Ferreira[d], José C.T. Carvalho[d], Ana C. G. Albuquerque de Freitas[e], Caio P. Fernandes[d], Raimundo N. P. Souto[e], Irlon M. Ferreira[a,*]

[a]Biocatalysis and Applied Organic Synthesis Laboratory, Federal University of Amapá, University Campus Marco Zero do Equador, Rodovia Juscelino Kubitschek de Oliveira, Km 02, Bairro Zerão, 68902-280, Macapá, AP, Brazil.
[b]Federal University of Western Pará, Institute of Collective Health (Tapajós Unit), 68035-110 Santarém, PA, Brazil.
[c]Department of Physical Chemistry, Institute of Chemistry of São Carlos, University of São Paulo. Av. João Dagnone, 1100, Ed. Prof. Douglas Wagner Franco, Santa Angelina, 13563–120, São Carlos, SP, Brazil.
[d]Drug Research Laboratory, Federal University of Amapá, University Campus Marco Zero do Equador, Rodovia Juscelino Kubitschek de Oliveira, Km 02, Bairro Zerão, 68902-280, Macapá, AP, Brazil.
[e]Drug Planning and Development Laboratory, Institute of Exact and Natural Sciences, Federal University of Pará, Belém, PA, Brazil.
[f]Arthropod Laboratory, Federal University of Amapá, University Campus Marco Zero do Equador, Rodovia Juscelino Kubitschek de Oliveira, Km 02, Bairro Zerão, 68902-280, Macapá, AP, Brazil.

*Corresponding author: irlon.ferreira@gmail.com /Orcid.org/0000-0002-4517-0105

Abstract

This work reports the preparation of nanoparticles of silk fibroin with esters obtained from the oils of two Amazonian plant species (*Carapa guianensis* Aublet and *Bertholletia excelsa*) with excellent physicochemical properties and activity against the larvae of the vector *Aedes aegypti*. The temporal stability of the nanoparticles was evaluated for 50 days at temperatures of 4 ºC and 32 ºC. The size of the nanoparticle was satisfactory, with sizes ranging from 207 ± 2.3 nm to 540.8 ± 23.8 nm, and PdI values ranging from 0.294 to 0.560, and zeta potential from -37.9 ± 0.3 mV to -62.9 ± 0.7 mV. Study of the morphology of nanoparticles, by transmission electron microscopy analysis, clearly showed spherical shapes. The nanoparticles presented slow and controlled release that induced a high mortality rate in the 3rd larval instar of *Ae. aegypti*, with LC_{50} of 27.45 µg. mL^{-1} for FABE-Cg-SF-NPs and LC_{50} of 21.14 µg.mL^{-1} for FABE-Be-SF-NPs, after 48 h of exposure. In addition, they were able to inhibit oviposition by *Ae. aegypti*. However, the nanoparticles did not present significant teratogenic effects on zebrafish embryos up to 72 h post-fertilization. Thus, the formation of nanoparticles by butyl esters in silk fibroin may become an (eco)alternative and effective in the control of *Ae. aegypti* larvae.

Keywords: Amazon oils; Nanobioinsecticide; Oviposition; Toxicity; Silk cocoon.

3.1. INTRODUCTION

The World Health Organization states that vector-transmitted infectious diseases such as dengue, yellow fever, Zika fever, chikungunya fever, malaria, filariasis, leishmaniasis and Chagas disease account for more than 17% of infectious diseases worldwide and cause more than 700,000 deaths per year (WHO, 2018). Arboviruses are groups of viruses of medical relevance for public health that can be transmitted to vertebrate hosts through several vectors such as hematophagous arthropods, sandflies and ticks, but mosquitoes are the principal vector for this group of viruses (Huang et al., 2019; Sukhralia et al., 2019; Young, 2018).

Dengue is a serious public health problem that affects millions of people worldwide. It is transmitted by mosquitoes that carry arboviruses. Dengue is endemic in more than 129 countries, especially in tropical and subtropical regions, where the climate and environmental conditions favor the breeding of mosquitoes (Duarte et al., 2021). An estimated 100-400 million cases of dengue occur per year, with 96 million symptomatic cases and 40,000 deaths worldwide (WHO, 2018). There is still no specific antiviral treatment for the different dengue serotypes (Beckham and Tyler, 2015; Donalisio et al., 2017). The strategy most used for controlling this disease is based on population control of the vector (Balasubramanian et al., 2017; WHO, 2018).

Thus, searching for alternatives for prevention of these diseases is essential, and nanotechnology has emerged as an alternative means for development of new techniques for vector control or development of new drugs for treating viral diseases (Singh et al., 2017). Furthermore, nanometric systems have been successfully used for management of vectors such as *Aedes aegypti* and other viral agents causing diseases (de Oliveira et al., 2014; Duarte et al., 2021; Kumar et al., 2019).

Brazil has a significant part of the planet's biodiversity, with 13% of all existing species (Silveira et al., 2020). Within this scenario, the Amazon region stands out because of its vast vegetation, which is rich in plant species that produce oils. Among the various oil-producing native species of this region, *Carapa guianensis* Aublet and *Bertholletia excelsa* can be highlighted. However, within this biodiversity, most of the secondary metabolites produced these plants have been little studied for biotechnological purposes, such as for production of bioproducts for application in managing disease-causing vectors and treating viral infections (Beltrão and Oliveira, 2007; Malheiros et al., 2022, 2020; Peniche et al., 2022).

The interaction between nanoparticles and bioactive compounds obtained from plants has led to sustainable development of various sectors of agriculture, the food industry and fine

chemical and drug production (Amiri et al., 2014; Ashna et al., 2022). For example, encapsulation of vegetable oils has expanded the application of these compounds, along with their bioactivity in aqueous systems (Bajerski et al., 2016; Malheiros et al., 2022; Oliveira et al., 2022). Nanoformulations have shown promise with regard to delivery of drug systems, for substances with low solubility in water or low permeability in membranes, due to their ability to dissolve lipophilic substances (Gupta et al., 2016). In addition, nanometric transport systems have the capacity to increase the stability and effectiveness of fixed oils and other natural products (Lucca et al., 2018).

Polymeric nano-dispersion is generally produced using surfactants that act at the interface between two immiscible phases by decreasing surface tension and serving as a barrier to coalescence of the nanoformulation. It is driven by a system that tries to achieve a minimal state of Gibbs free energy (Kabalnov, 1998). The use of proteins as surfactants for stabilizing nanosystems is already well established, given their amphiphilic nature, consisting of sequences of hydrophilic and hydrophobic groups that act at the interface of the two nanoformulation phases (Lam and Nickerson, 2013).

Silk fibroin is a natural protein produced by the silkworm, *Bombyx mori*, that is formed by hydrophobic amino acid sets such as glycine, alanine, serine and tyrosine. This composition gives it interesting mechanical, physical and chemical properties (Ferreira et al., 2014; Zhang et al., 2007) that have been shown to be useful in a variety of applications, such as tissue engineering, bioactive organic compound delivery systems, production of films, hydrogels, microspheres, nanoparticles, among others (Araújo et al., 2020; Ferreira et al., 2017; Holanda et al., 2022; Koh et al., 2015; Zaharia et al., 2012). The amphiphilic nature of silk fibroin enables preparation of products such as nanoparticle formulations, in stable water/oil systems with controlled release (Nong et al., 2021).

In this light, the aim of the present work was to develop polymeric nanoparticles from silk fibroin in association with butyl esters obtained from Amazon oils (*C. guianensis* and *B. excelsa*). The larvicidal potential of this bionanomaterial against *Ae. aegypti* was also evaluated as an alternative to synthetic insecticides. The nanoparticles did not show any toxicological effect on zebrafish (*Danio rerio*) embryos.

3.2. MATERIAL AND METHODS

3.2.1. Reagents and solvents

B. excelsa (Brazil nut) oil was obtained from the Jari Farmers' mixed cooperative (Laranjal do Jari, Amapá, Brazil). *C. guianensis* (andiroba) oil was obtained from Embrapa (Macapá, Amapá, Brazil). Butyl alcohol (99.5%) was purchased from Cromato Chemicals (São Paulo, Brazil). Solvents for use in ester purification through column chromatography (98.5% *n*-hexane, 98% ethyl acetate and silica gel 60 [70-230 mesh]) were purchased from Synth (São Paulo, Brazil). Amano AK lipase from *Pseudomonas fluorescens* (20,000 U/g) was purchased from Sigma-Aldrich (São Paulo, Brazil).

3.2.2. Physicochemical analysis on vegetable oils from C. guianensis and B. excelsa

The acidity index (mg $KOH.g^{-1}$), saponification index, density ($mg.mL^{-1}$) and peroxide content ($meq.kg^{-1}$) determined from the vegetable oils were analyzed using the methods described in the analytical standards of the Adolfo Lutz Institute (Lutz, 2008).

3.2.3. Synthesis of butyl esters from andiroba and Brazil nut oils, catalyzed by Amano AK lipase from Pseudomonas fluorescens

The enzymatic transesterification reaction was performed separately for andiroba and Brazil nut oils to generate the respective esters (FABE-Cg and FABE-Be), as reported by Ferreira et al. (2017). It was done in a 50 mL reaction flask containing 1.0 g of oil, 3 mL of butyl alcohol and 0.1 g (10%) of Amano AK lipase from *Pseudomonas fluorescens*. The reaction mixtures were magnetically stirred for 24 h at room temperature. Afterwards, the reaction solutions were filtered, the organic phases were dried using anhydrous sodium sulfate and filtered, and the solvents were removed under reduced-pressure vacuum. The products were purified by means of silica gel column chromatography, using a mixture of *n*-hexane and ethyl acetate (9:1) as the mobile phase. The isolated products were characterized according to their spectroscopic data (using GC-MS and FTIR, as described below).

3.2.4. Gas chromatography-mass spectrometry (GC-MS)

The vegetable oil samples transesterified with *n*-butyl alcohol were analyzed by means of gas chromatography coupled to mass spectrometry (GC-MS). These analyses were

performed in a Shimadzu GC2010 system with a selective mass detector (Shimadzu MS2010plus) in electron ionization (EI, 70 eV) mode. The system was equipped with an RTX-5MS column (30 m × 0.25 mm × 0.25 µm). The GC-MS conditions started with an oven temperature of 130 °C, which was maintained for 2 min and then increased to 290 °C at a rate of 5 °C.min^{-1}. The final temperature was maintained for 2 min. The total analysis time was 36 min. The injector and detector temperatures were maintained at 210 ºC; 1 µL of sample was injected with 1:15 split; and helium was used as the carrier gas at a flow rate of 1.0 mL.min^{-1}. The ions were monitored from 3 to 36 min for m/z 40-500. Components present in the samples were identified by comparing spectral data with those described in the Wiley library.

3.2.5. FT-IR spectroscopy analysis

A Fourier-transform infrared spectrophotometer (Spectrum Two FT; PerkinElmer, Inc., Waltham, MA, USA), with an attenuated total reflection (ATR) sampling accessory, a diamond plate and a deuterated triglycine sulfate detector, was used to record the spectra of vegetable oils transesterified with *n*-butyl alcohol and FABE-Cg-SF-NPs and FABE-Be-SF-NPs nanoparticles. The spectral range was set at between 350 and 4,000 cm^{-1}, and the resolution was set to 0.5 cm^{-1} (de Oliveira Penido et al., 2017).

3.2.6. ^{13}C nuclear magnetic resonance (NMR) analysis

The ^{13}C NMR experiments were performed in an Agilent Technologies 400 MHz Premium Shielded spectrometer. All samples (vegetable oils and FABE-Cg and FABE-Be; 20 µL) were prepared by dissolving them in 600 µL of deuterated chloroform ($CDCl_3$, 99.99%; Cambridge Isotope Laboratories, Andover, USA) and tetramethylsilane (TMS) as the internal standard. The chemical shifts were expressed in ppm (Ferreira et al., 2019).

3.2.7. Preparation of the silk fibroin solution

The silk fibroin solution was prepared based on the method developed by Ferreira et al. (2014). Silkworm cocoons (3.0 g; from Bratac, Brazil) were degummed in a boiling aqueous Na_2CO_3 solution (2%, w/v) for 30 min. The resultant fibers were filtrated and washed with distilled water (3 x 500 mL). Subsequently, the silk fibers were dissolved in a 50 mL ternary solution with H_2O:EtOH:$CaCl_2$ molar proportions of 8:2:1 at 30 ºC for 4 h. This mixture was then dialyzed (cellulose tube with an exclusion limit of 16 kDa; from Viskase, Brazil) for 3 days at room temperature, and the water was changed every 24 h. The fibroin solution was

centrifuged (6000 rpm for 10 min) to remove impurities and larger particles. The concentration of the silk fibroin solution was adjusted with water to 2% (w/w).

3.2.8. Preparation of polymeric silk fibroin nanoparticles with the synthesized esters FABE-Cg and FABE-Be

A volume of 10 mL of the nanoparticles was produced by homogenizing the silk fibroin solution with the butyl esters synthesized (Section 2.3). In summary, the 1% (v/v) esters FABE-Cg or FABE-Be were separately added to a mixture of 5% (v/v) ethanol and isopropanol (1:1) and stirred for 30 min using a magnetic stirrer. Then, the 94% (v/v) silk fibroin solution (2%) was separately added dropwise to the previous mixture of FABE-Cg and FABE-Be esters and the formulation was vortex-stirred at 300 rpm for 1 h, as described by Sarquis et al. (2020). The polymeric silk fibroin nanoparticles in association with butyl esters were named with the codes FABE-Cg-SF-NPs (silk fibroin nanoparticles with *C. guianensis*) and FABE-Be-SF-NPs (silk fibroin nanoparticles with *B. excelsa*).

3.2.9. Characterization of the polymeric silk fibroin nanoparticles (FABE-Cg-SF-NPs and FABE-Be-SF-NPs)

3.2.9.1. Particle size and distribution

The nanoparticles (FABE-Cg-SF-NPs and FABE-SF-Be-NPs) were characterized by means of dynamic light scattering using a Zetasizer Nano ZS (Malvern Pananalytical, Malvern, UK), with application of noninvasive back-scatter (scattering angle 173°) at a temperature of 25 °C. The nanoparticles were diluted (1:10) with ultrapure water prior to measurements. The average particle size (Z-average) and polydispersity index (PdI) were obtained through cumulative analysis on the scatter data recorded by the instrument software (measurements in triplicate) and the results were expressed as means and standard deviations, as described by Anarjan and Tan, (2013).

3.2.9.2. Zeta potential

The zeta potential, which represents the particle surface electrostatic charge, was determined through electrophoretic mobility (Zetasizer Nano ZS; Pananalytical, Malvern, UK) for FABE-Cg-SF-NPs and FABE-Be-SF-NPs. The samples of polymeric silk fibroin nanoparticles were diluted in ultrapure water (1:10). The Helmholtz-Smoluchowski equation

was used to calculate the zeta potential, in the instrument software, as described by Anarjan and Tan (2013).

3.2.9.3. Stability analysis on polymeric silk fibroin nanoparticles (FABE-Cg-SF-NPs and FABE-Be-SF-NPs)

The nanoparticles (FABE-Cg-SF-NPs and FABE-Be-SF-NPs) were stored at different temperatures, at 4 °C in a refrigerator and at 32 °C in a drying oven. Then, the particle sizes, polydispersity index and zeta potential of the nanoparticles were evaluated from day 1 to day 50 after preparation using a ZS zetasizer (Malvern, UK). Each polymeric silk fibroin nanoparticle sample was diluted with distilled water (1:10) to avoid multiple dispersion effects, as described by Anarjan and Tan (2013). Measurements were made in triplicate. The mean droplet size was expressed in terms of the mean diameter. All analyses were performed at 25 °C.

3.2.9.4. Oxidative stability of polymeric silk fibroin nanoparticles (FABE-Cg-SF-NPs and FABE-Be-SF-NPs)

The nanoparticles (FABE-Cg-SF-NPs and FABE-Be-SF-NPs) were placed in an amber glass and then incubated in the dark at 4 °C in a refrigerator and at 32 °C in a drying oven for 50 days. Samples, were collected periodically over the course of this storage, to analyze their oxidative stability. The lipid hydroperoxide content was measured using a method adapted from Walker et al. (2017). Lipid extraction was performed by adding an aliquot of the nanoparticles (0.7 mL) to an isooctane/2-propanol mixture (3:1 v/v; 2 mL) and then vortexing the sample three times for 10 s, followed by centrifugation at 1300 g for 3 min. The supernatant (0.2 mL) was mixed with methanol/1-butanol (2:1 v/v; 2.8 mL), followed by addition of 3.94 M ammonium thiocyanate/ferrous sulfate solution (1:1 v/v; 30 μL). After 20 min in the dark, this mixture was analyzed at 510 nm wavelength in a UV-vis spectrophotometer (Beckman Coulter Inc., USA). Each sample was analyzed in triplicate.

3.2.9.5. Differential scanning calorimetry (DSC)

The samples of nanoparticles (FABE-Cg-SF-NPs and FABE-Be-SF-NPs) were air-dried for 4 h at room temperature for DSC analysis. This was performed using DSC-60 plus equipment (Shimadzu, Kyoto, Japan). A total of 5 mg of each sample of fibroin nanoparticles

was placed in a closed aluminum pan and subjected to a heating rate of 10 °C.min^{-1}, up to a temperature of 100 °C with a nitrogen atmosphere at 50 cm^3.min^{-1}, as described by (Pereira et al., 2019).

3.2.9.6. Morphology of polymeric silk fibroin nanoparticles (FABE-Cg-SF-NPs and FABE-Be-SF-NPs)

Transmission electron microscopy (TEM) analyses on the nanoparticles (FABE-Cg-SF-NPs and FABE-Be-SF-NPs) were performed using a JEM 2100-FS microscope (JEOL Ltd., Tokyo, Japan) operated at 200 kV. For sample preparation, a drop of the suspension was deposited on formvar/carbon-coated copper grids (300 mesh, Electron Microscopy Sciences, Hatfield, PA, USA). After 60 s, the excess was gently dried with filter paper and the grid was stained using a drop of 2% w/v of uranyl acetate solution (Sigma-Aldrich, St. Louis, MO, USA) for 120 s. The staining solution was gently eliminated using filter paper and the grid was rapidly dipped in particle-free ultrapure water to further eliminate loosely bound material and excess staining. The images were processed using the Digital Micrograph software (Gatan Inc., Pleasanton, CA, USA), as described by Pereira et al., (2019).

3.2.9.7. In vitro drug release

In vitro release of esters (FABE-Cg and FABE-Be) in the nanoparticles (FABE-Cg-SF-NPs and FABE-Be-SF-NPs) was performed using the dialysis bag method, with modifications (Zhao et al., 2012). The experiment was performed at 37 °C using phosphate buffer (pH 7.4) as the release medium. The dialysis bag (MWCO 12,000 to 14,000 Da, Sigma-Aldrich, St. Louis, MO, USA) containing 2 mL of the FABE-Cg-SF-NPs and FABE-Be-SF-NPs samples was placed in contact with 100 mL of release medium, thus ensuring sinking conditions, under moderate magnetic stirring. 2 mL of the release medium was removed and replaced with the same volume of fresh medium at predetermined times (0, 1, 2, 3, 4, 5, 6, 7, 8 and 24 h) for analysis. The concentrations of the released esters (FABE-Cg and FABE-Be) from the samples were obtained at 250 nm using a spectrophotometer (PerkinElmer Lambda 35 UV-Vis, Canada). The data were analysed using mathematical modelling (KinetDS software, version 3.0, Krakow, Poland) in order to gain a better understanding of the ester release behaviour of the nanoparticles. The model that best described the release profile was selected based on the correlation coefficient (r).

3.2.10. Larvicidal activity and oviposition-deterrence analyses

Polymeric silk fibroin nanoparticles associated with butyl esters (FABE-Cg-SF-NPs and FABE-Be-SF-NPs) were prepared at different concentrations (7.5, 15, 25, 50 and 75 µg.mL^{-1}) for larvicidal tests on *Ae. aegypti*. The Rockefeller colony maintained by the Arthropod Laboratory (ARTHROLAB) of the Federal University of Amapá was the source of the specimens used. Five replications were performed with 10 larvae each. Silk fibroin solution (2%) without the active agent was used as a negative control, and a dichlorvos solution (6.25 ng.mL^{-1}) was used as a positive control. Larval mortality was determined after 24 and 48 h of incubation at a temperature of 25 ºC and humidity of 75%. Larvae were considered dead when they did not respond to any stimuli or did not move on the surface of the solution, compared with what was observed in the control. Bioassays were performed in accordance with the recommendations of WHO (2005).

The oviposition deterrence evaluation was conducted in accordance with the WHOPES guidelines (WHO, 2005). For this assay, 50 pregnant females (fed with blood) were transferred to cages measuring 40 cm × 40 cm × 40 cm under conditions of 25 ± 2 °C and relative humidity of 75 ± 5% and 12-h photoperiods. The cages contained dark ovitraps containing nanoparticles (FABE-Cg-SF-NPs and FABE-Be-SF-NPs) at concentrations of 25, 50 and 100 µg.mL^{-1}. The control solution for this assay was prepared with water and silk fibroin (2%). The oviposition response was determined by counting the numbers of eggs laid on filter papers. The test was done in quadruplicate and the number of eggs was determined after 96 h with the aid of a stereoscopic magnifying glass.

3.2.11. Morphological analysis on larvae of Ae. aegypti

After the larvicide test, the larvae were fixed in 10% formalin. Their external morphology was then analyzed under an optical microscope and photographed with a digital camera (MDCE - SC USB 2.0) using the ScopeImage 9.0 software, as described by Araújo et al. (2022).

3.2.12. Toxicity assay on zebrafish embryos

Zebrafish (*Danio rerio*) were purchased from the company Power Fish, located in Itaguari-RJ, Brazil. They were kept in tanks in which the water conditions were controlled (23 ± 2 ºC and light/dark cycle 14/10 h) for 8 months before the trials, as described by Borges et al. (2018) and Tavares Carvalho et al. (2016).

Sexually mature zebrafish were selected and placed in a breeding aquarium in the proportions of two males per female, separated by a glass partition and by a titanium mesh held horizontally 5 cm above the bottom of the aquarium to keep the fish apart from the eggs, which sink to the bottom of the tank. After overnight, lights were switched on to simulate the dawn and incite oviposition (Yang et al., 2018). After collection, the eggs were washed with aquarium water.

The reproduction test followed the recommendations of the Organization for Economic Cooperation and Development (OECD, 236)/(OECD, 2013). The eggs were washed with aquarium water, randomized, separated into 7 groups with N = 50 eggs and treated in triplicate. The groups were treated with FABE-Cg-SF-NPs and FABE-Be-SF-NPs at concentrations of 20.5 µg.mL^{-1} and 26.5 µg.mL^{-1}, respectively, and transferred to wells of a 96-well plate containing a final volume of 250 µL. Solutions of silk fibroin (2%) and dichlorvos (6.25 ng.mL^{-1}) were used as negative and positive controls, respectively. Microplates containing the treated and control groups were maintained at a controlled temperature (28 ± 2 °C) in an incubator (SOLAB - SL, Brazil). Teratogenic alterations, vitality and absence of pigments were observed through analysis under an optical microscope (Model BIO3 research, W LED 6 V DC, 1200 mA) at 24, 48, 72 and 96 h post-fertilization (hpf) (OECD, 1997).

3.2.13. Statistical analysis

Lethal concentrations (LC_{50} and LC_{90}) were determined after 24 and 48 h of incubation and were calculated using Probit analysis in the StatGraphics Centurion XV software, version 15.2.11. If the control mortality of the treated groups was between 5 and 20%, the analysis was corrected in accordance with the WHO (2005) formula: mortality (%) = X–Y⁄X × 100, where X = percentage survival in the untreated control and Y = percentage survival in the treated sample.

3.3. RESULTS AND DISCUSSION

3.3.1. GC-MS analysis on andiroba and Brazil nut oil transesterification by P. fluorescens lipase

The economic and biological importance of oils (both fixed and volatile) from plant species of the Amazon region, such as those from andiroba and Brazil nut, stimulated us to expand their potential through use of biotechnology, with the aim of obtaining bioactive nanoformulations through a sustainable approach.

Firstly, through GC-MS analyses on triglycerides esterified from andiroba and Brazil nut oils, through use of *P. fluorescens* lipase (Fig. 3.1), high similarity was observed between the main fatty acid derivatives identified in both oils (Table 3.1). The esterified andiroba and Brazil nut oils presented 43.95% and 36.6% saturated fatty acids in their compositions, respectively, with highlighting of palmitic and stearic acids. In both samples, oleic acid (C18:1, ω-9) was identified at a greater proportion, with 46.61% for andiroba oil and 31.8% for Brazil nut oil. In contrast, linoleic acid (C18:2, ω-6) was identified with proportions of 2.35% in andiroba oil and 28.8% in Brazil nut oil.

The fatty acid profile identified in andiroba and Brazil nut oils was in accordance with what had previously been observed in the literature (Barata et al., 2020; Sarquis et al., 2020). The relationship between the compositions of saturated and unsaturated fatty acids of oils influences the physical-chemical properties of their polymeric nanoparticles, as well as their biological activity (da Costa Vieira et al., 2020).

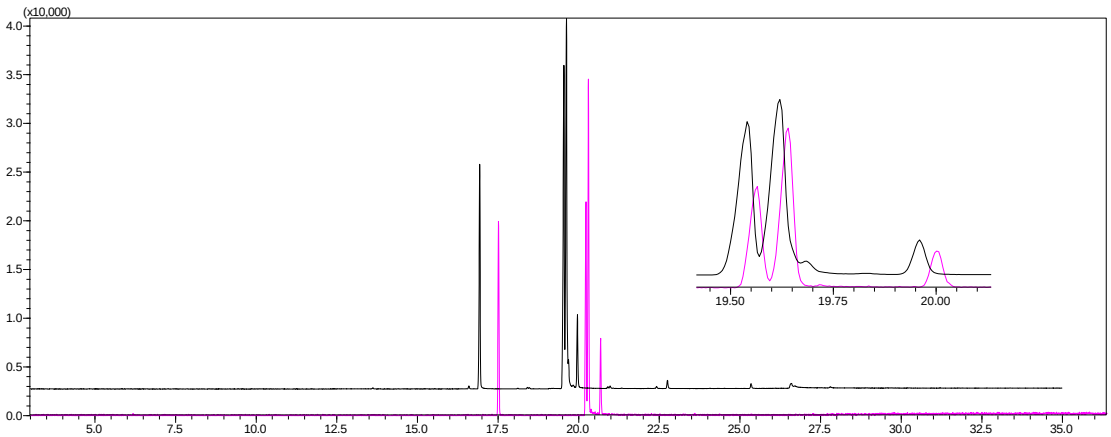

Fig. 3.1. Chromatographic profile of FABEs (butyl esters of acids fatty) from *C. guianensis* (in black) and *B. excelsa* (in pink) oils, as determined by CG-MS analysis.

Table 3.1 Composition of FABEs from *C. guianensis* (andiroba) and *B. excelsa* (Brazil nut), determined by means of CG-MS analysis.

Fatty esters in *n*-butyl[a]	Relative concentration (%)[b] *C. guianensis*	Relative concentration (%)[b] *B. excelsa*
Palmitic (C16:0)	40.5	19.0
Linoleic (C18:2, ω-6)	2.35	28.8
Oleic (C18:1, ω-9)	43.61	31.8
Vaccenic (18:1, ω-7)	0.53	2.0
Stearic (C18:0)	3.45	17.6
Unidentified	1.95	-
Σ Saturated	43.95	36.6
Σ Monounsaturated	44.14	33.8
Σ Polyunsaturated	2.35	28.8

[a] MS database (NIST 5.0). [b] Values selected through integration of the peaks.
Note: The oils were previously transesterification by lipase from *P. fluorescens* using *n*-butyl alcohol.

3.3.2. Physical-chemical properties of in natura oils from andiroba and Brazil nut

The physical-chemical parameters of *in natura* oils from andiroba and Brazil nut were determined in accordance with previously developed protocols (Lutz, 2008). The acidity index for andiroba oil and Brazil nut were 3.73 (± 0.15) mgNaOH.g^{-1} and 0.54 (± 0.01) mgNaOH.g^{-1}, respectively. The peroxide indices for andiroba and Brazil nut oils were 8.15 (± 0.01) meq.kg^{-1} and 7.15 (± 0.01) meq.kg^{-1}, respectively. Andiroba oil presented a saponification index of 152.05 (± 1.00) mgKOH.g^{-1} and Brazil nut oil, 156.70 (± 0.70) mgKOH.g^{-1}. In addition, andiroba and Brazil nut oils presented density values of 1.010 (± 0.010) g.mL^{-1} and 1.030 (± 0.010) g.mL^{-1}, respectively (Table 3.2). This similarity of results regarding the physical and chemical properties of these *in natura* oils was also reported by Elson et al. (2014) and Vilhena et al. (2020). Quality control on *in natura* oils provides important information that can influence the physical-chemical characteristics of formulations that may arise from them or their derivatives. Such characteristics can impact on the size and structure of the dispersed phase, as well as on its distribution. In addition, these factors are closely linked to the intrinsic characteristics of each oil, such as interfacial tension and hydrophobic character (Vergallo, 2020).

Table 3.2 Physical-chemical properties of *C. guianensis* and *B. excelsa* fixed oils *in natura*[a]

Oils	Acidity index (mgNaOH.g^{-1})	Peroxide value (meq.kg^{-1})	Saponification index (mgKOH.g^{-1})	Density (g.mL^{-1})
Carapa guianensis	3.73 ±0.15	8.15 ±0.01	152.05 ±1.00	1.01 ±0.01
Bertholletia excelsa	0.54 ±0.01	7.15 ±0.01	156.70 ±0.70	1.03 ±0.00

[a]Average values ± standard error of average determinations in triplicate.

3.3.3. Characterization of polymeric silk fibroin nanoparticles (FABE-Cg-SF-NPs and FABE-Be-SF-NPs)

3.3.3.1. Temporal stability of polymeric silk fibroin nanoparticles (FABE-Cg-SF-NPs and FABE-Be-SF-NPs)

Polymeric nanoparticles are essential components of nanometric-sized drug transporters (Bigaj-Józefowska and Grześkowiak, 2022). The best way to evaluate the temporal stability of a nanosystem is by monitoring particle size, polydispersity index and zeta potential over the storage time. Through the technique of dynamic light dispersion, the changes to these parameters can be ascertained. The smaller the particle size is, the greater its resistance to gravitational forces will be, thus decreasing the probability of aggregation and flocculation (McClements, 2012; Ostertag et al., 2012). Table 3.3 shows the size, polydispersity index and zeta potential of the FABE-Cg-SF-NPs and FABE-Be-SF-NPs nanoparticles during the 50 days monitoring period, while stored at 4º and 32 ºC.

The FABE-Cg-SF-NPs nanoparticles stored at 4 ºC exhibited sizes between 330.7 ± 1.8 nm and 207 ± 2.3 nm. In contrast, when stored at 32 ºC, they exhibited particle sizes between 330.7 ± 1.8 nm and 306.5 ± 3.9 nm, over the 50 days of monitoring (Table 3.3). FABE-Be-SF-NPs stored at 4 ºC exhibited sizes ranging from 383.2 ± 36.8 nm to 239.9 ± 4.8 nm. When stored at 32 ºC the sizes of the nanoparticles ranged from 383.2 ± 36.8 nm to 540.8 ± 23.8 nm, over the course of the monitoring days (Table 3.3).

In this study, the formulations obtained from polymeric silk fibroin nanoparticles associated with butyl esters (FABE-Cg-SF-NPs and FABE-Be-SF-NPs) showed good stability in relation to their sizes during the period of up to 50 days of monitoring. The only exception was FABE-Be-SF-NPs stored at 32 ºC, which showed a small increase in their sizes on the 50th day (Table 3.3).

These changes in nanoparticle sizes may have been influenced by the chain lengths and types of the fatty acid esters present in the formulation (Marinho et al., 2022). Furthermore, the β-sheet structure of silk fibroin can be induced by the ethanol present in the formulation and in this way can form silk fibroin microcrystals. These microcrystals can grow and aggregate along with the conformational transition process due to the free chains of silk fibroin in the formulation (Cao et al., 2007).

The increase in the chain of solid lipid-based nanocarriers from C16:0 to C18:0, had a slight influence on the particle size of these nanocarriers (162 ± 26.9 nm to 360 ± 31.7). This phenomenon was also observed previously in vegetable oil-based nanocarriers that had high content of fatty acids of the C16:0 to C18:0 types in their lipid composition (Pinto et al., 2018). This phenomenon can be explained by the formation of a more viscous lipid phase, which leads to increased surface tension and consequently can lead to formation of larger particles (Ekambaram et al., 2012; Niculae et al., 2014).

In the present study, the good stability of the nanoparticles over the 50 days period consisted of storage of the formulation developed from silk fibroin associated with butyl esters derived from the fixed oils of the andiroba and Brazil nut plants. This stability can be attributed to adsorption of silk fibroin to the oil/water interface, which effectively reduces the interfacial tension and exhibits a good emulsifying effect. Silk fibroin is able to form a film at the oil/water interface, which improves the viscoelastic properties and thus plays an important role in stabilizing this type of nanoformulation (Tang et al., 2015).

The polydispersity index (PdI) is defined as the ratio of standard deviation to average particle size. It thus indicates the degree of uniformity of particle size within a formulation (Jadhav and Yadav, 2020). Hence, the scatter effect is better and stability is greater when the PdI value is less than 0.5 (McClements and Jafari, 2018).

FABE-Cg-SF-NPs showed PdI values between 0.315 and 0.294 at 4 ºC, and ranged from 0.315 to 0.308 when stored at 32 ºC for up to 50 days (Table 3.3). The PdI values for FABE-Be-SF-NPs ranged from 0.484 to 0.278 when stored at 4 ºC for up to 50 days. When FABE-Be-SF-NPs were stored at 32 °C for up to 50 days, their PdI values ranged from 0.484 to 0.486 (Table 3.3).

With these PdI values, the nanoformulations showed less dispersed particle size distribution. This provides nanoformulations that are less susceptible to delamination or precipitation, in addition to conferring greater stability for the biomaterial (Shi et al., 2021).

The interfacial tension between the two phases of the nanoformulations is maintained by various attractive interactions between the molecules of the two liquid phases. These

interactions may be minimized by the amphiphilicity of silk fibroin, which has a polypeptide chain containing a mixture of hydrophilic and hydrophobic amino acids. The amphiphilic nature of silk fibroin may be responsible for decreasing the interfacial tension and thereby decreasing its free energy. Consequently, it reduces the particle size and favors less polydispersion, thus improving the emulsification process and the stability of the nanoparticles (Schroën, 2020).

Zeta potential is a measure of electrostatic stability. The higher the surface load of the nanoformulation is, the more stable it will be. In cases of low load values, the particles tend to collide with each other and thus increase their sizes, which diminishes the stability of the reformulated nanoparticles (Jafarizadeh-Malmiri, 2020). Thus, stability of nanoformulations is associated with a zeta potential value of ± 30 mV, which is usually indicative of a stable nanoformulation (Aswathanarayan and Vittal, 2019).

The zeta potential for FABE-Cg-SF-NPs was between -46.8 ± 0.7 mV and -41 ± 0.5 mV when maintained at 4 ºC and between -46.8 ± 0.7 mV and -62.9 ± 0.7 mV when maintained at 32 ºC. For FABE-Be-SF-NPs, the zeta potential was from -50.7 ± 2.1 mV to -47 ± 0.9 mV when stored at 4 ºC and from -50.7 ± 2.1 mV to -51.0 ± 0.6 mV when kept at 32 ºC. Monitoring of zeta potential analyses was performed for all synthesized nanoparticles during the 50 days storage period (Table 3.3).

The process of stabilization of polymeric nanoformulations is governed by the properties of the layers that are adsorbed on to the surface of the oil droplets (Wlastra, 1996). Macromolecules such as proteins form an adsorbed film on the nanoparticle surface, thus creating an energy barrier against coalescence. When adsorbed, the protein molecules can unfold and reorient their amino groups so that the hydrophobic groups align with the oil molecules and the hydrophilic groups align with the aqueous phase. Therefore, a viscoelastic or gelatinous layer can form at the interface (Song and Forciniti, 2000). Because of these characteristics, it can be inferred that there are attractive interactions between butyl esters derived from *in natura* oils and the amino acids alanine and glycine, which are found in the outer layer of silk fibroin.

Table 3.3 Particle size distribution, PdI and zeta potential of polymeric silk fibroin nanoparticles (FABE-Cg-SF-NPs and FABE-Be-SF-NPs).

	4 ºC				32 ºC			
	Time (days)	**Size (nm)**	**PdI**	**Zeta (mV)**	**Time (days)**	**Size (nm)**	**PdI**	**Zeta (mV)**
FABE-Cg-SF-NPs	0	330.7 (±1.8)	0.315	-46.8 (±0.7)	0	330.7 (±1.8)	0.315	-46.8 (±0.7)
	7	305.1 (±13.0)	0.439	-46.7 (±4.8)	7	329.1 (±12.2)	0.359	-45.5 (±3.4)
	14	267.3 (±7.2)	0.477	-42.7 (±4.8)	14	334.5 (±6.6)	0.350	-43.1 (±2.3)
	21	229 (±6.5)	0.348	-44.5 (±0.2)	21	328.4 (±2.2)	0.323	-46.7 (±0.8)
	28	226.3 (±2.6)	0.320	-38.1 (±0.4)	28	323.2 (±14.6)	0.343	-45.3 (±1.4)
	50	207 (±2.3)	0.294	-41 (±0.5)	50	306.5 (±3.9)	0.308	-62.9 (±0.7)
FABE-Be-SF-NPs	0	383.2 (±36.8)	0.484	-50.7 (±2.1)	0	383.2 (±36.8)	0.484	-50.7 (±2.1)
	7	334.5 (±11.6)	0.451	-42.9 (±1.1)	7	381.8 (±26.8)	0.449	-50.2 (±1.1)
	14	301.6 (±2.1)	0.413	-42.4 (±1.6)	14	361.4 (±16.8)	0.430	-44.9 (±0.26)
	21	274.3 (±3.7)	0.374	-43.2 (±4.5)	21	334.1 (±9.3)	0.505	-49.7 (±1.6)
	28	255.6 (±7.4)	0.271	-37.9 (±0.3)	28	363.7 (±41.3)	0.560	-43.4 (±1.5)
	50	239.9 (±4.8)	0.278	-47.0 (±0.9)	50	540.8 (±23.8)	0.486	-51.0 (±0.6)

3.3.3.2. Oxidative stability of polymeric silk fibroin nanoparticles (FABE-Cg-SF-NPs and FABE-Be-SF-NPs)

The oxidative stability of FABE-Cg-SF-NPs and FABE-Be-SF-NPs was monitored during the period of up to 50 days of storage, at temperatures of 4 ºC and 32 ºC, by measuring the primary lipid oxidation products (lipid hydroperoxides). In both nanoformulations, lipid oxidation products gradually increased during the monitoring period (Fig. 3.2). However, the formulations showed low lipid oxidation values in comparison with the oxidation values of their oils *in natura*.

The FABE-Cg-SF-NPs and FABE-Be-SF-NPs showed similar lipid hydroperoxide values, ranging from 0.3 to 0.4 meq.kg^{-1} at the different temperatures studied. These were comparable with those of *in natura* oils, which showed similar lipid hydroperoxide values ranging from 0.1 to 0.7 meq.kg^{-1} (Fig. 3.2).

(Yan et al., 2022) also evaluated the oxidative stability of emulsions stabilized by soybean protein nanoparticles and found values similar to ours. The low lipid oxidation found in these studies may be related to a compact layer formed by the protein at the oil/water interface, which would prevent water-soluble pro-oxidants from approaching lipids (Zhang et al., 2020). In addition, proteins not adsorbed at the interface can bind to pro-oxidants, thus inhibiting their ability to adsorb on the surface of drops and promote their oxidation (Gumus et al., 2017).

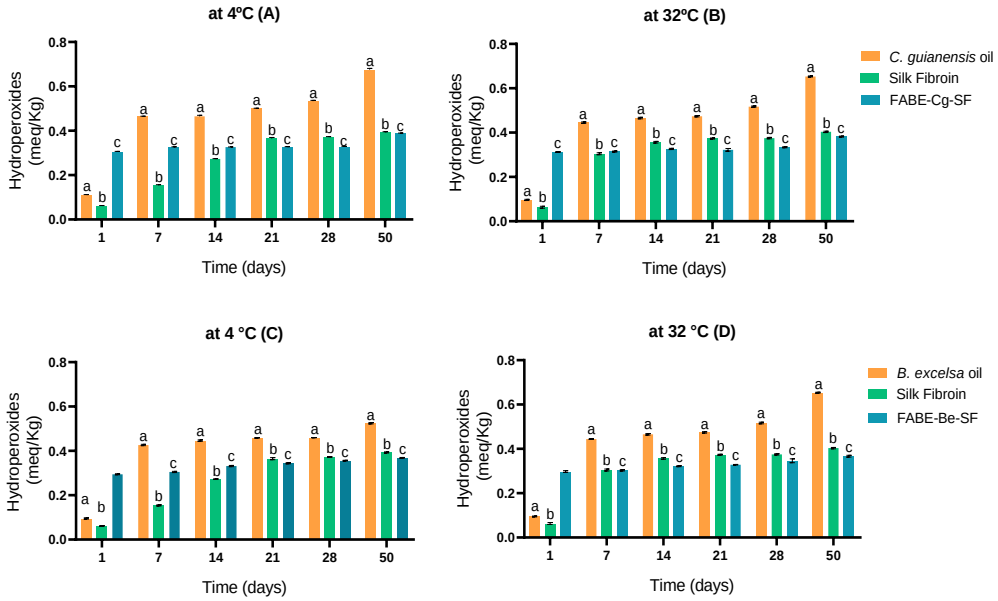

Fig. 3.2. Influence of temperature on hydroperoxides values in silk fibroin polymeric nanoparticles associated with butyl esters during 50 days storage. Hydroperoxides values are also presented for the *in natura* oils and the silk fibroin solution (2%). (A) FABE-Cg-SF-NPs sample at 4 ºC. (B) FABE-Cg-SF-

NPs sample at 32 ºC. (C) FABE-Be-SF-NPs sample at 4 ºC. (D) FABE-Be-SF-NPs sample at 32 ºC. Statistical significance is shown by different lower-case letters, based on the ANOVA test ($p < 0.05$).

3.3.3.3. Differential exploratory calorimetry (DSC)

The DSC thermogram characterized the energies involved in the pyrolysis process of the FABE-Cg-SF-NPs and FABE-Be-SF-NPs. The Fig. 3.3 shows an endothermic event from 50 to 100 °C, attributed to moisture evaporation. The formulations of FABE-Cg-SF-NPs and FABE-Be-SF-NPs showed peaks similar to the peaks of silk fibroin nanoparticles. Sharp peaks were observed at 218 °C for FABE-Cg-SF-NPs and 221 °C for FABE-Be-SF-NPs. There was also an exothermic peak at 250 °C for both formulations, which indicated a thermal transformation from silk I to silk II.

In the literature, a similar profile was observed for polymeric silk fibroin nanoparticles with the butyl ester of *Astrocaryum murumuru* Mart. fat (Marinho et al., 2022). Another similar result was observed for cross-linked silk fibroin nanoparticles designed for drug delivery (Pham et al., 2018).

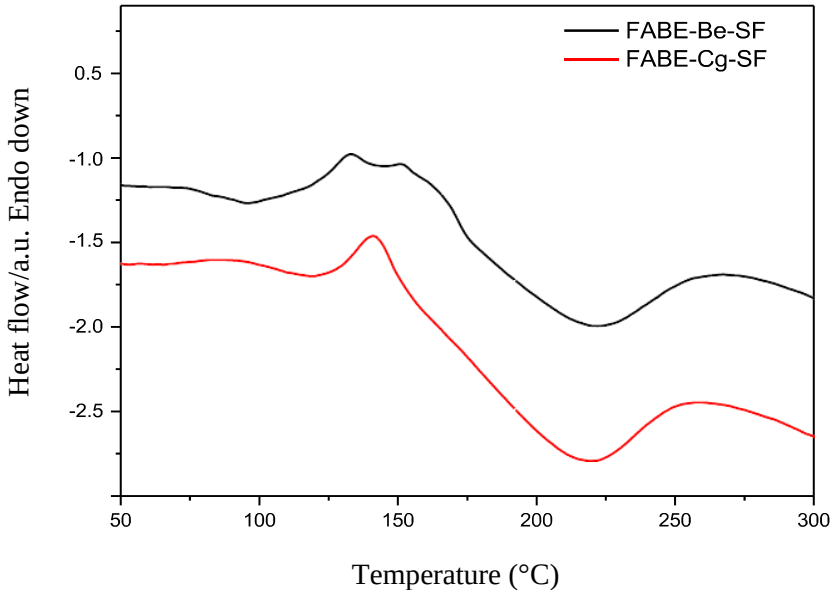

Fig. 3.3. DSC curves from silk fibroin nanoparticles (FABE-Cg-SF-NPs and FABE-Be-SF-NPs) at a heating rate of 10 °C.min^{-1}, nitrogen atmosphere at 50 cm^3.min^{-1}.

3.3.3.4. Transmission electron microscopy (TEM)

The micrographs of Transmission electron microscopy showed that the nanoparticles of FABE-Cg-SF-NPs and FABE-Be-SF-NPs exhibited uniform distribution and spherical particles, surrounded by the silk fibroin polymer wall (Fig. 3.4). Through TEM, it was observed

that the nanoparticles (FABE-Cg-SF-NPs and FABE-Be-SF-NPs) showed some aggregation between two or more particles, causing the particles to vary in sizes from 200 to 300 nm, which corroborates with the polydispersity index values obtained with the DLS measurements presented in Table 3.3. However, the FABE-Cg-SF-NPs and FABE-Be-SF-NPs exhibited compact stable structures. This may have been induced by the reticulation effect of the silk fibroin chains when they approached for formation of amidic bonds (Pham et al., 2018).

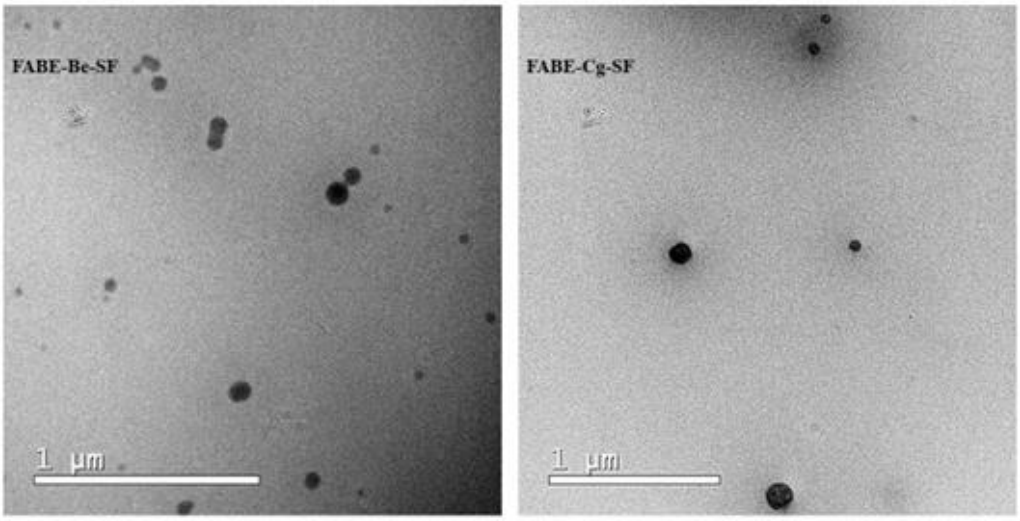

Fig. 3.4. TEM analysis on polymeric silk fibroin nanoparticles (FABE-Be-SF-NPs and FABE-Cg-SF-NPs).

3.3.3.5. FT-IR analysis on polymeric silk fibroin nanoparticles (FABE-Cg-SF-NPs and FABE-Be-SF-NPs)

The FT-IR analyses on the solution of silk fibroin and the nanoparticles (FABE-Cg-SF-NPs and FABE-Be-SF-NPs) exhibited characteristic bands for silk fibroin (Fig. 3.5). Bands in the region from 1600 to 1640 cm^{-1} were observed, corresponding to the (C = O) group of amide I. Bands present in the region from 1520 to 1540 cm^{-1} corresponded to the (N – H) group of amide II and those between 1230 and 1270 cm^{-1} were characteristic of the (C – N) and (N – H) groups of amide III. Together, these bands corresponded to the conformations of the protein material and represented the β-sheet structure of silk fibroin II. Intramolecular β-sheet bands increase during the process of formation of polymeric silk fibroin nanoparticles, due to interactions between the organic solvent and the hydrophobic region of the fibroin (Carvalho et al., 2018).

The FT-IR spectra for FABE-Cg-SF-NPs and FABE-Be-SF-NPs were similar to that of silk fibroin. Therefore, it could be deduced that silk fibroin forms the wall of the nanoparticles, while esters are at their core, as seen in TEM micrographs.

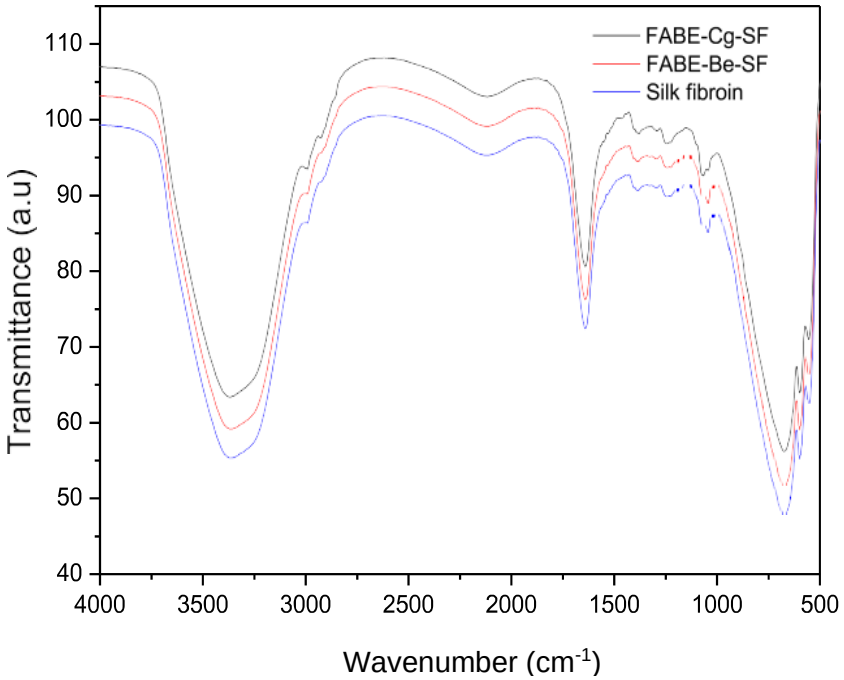

Fig. 3.5. FT-IR spectra of silk fibroin (SF) and nanoparticles (FABE-Be-SF-NPs and FABE-Cg-SF-NPs).

3.3.3.6. In vitro release of butyl esters from FABE-Be-SF-NPs and FABE-Cg-SF-NPs

The *in vitro* release profiles of the butyl esters from the nanoparticles (FABE-Cg-SF-NPs and FABE-Be-SF-NPs) were determined through a 24 h dissolution assay. Quantification of the free esters dispersed in the release medium was performed using the UV-vis technique. FABE-Cg-SF NPs showed release rates of 45% in the first 8 h and 70% in 24 h. While FABE-Be-SF NPs showed release rates of 20% in the first 8 h and 40% in 24 h (Fig. 3.6). This seemed indicate that the nanoparticles (FABE-Cg-SF-NPs and FABE-Be-SF-NPs) exhibited slow and sustained release profiles.

Generally, in the case of polymeric nanoparticles, the drug release profile is attributed to the diffusion process through the pores of the polymer wall (Schaffazick et al., 2003). Thus, the diffusion process seems to be the main release mechanism of the butyl esters contained in the nanoparticles. Moreover, the differences in the lipid composition of the esters influenced not only the particle size but also the PdI of the nanoparticles which may have influenced the release of the lipids.

The ester release data were fitted using various kinetic models to better understand the release mechanism of the esters in the formulations. However, the release profile obtained for both formulations was best fitted by the Korsmeyer-Peppas kinetic model, which confirms that the initial release model may be by diffusion or swelling (Pourtalebi Jahromi et al., 2020). FABE-Cg-SF-NPs and FABE-Be-SF-NPs nanoparticles showed correlation coefficient (R^2) values of 0.999 and 0.995, respectively.

The FABE-Be-SF-NPs showed a slower release rate than FABE-Cg-SF-NPs, inferring this fact to a better interaction of the butyl esters of *B. excelsa* to the polymer matrix of the silk fibroin nanoparticles. This results was interesting, since this change in the release profile can lead to several positive factors, among them we highlight the reduction of the amount of chemical necessary for pest control, reduction of the risk of environmental contamination, reduction of the amount of energy spent, since the number of necessary applications compared to conventional formulations is reduced, in addition to other (Silva et al., 2010).

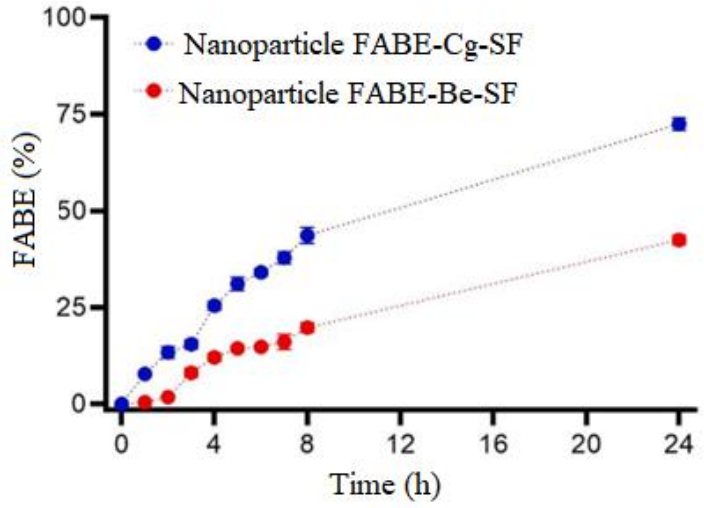

Fi**g. 3.6**. Release profile of polymeric silk fibroin nanoparticles (FABE-Cg-SF-NPs and FABE-Be-SF-NPs), over a 24 h period (n = 3).

3.4. Larvicidal activity of polymeric silk fibroin nanoparticles (FABE-Cg-SF-NPs and FABE-Be-SF-NPs) and oviposition deterrence test against Ae. aegypti

The results regarding the larvicidal efficacy of FABE-Cg-SF-NPs and FABE-Be-SF-NPs are presented in Table 3.4. The FABE-Cg-SF-NPs showed better larvicidal effect after 24 h of contact with larvae of *Ae. aegypti*, with 94% mortality at the highest concentration (75 $\mu g.mL^{-1}$) and 8% at the lowest concentration (7.5 $\mu g.mL^{-1}$). For FABE-Be-SF-NPs, the

mortality rate was 66% at the concentration of 75 µg.mL^{-1} and 4% at the concentration of 7.5 µg.mL^{-1} (Fig. 3.7A).

After 48 h of treatment, a slight increase in larvicidal effect was observed for FABE-Be-SF-NPs, with 100% mortality at the concentration of 75 µg.mL^{-1} and 20% at the concentration of 7.5 µg.mL^{-1}. The nanoformulation of FABE-Cg-SF-NPs showed 98% mortality at the concentration of 75 µg.mL^{-1} and 20% at the concentration of 7.5 µg.mL^{-1} (Fig. 3.7B). In contrast, a negative control consisting solely of fibroin solution exhibited no larvicidal action.

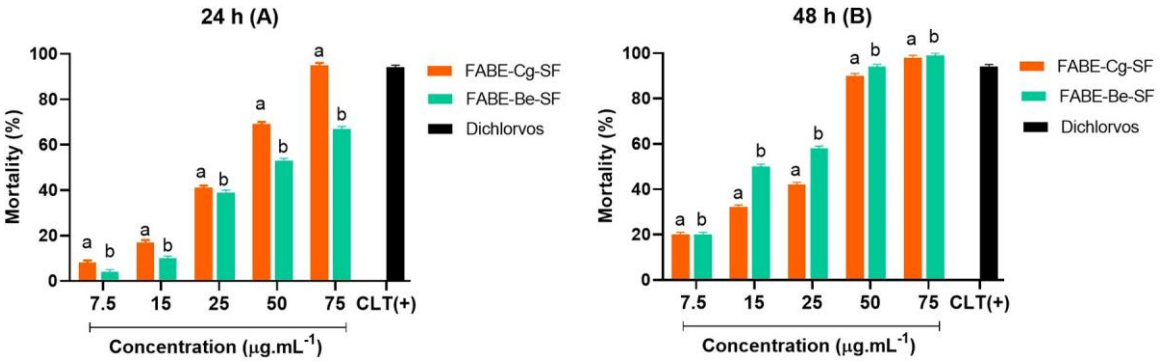

Fig. 3.7. Percentage mortality of *Ae. aegypti* after 24 h (**A**) and 48 h (**B**) of exposure to the nanoparticles (FABE-Cg-SF-NPs and FABE-Be-SF-NPs) at different concentrations. CLT (+): dichlorvos solution (6.25 ng.mL^{-1}). Each value in the column graph is the mean of five repetitions ± standard deviation and represents the mortality rate of the two nanoformulations. Statistical significance is shown by different lower-case letters, based on the ANOVA test ($p < 0.05$).

We also evaluated the LC_{50} and LC_{90} values for the nanoparticles at 24 and 48 h (Table 3.4). After 24 h of larval exposure to the formulations, the FABE-Cg-SF-NPs showed better larvicidal activity, with LC_{50} of 40.88 µg.mL^{-1} and LC_{90} of 68.22 µg.mL^{-1}. FABE-Be-SF-NPs showed LC_{50} of 52.99 µg.mL^{-1} and LC_{90} of 95.57 µg.mL^{-1}. After 48 h, FABE-Be-SF-NPs showed LC_{50} of 21.14 µg.mL^{-1} and LC_{90} of 41.11 µg.mL^{-1}; and FABE-Cg-SF-NPs exhibited LC_{50} of 27.45 µg.mL^{-1} and LC_{90} of 51.87 µg.mL^{-1}. These results showed that the larvicidal action of the nanoparticles was dependent on the composition of fatty acids present in the lipid matrix.

Table 3.4 LC_{50} and LC_{90} values for *Ae. aegypti* in contact with the polymeric silk fibroin nanoparticles (FABE-Be-SF-NPs and FABE-Cg-SF-NPs).

	24 hours				**48 hours**			
	LC_{50} (µg.mL^{-1}) (LCL-UCL)	LC_{90} (µg.mL^{-1}) (LCL-UCL)	X^2 (df = 4)	P	LC_{50} (µg.mL^{-1}) (LCL-UCL)	LC_{90} (µg.mL^{-1}) (LCL-UCL)	X^2 (df = 4)	P
FABE-Cg-SF-NPs	40.88 (2.22 – 45.62)	68.22 (3.92 – 77.37)	3.68820	0.450	27.45 (1.86 – 31.40)	51.87 (3.51 – 60.25)	8.0158	0.091
FABE-Be-SF-NPs	52.99 (3.44 – 60.82)	95.57 (7.29 – 113.63)	17.3142	0.002	21.14 (1.54 – 24.45)	41.11 (3.06 – 48.63)	11.3448	0.023

*LC – lethal concentration (50% and 90%); LCL – lower confidence limit; UCL – upper confidence limit; X^2 – chi-square; df – degree of freedom; significant at $P < 0.05$.

Use of natural compounds from plants and/or their derivatives has been investigated for mosquito control. For example, vegetable oils rich in fatty acids have shown larvicidal action against *Culex quinquefasciatus* (Kannathasan et al., 2008; Perumalsamy et al., 2015). This action is seen especially when long-chain unsaturated fatty acids are present in the composition of these oils (Bury et al., 1998). However, in another study, it was observed that oleic, linoleic and linolenic fatty acids and their respective methyl esters had lower LC_{50} than saturated fatty acids (palmitic and stearic), against *C. quinquefasciatus* larvae (Rocha et al., 2018).

Sarquis et al. (2020) evaluated the larvicidal activity of a nanoemulsion of *C. guianensis* free fatty acid in association with silk fibroin against third-instar larvae of *Ae. aegypti*. They found 68% larval mortality at 50 $\mu g.mL^{-1}$ (LC_{50} = 16.79 $\mu g.mL^{-1}$) after 48 h of exposure. Furthermore, Marinho et al. (2022) produced polymeric silk fibroin nanoparticles combined with fatty acid esters from *Astrocaryum murumuru* fat and observed that the nanoparticles thus produced induced 100% mortality of third-instar larvae of *Ae. aegypti* at 75 $\mu g.mL^{-1}$ (LC_{50} = 21.35 $\mu g.mL^{-1}$) after 48 h of treatment.

The larvicidal effect of nanosystems such as nanoparticles has been correlated with denaturation of proteins essential to larvae (Byrne, 1988). Penetration and transmission of the nanoinsecticide formulation occurs through the larval exoskeleton (Lomonaco et al., 2009). In addition, other mechanisms of action such as inhibition of chitin synthesis (inhibiting larvae growth), inhibition of acetylcholinesterase and inhibition of GABA have been observed (Marcombe et al., 2018).

The toxicity of the nanoparticles has been correlated with their nanoscale particle size and the slow and gradual release of the active agents present in the formulation (Anjali et al., 2012; Oliveira et al., 2016). However, the diversity of compounds present in the oils needs to be taken into account, and it is likely that the efficacy of larvicidal action also occurs through several other mechanisms that may be acting synergistically (Amado et al., 2020).

In the oviposition deterrence assay, it was observed that the polymeric silk fibroin nanoparticles associated with butyl esters inhibited the oviposition action of females of *Ae. aegypti*. Females preferred ovitraps in the control group containing water only, which gave rise to an oviposition rate of 39%. On the other hand, the control group containing silk fibroin solution showed oviposition rates of 25.3% and 28.8% for the trials with FABE-Cg-SF-NPs and FABE-Be-SF-NPs, respectively (Table 3.5). Females showed only 6% preference for the ovitraps containing FABE-Cg-SF-NPs at the concentration of 100 $\mu g.mL^{-1}$ and 8% for FABE-Be-SF-NPs at the same concentration.

The analysis of variance presented $p<0.05$, thus demonstrating that this assay showed a significant difference between the concentrations administered (100, 50 and 25 µg.mL^{-1}), in relation to the control groups. Thus, it can be suggested that the nanoparticles presented repellency in relation to the females, such that they helped prevent egg-laying (Fig. 3.8).

Table 3.5 Effects of polymeric silk fibroin nanoparticles (FABE-Be-SF-NPs and FABE-Cg-SF-NPs) on the oviposition action of females of *Ae. aegypti.*

	OA (%) Water	**OA (%) Silk Fibroin 2%**	**OA (%) 100 µg.mL^{-1}**	**OA (%) 50 µg.mL^{-1}**	**OA (%) 25 µg.mL^{-1}**	**P value**
FABE-Cg-SF-NPs	39	25.3	6	11.1	14.6	p<0.0001
FABE-Be-SF-NPs	39	28.8	8	11.6	15.1	p<0.0001

OA = Oviposition activity.

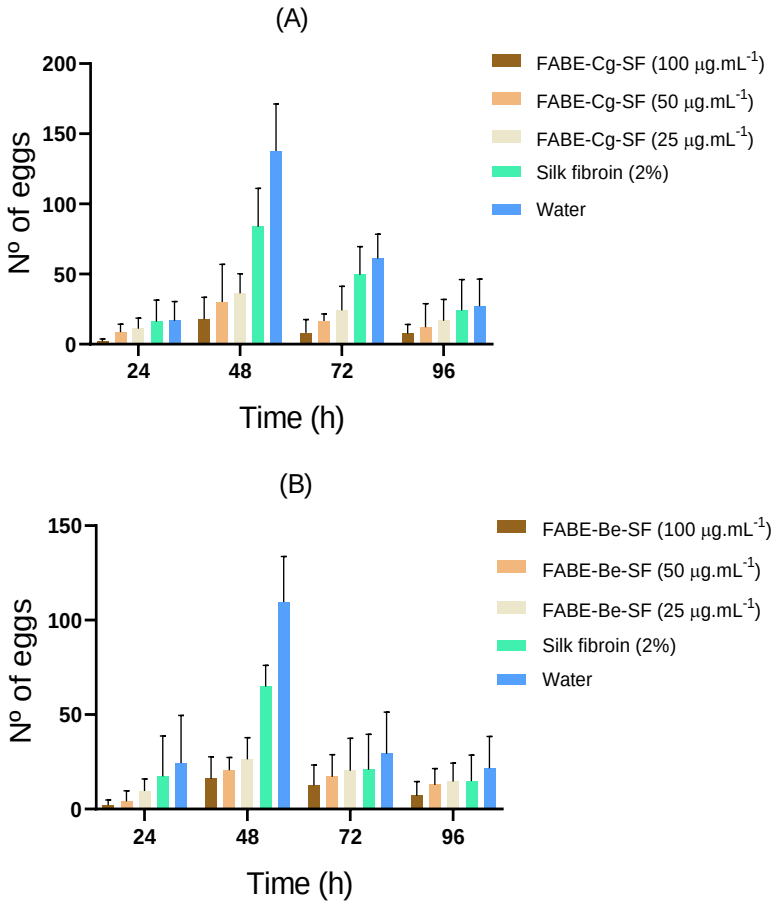

Fig. 3.8. Effect of polymeric silk fibroin nanoparticles (FABE-Cg-SF-NPs and FABE-Be-SF-NPs) on oviposition of pregnant females of *Ae. aegypti*. The bars represent the percentage corresponding to the average number of eggs laid by the females in the controls (water and 2% silk fibroin solution).

A study on the oviposition effect of *Syagrus coronata* oil showed that this oil yielded an oviposition index among females of *Ae. aegypti* of -0.35 to 50 µg.mL^{-1}. In the same study, the deterrent effect of octanoic acid was observed, with a deterrence index of -0.31 at the same concentration (Nascimento et al., 2017). Water-dispersible tablets containing neem oil, which is rich in oleic, linoleic, palmitic, stearic and arachidonic acid, were able to deter oviposition among females of *Anopheles culicifacies*, with 89% efficiency (Kala et al., 2019).

Previous studies have shown that oxygenated hydrocarbons are capable of stimulating responses in the antennae of *Ae. aegypti* females, thus interfering with egg laying by these females (Bezerra-Silva et al., 2016). Thus, it can be inferred that the deterrent effect of silk fibroin nanoparticles associated with butyl esters of Amazonian oils may be related to the stimulus caused by the butyl esters to the antennal sensillae of *Ae. aegypti* females.

3.5. Morphological analysis on larvae of Ae. aegypti

The effect of nanoparticles (FABE-Be-SF-NPs and FABE-Cg-SF-NPs) on the external morphology of larvae of *Ae. aegypti* was observed (Fig. 3.9). Optical microscopy images revealed the presence of precipitates of nanoparticles in the bodies of the larvae, causing damage to the cuticles. This, possibly contributed to the penetration of the nanoparticles into the interior of the larvae. Their bodies became dark, distorted and contracted. In addition, the final segment of the larvae, which includes the abdomen (**AB**), respiratory siphon (**S**) and anal papilla (**AP**), presented swelling (Fig. 3.9A). In contrast, these changes to the external morphology of the larvae were not observed in the control group treated with 2% silk fibroin solution (Fig. 3.9B). Results similar to these were reported by Sarquis et al. (2020), who used nanoemulsions of ethyl esters of *C. guianensis* combined with fibroin, and by Araújo et al. (2020), who used a hexanic extract from the leaves of *Acmella oleracea* dissolved in a solution of silk fibroin.

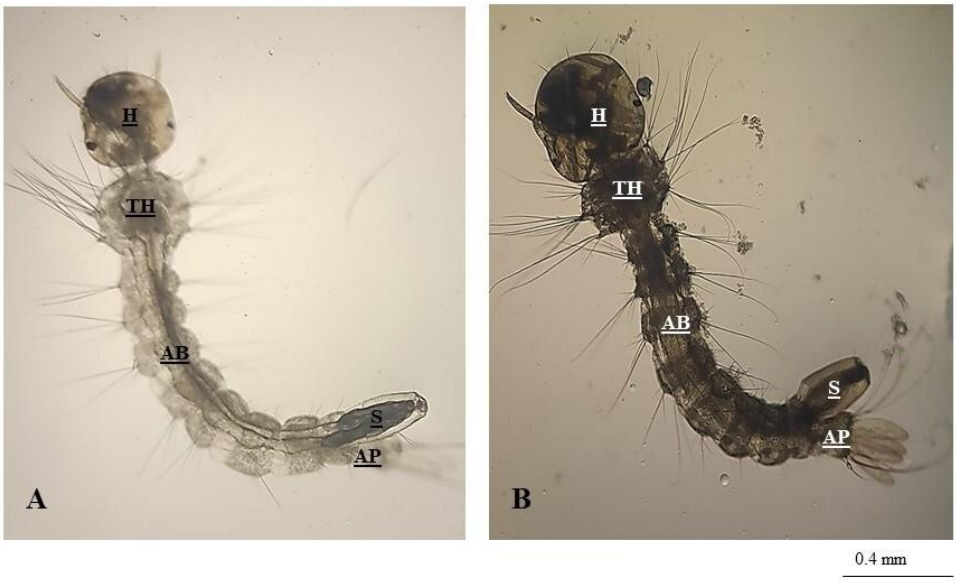

Fig. 3.9. Optical microscopy image of *Ae. aegypti* larva (0.4 mm). (A) Larva exposed to negative control (2% silk fibroin). (B) Larva treated with polymeric silk fibroin nanoparticles (FABE-Cg-SF-NPs) showing deformation, darkening and swelling of its abdomen (**AB**), respiratory siphon (**S**) and anal papilla (**AP**).

3.6. Evaluation of the toxicity of polymeric silk fibroin nanoparticles (FABE-Cg-SF-NPs and FABE-Be-SF-NPs) in zebrafish embryos

Use of zebrafish embryos in a toxicity assay has several advantages as an experimental model, because the embryos are transparent and have high reproduction and fertilization rates, rapid growth and a short life cycle. This enables a variety of experimental tests that make it possible to observe the toxic effects of different pollutants, such as nanomaterials, pesticides, pharmaceuticals, industrial chemical residues and heavy metals, among others (Busquet et al., 2014).

The main changes to embryotoxicity in zebrafish are evaluated within 96 h after exposure to the test substance. These trials evaluate mortality rate changes, head malformations, cardiac edema, calf sac edema, malformations and tail detachment (Verma et al., 2021).

In our study, the nanoparticles (FABE-Cg-SF-NPs and FABE-Be-SF-NPs) in zebrafish embryos (*Danio rerio*) showed no significant toxicity at concentrations tested at up to 96 hpf (Fig. 3.10). However, the positive control performed with dichlorvos (6.25 ng.mL^{-1}) gave rise to embryonic toxicity with 100% mortality in the initial hours of embryo development. On the other hand, the groups of negative controls treated with water and 2% silk fibroin solution did not present morphological damage or mortality.

In the literature, biogenic silica nanoparticles loaded with thymol did not induce lethal or sublethal effects on zebrafish embryos, even at the highest tested concentration of 793 $mg.L^{-1}$ (Pereira et al., 2021). A toxicological evaluation on titanium dioxide nanoparticles also showed no teratogenic effects on zebrafish embryos up to 96 hpf, at a concentration of 100 $mg.L^{-1}$ (Vranic et al., 2019).

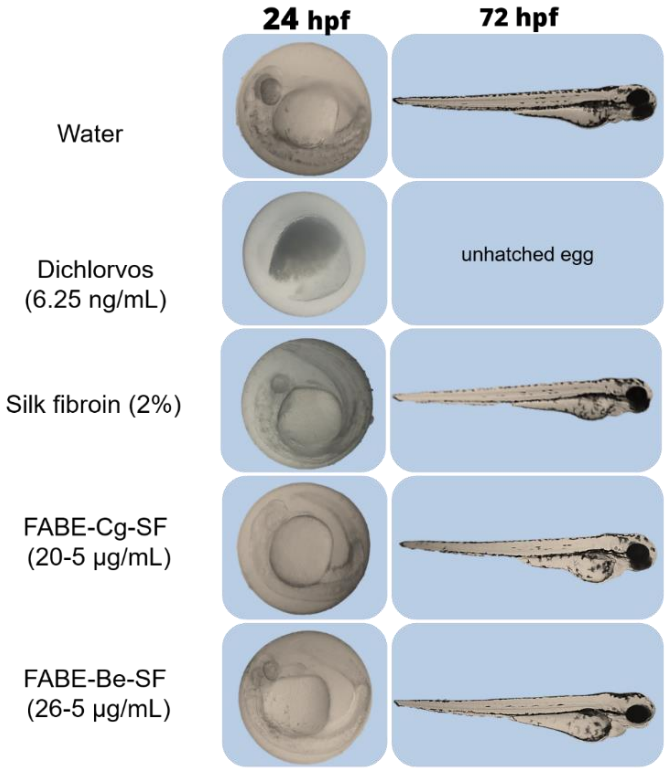

Fig. 3.10. Representative image of zebrafish embryos exposed to polymeric silk fibroin nanoparticles up to 72 hours after fertilization (hpf).

3.7 CONCLUSION

Polymeric nanoparticles of silk fibroin (FABE-Cg-SF-NPs and FABE-Be-SF-NPs) preparate with butyl esters derived from *C. guianensis* and *B. excelsa* oils showed temporal good stability up to 50 days of storage at temperatures of 4 and 32 ºC. The nanoparticles were spherical in shape, with diameters ranging from 200 to 300 nm. The release profile of the nanoparticles was considered slow and gradual, which favored a high larvicidal action at low lethal concentrations. FABE-Cg-SF-NPs and FABE-Be-SF-NPs showed CL_{50} of 27.45 $\mu g.mL^{-1}$ and 21.14 $\mu g.mL^{-1}$, respectively, after 48 h of treatment against the larvae of the vector *Aedes aegypti*. The nanoparticles produced morphological damage in the larvae and were effective in

inhibiting oviposition of gravid females of *Ae. aegypti*. Furthermore, no teratogenic effect of the nanoparticles was observed in zebrafish embryos up to 72 h after fertilization. Thus, silk fibroin nanoparticles can be an interest sustainable alternative and effective tool to improve the control of *Ae. aegypti* larvae.

Credit authorship contribution statement

Victor H. Marinho, Fabricio H. Holanda and Irlon M. Ferreira: Conceptualization, Methodology, Validation, Software, Formal analysis, Investigation, Data curation, Writing – original draft. **Inana F. Araújo,** Ricardo M. A. Ferreira**, David E. J. Quintero, Rayanne R. Pereira, Ana C. G. Albuquerque de Freitas, Adriana M. Ferreira:** Methodology, Investigation, Writing – original draft, Writing – review & editing, Visualization. **Irlon M. Ferreira, Raimundo N. P. Souto, André L. M. Porto and José C. T. Carvalho:** Conceptualization, Supervision, Project administration, Funding acquisition.

Declaration of Competing Interest

The authors declare that they have no known competing financial interests or personal relationships that could have influenced the present study.

Acknowledgements

The authors would like to acknowledge the Research Support Foundation of the State of Amapá (Fundação de Amparo à Pesquisa do Estado do Amapá, FAPEAP; grant no. 34568.515.22257.28052017) and the Coordination Office for the Improvement of Higher Education Personnel - Brazil (CAPES), for partial funding of the present work; and the Graduate Program in Biodiversity and Biotechnology of the BIONORTE Network (PPG-BIONORTE) for financial support.

Supplementary data associated with this article can be found in the online version at doi: 10.1016/j.indcrop.2023.117133.

3.8 REFERENCES

Amado, J R.R., Prada, A.L., Diaz, J.G., Nonato, R., Souto, P., Cesar, J., Arranz, E., Souza, T.P. De, 2020. Development, larvicide activity, and toxicity in nontarget species of the *Croton linearis* Jacq essential oil nanoemulsion. Environ. Sci. Pollut. Res. Int. 27, 9410–9423.

Amiri, M.S., Joharchi, M.R., TaghavizadehYazdi, M.E., 2014. Ethno-medicinal plants used to cure jaundice by traditional healers of Mashhad, Iran. Iran. J. Pharm. Res. 13, 157–162.

Anarjan, N., Tan, C.P., 2013. Chemical stability of astaxanthin nanodispersions in orange juice and skimmed milk as model food systems. Food Chem. 139, 527–531.

Anjali, C.H., Sharma, Y., Mukherjee, A., Chandrasekaran, N., 2012. Neem oil (*Azadirachta indica*) nanoemulsion: a potent larvicidal agent against *Culex quinquefasciatus*. 158–163.

Araújo, I.F., Loureiro, H.A., Marinho, V.H.S., Neves, F.B., Sarquis, R.S.F., Faustino, S.M.M., Yoshioka, S.A., Ferreira, R.M.A., Souto, R.N.P., Ferreira, I.M., 2020. Larvicidal activity of the methanolic, hydroethanolic and hexanic extracts from *Acmella oleracea*, solubilized with silk fibroin, against *Aedes aegypti*. Biocatal. Agric. Biotechnol. 24, 101550.

Araújo, I.F., Marinho, V.H. de S., Sena, I. da S., Curti, J.M., Ramos, R. da S., Ferreira, R.M.A., Souto, R.N.P., Ferreira, I.M., 2022. Larvicidal activity against *Aedes aegypti* and molecular docking studies of compounds extracted from the endophytic fungus *Aspergillus sp*. isolated from Bertholletia excelsa Humn. & Bonpl. Biotechnol. Lett. 44, 439–459.

Ashna, M., Es-Haghi, A., Karimi Noghondar, M., Al Amara, D., Yazdi, M.E.T., 2022. Greener synthesis of cerium oxide nanoemulsion using pollen grains of *Brassica napus* and evaluation of its antitumour and cytotoxicity properties. Mater. Technol. 37, 525–532.

Aswathanarayan, J.B., Vittal, R.R., 2019. Nanoemulsions and their potential applications in food industry. Front. Sustain. Food Syst. 3, 1–21.

Bajerski, L., Michels, L.R., Colomé, L.M., Bender, E.A., Freddo, R.J., Bruxel, F., Haas, S.E., 2016. The use of Brazilian vegetable oils in nanoemulsions: an update on preparation and biological applications. Brazilian J. Pharm. Sci. 52, 347–363.

Balasubramanian, A., Teramoto, T., Kulkarni, A.A., Bhattacharjee, A.K., Padmanabhan, R., 2017. Antiviral activities of selected antimalarials against dengue virus type 2 and Zika virus. Antiviral Res. 137, 141–150.

Barata, P.H.S., Sarquis, Í.R., Carvalho, H.O., Barros, A.S., Rodrigues, A.B., Galue-Parra, A.J., Silva, E.O., Carvalho, J.C.T., Ferreira, I.M., 2020. Chemoenzymatic synthesis and anti-inflammatory activity of fatty acid amides prepared from *Bertholletia excelsa* (Brazil Nut) triglycerides. J. Braz. Chem. Soc. 31, 1557–1565.

Beckham, J.D., Tyler, K.L., 2015. Arbovirus infections. Contin. Lifelong Learn. Neurol. 21, 1599–1611.

Beltrão, N.E.M., Oliveira, M.I.P., 2007. Oleaginosas potenciais do nordeste para a produção de biodiesel. Documentos 177, 1–54.

Bezerra-silva, P.C., Dutra, K.A., Santos, G.K.N., Silva, R.C.S., 2016. Evaluation of the activity of the essential oil from an ornamental flower against *Aedes aegypti*: electrophysiology, molecular dynamics and behavioral assays 1–15.

Bigaj-Józefowska, M.J., Grześkowiak, B.F., 2022. Polymeric nanoparticles wrapped in biological membranes for targeted anticancer treatment. Eur. Polym. J. 176.

Borges, R.S., Keita, H., Ortiz, B.L.S., dos Santos Sampaio, T.I., Ferreira, I.M., Lima, E.S., de Jesus Amazonas da Silva, M., Fernandes, C.P., de Faria Mota Oliveira, A.E.M., da Conceição, E.C., Rodrigues, A.B.L., Filho, A.C.M.P., Castro, A.N., Carvalho, J.C.T., 2018. Anti-inflammatory activity of nanoemulsions of essential oil from *Rosmarinus officinalis* L.: in vitro and in zebrafish studies. Inflammopharmacology 26, 1057–1080.

Bury, N.R., Codd, G.A., Bonga, S.E.W., Flik, G., 1998. Fatty acids from the cyanobacterium *Microcystis aeruginosa* with potent inhibitory effects on fish gill Na^+/K^+-ATPase activity. J. Exp. Biol. 89, 81–89.

Busquet, F., Strecker, R., Rawlings, J.M., Belanger, S.E., Braunbeck, T., Carr, G.J., Cenijn, P., Fochtman, P., Gourmelon, A., Hübler, N., Kleensang, A., Knöbel, M., Kussatz, C., Legler, J., Lillicrap, A., Martínez-jerónimo, F., Polleichtner, C., Rzodeczko, H., Salinas, E., Schneider, K.E., Scholz, S., Brandhof, E. Van Den, Ven, L.T.M. Van Der, Walter-rohde, S., Weigt, S., Witters, H., Halder, M., 2014. OECD validation study to assess intra- and inter-laboratory reproducibility of the zebrafish embryo toxicity test for acute aquatic toxicity testing 69, 496–511.

Byrne, M.F.R., 1988. Plant-insect coevolution and inhibition of acetylcholinesterase. J. Chem. Ecol. 14.

Cao, Z., Chen, X., Yao, J., Huang, L., Shao, Z., 2007. The preparation of regenerated silk fibroin microspheres. Soft Matter 3, 910–915.

Carvalho, L., Araújo, P., Martins, J., Júnior, D.O., 2018. Synthesis and characterization of fibroin scaffolds. Rev. Mat. 23, 1-9.

da Costa Vieira, M., Bakof, K.K., Schuch, N.J., Skupien, J.A., Boeck, C.R., 2020. The benefits of omega-3 fatty acid nanocapsulation for the enrichment of food products: a review. Rev. Nutr. 33, 1–12.

de Oliveira, J.L., Campos, E.V.R., Bakshi, M., Abhilash, P.C., Fraceto, L.F., 2014. Application of nanotechnology for the encapsulation of botanical insecticides for sustainable agriculture: Prospects and promises. Biotechnol. Adv. 32, 1550–1561.

de Oliveira Penido, C.A.F., Pacheco, M.T.T., Novotny, E.H., Lednev, I.K., Silveira, L., 2017. Quantification of cocaine in ternary mixtures using partial least squares regression applied

to Raman and Fourier transform infrared spectroscopy. J. Raman Spectrosc. 48, 1732–1743.

Donalisio, M.R., Freitas, A.R.R., Zuben, A.P.B. Von, 2017. Arboviruses emerging in Brazil: challenges for clinic and implications for public health. Rev. Saude Publica 51, 10–15.

Duarte, J.L., Filippo, L.D. Di, Araujo, V.H.S., Oliveira, A.E.M. de F.M., de Araújo, J.T.C., Silva, F.B. da R., Pinto, M.C., Chorilli, M., 2021. Nanotechnology as a tool for detection and treatment of arbovirus infections. Acta Trop. 216.

Ekambaram, P., Sathali, A.A.H., Priyanka, K., 2012. Solid lipid nanoparticles: a review 2, 80–102.

Elson, F., Montero, I.F., Melo, A. a, Santos, R.C., Romulo, P., Ribeiro, E., Karina, A., Costa, P., Cristina, A., Melo, G. De, 2014. Full paper propiedades físico-químicas por RMN de 1 H y constituyentes en el aceite de *Carapa guianensis* por ESI-MS. Orbital-The Electron. J. Chem. 6.

Ferreira, A.M., da S. Sena, I., Magalhães, K.F., Oliveira, S.L., Ferreira, I.M., Porto, A.L.M., 2019. Amazon Oils from Andiroba (*Carapa* sp.) and Babassu (*Orbignya* sp.) for Preparation Biodiesel by Enzymatic Catalysis. Curr. Biotechnol. 7, 428–437.

Ferreira, I.M., Ganzeli, L.D.S., Rosset, I.G., Yoshioka, S.A., 2017. Ethylic biodiesel production using lipase immobilized in silk fibroin-alginate spheres by encapsulation. Catal. Letters 147, 269–280.

Ferreira, I.M., Nishimura, R.H.V., Souza, A.B.D.A., Clososki, G.C., Yoshioka, S.A., Porto, A.L.M., 2014. Highly enantioselective acylation of chlorohydrins using Amano AK lipase from *P. fluorescens* immobilized on silk fibroin-alginate spheres. Tetrahedron Lett. 55, 5062–5065.

Gumus, C.E., Decker, E.A., Julian, D., 2017. Impact of legume protein type and location on lipid oxidation in fish oil-in-water emulsions: Lentil, pea, and faba bean proteins, Food Research International, Part 2, 175-185.

Gupta, A., Eral, H.B., Hatton, T.A., Doyle, P.S., 2016. Nanoemulsions: Formation, properties and applications. Soft Matter 12, 2826–2841.

Holanda, F.H., Ribeiro, A.N., Sánchez-Ortiz, B.L., de Souza, G.C., Borges, S.F., Ferreira, A.M., Florentino, A.C., Yoshioka, S.A., Moraes, L.S., Carvalho, J.C.T., Ferreira, I.M., 2022. Anti-inflammatory potential of baicalein combined with silk fibroin protein in a zebrafish model (*Danio rerio*). Biotechnol. Lett. 45, 235–253.

Huang, S., Gu, J., Ye, J., Fang, B., Wan, S., Wang, C., Ashraf, U., Li, Q., Wang, X., Shao, L., Song, Y., Zheng, X., Cao, F., Cao, S., 2019. Benzoxazine monomer derived carbon dots

as a broad-spectrum agent to block viral infectivity. J. Colloid Interface Sci. 542, 198–206.

Jadhav, P.A., Yadav, A. V, 2020. Polymeric Nanosuspension loaded oral thin films of flurbiprofen: design , development and *in vitro* evaluation 13, 1905–1910.

Jafarizadeh-malmiri, O.A.H., 2020. Green approach in food nanotechnology based on subcritical water: effects of thyme oil and saponin on characteristics of the prepared oil in water nanoemulsions. Food Sci. Biotechnol. 29, 783–792.

Kabalnov, A., 1998. Thermodynamic and theoretical aspects of emulsions and their stability. Curr. Opin. Colloid Interface Sci. 3, 270–275.

Kala, S., Naik, S.N., Patanjali, P.K., Sogan, N., 2019. Neem oil water dispersible tablet as effective larvicide, ovicide and oviposition deterrent against *Anopheles culicifacies*. South African J. Bot. 123, 387–392.

Kannathasan, K., Senthilkumar, A., Venkatesalu, V., Chandrasekaran, M., 2008. Larvicidal activity of fatty acid methyl esters of *Vitex* species against *Culex quinquefasciatus*. Parasitol. Res. 103, 999–1001.

Koh, L.D., Cheng, Y., Teng, C.P., Khin, Y.W., Loh, X.J., Tee, S.Y., Low, M., Ye, E., Yu, H.D., Zhang, Y.W., Han, M.Y., 2015. Structures, mechanical properties and applications of silk fibroin materials. Prog. Polym. Sci. 46, 86–110.

Kumar, S., Nehra, M., Dilbaghi, N., Marrazza, G., Hassan, A.A., Kim, K.H., 2019. Nano-based smart pesticide formulations: emerging opportunities for agriculture. J. Control. Release 294, 131–153.

Lam, R.S.H., Nickerson, M.T., 2013. Food proteins: a review on their emulsifying properties using a structure-function approach. Food Chem. 141, 975–984.

Lomonaco, D., Pinheiro, M., Ferreira, S., Arriaga, M.C., Mazzetto, E., Vasapollo, G., 2009. Study of technical CNSL and its main components as new green larvicides 31–33.

Lucca, L.G., de Matos, S.P., Kreutz, T., Teixeira, H.F., Veiga, V.F., de Araújo, B. V., Limberger, R.P., Koester, L.S., 2018. Anti-inflammatory effect from a hydrogel containing nanoemulsified Copaiba oil (*Copaifera multijuga* Hayne). AAPS PharmSciTech 19, 522–530.

Lutz, I.A., 2008. Métodos físicos-químicos para análise de alimentos. Inst. Adolfo Lutz 1020.

Malheiros, D.F., Sarquis, I.R., Ferreira, I.M., Mathews, P.D., Mertins, O., Tavares-Dias, M., 2020. Nanoemulsions with oleoresin of *Copaifera reticulata* (Leguminosae) improve anthelmintic efficacy in the control of monogenean parasites when compared to oleoresin without nanoformulation. J. Fish Dis. 43, 687–695.

Malheiros, D.F., Videira, M.N., Ferreira, I.M., Tavares-Dias, M., 2022. Anthelmintic efficacy of *Copaifera reticulata* oleoresin in the control of monogeneans and haematological and histopathological effects on *Colossoma macropomum*. Aquac. Res. 53, 4087–4094.

Marcombe, S., Chonephetsarath, S., Thammavong, P., Brey, P.T., 2018. Alternative insecticides for larval control of the dengue vector *Aedes aegypti* in Lao PDR : insecticide resistance and semi-field trial study 1–8.

McClements, D.J., 2012. Nanoemulsions versus microemulsions: Terminology, differences, and similarities. Soft Matter 8, 1719–1729.

McClements, D.J., Jafari, S.M., 2018. Improving emulsion formation, stability and performance using mixed emulsifiers: a review. Adv. Colloid Interface Sci. 251, 55–79.

Nascimento, S., Santos, M.A.G., Marriel, N.B., Bezerra-silva, P.C., Rocha, S.K.L., Silva, A.G., Correia, M.T.S., Silva, V., Paiva, P.M.G., Martins, G.F., Navarro, D.M.A.F., 2017. Physiological and Molecular Plant Pathology fatty acid-rich volatile oil from *Syagrus coronata* seeds has larvicidal and oviposition-deterrent activities against *Aedes aegypti* 100, 35–40.

Niculae, G., Lacatusu, I., Badea, N., Meghea, A., Stan, R., 2014. Influence of vegetable oil on the synthesis of bioactive nanocarriers with broad spectrum photoprotection. Cent. Eur. J. Chem. 12, 837–850.

Nong, Y., Ren, Y., Wang, P., Zhou, M., Yu, Y., Yuan, J., Xu, B., Wang, Q., 2021. A facile strategy for the preparation of photothermal silk fibroin aerogels with antibacterial and oil-water separation abilities. J. Colloid Interface Sci. 603, 518–529.

OECD, 1997. OECD guideline for the testing of chemicals: Fish embryo toxicity (FET) test. Draft Propos. a new Guid. 2006, 1–4.

Oliveira, A.E.M.F.M., Duarte, J.L., Amado, J.R.R., Rodrigo, A., 2016. Development of a Larvicidal Nanoemulsion with Pterodon emarginatus Vogel Oil. Plos one 11(1): e0145835.

Oliveira, S. do S. do C., Sarmento, E. dos S., Marinho, V.H., Pereira, R.R., Fonseca, L.P., Ferreira, I.M., 2022. Green extraction of Annatto seed oily extract and its use as a pharmaceutical material for the production of lipid nanoparticles. Molecules 27.

Ostertag, F., Weiss, J., McClements, D.J., 2012. Low-energy formation of edible nanoemulsions: factors influencing droplet size produced by emulsion phase inversion. J. Colloid Interface Sci. 388, 95–102.

Peniche, T., Duarte, J.L., Ferreira, R.M.A., Sidônio, I.A.P., Sarquis, R.S.F.R., Sarquis, Í.R., Oliveira, A.E.M.F.M., Cruz, R.A.S., Ferreira, I.M., Florentino, A.C., Carvalho, J.C.T.,

Souto, R.N.P., Fernandes, C.P., 2022. Larvicidal effect of *Hyptis suaveolens* (L.) Poit. essential oil nanoemulsion on *Culex quinquefasciatus* (Diptera: Culicidae). Molecules 27.

Pereira, I.B., Sousa, H. De, Rodrigues, D.B., Mattos, D., 2021. Thymol-loaded biogenic silica nanoparticles in an aquatic environment: the impact of particle aggregation on ecotoxicity. 40, 333–341.

Pereira, R.R., Testi, M., Rossi, F., Silva Junior, J.O.C., Ribeiro-Costa, R.M., Bettini, R., Santi, P., Padula, C., Sonvico, F., 2019. Ucuùba (Virola surinamensis) fat-based nanostructured lipid carriers for nail drug delivery of ketoconazole: development and optimization using box-behnken design. Pharmaceutics 11.

Perumalsamy, H., Jang, M.J., Kim, J.R., Kadarkarai, M., Ahn, Y.J., 2015. Larvicidal activity and possible mode of action of four flavonoids and two fatty acids identified in Millettia pinnata seed toward three mosquito species. Parasites and Vectors 8, 1–14.

Pham, D.T., Saelim, N., Tiyaboonchai, W., 2018. Crosslinked fibroin nanoparticles using EDC or PEI for drug delivery: physicochemical properties, crystallinity and structure. J. Mater. Sci. 53, 14087–14103.

Pinto, F., de Barros, D.P.C., Fonseca, L.P., 2018. Design of multifunctional nanostructured lipid carriers enriched with α-tocopherol using vegetable oils. Ind. Crops Prod. 118, 149–159.

Pourtalebi Jahromi, L., Ghazali, M., Ashrafi, H., Azadi, A., 2020. A comparison of models for the analysis of the kinetics of drug release from PLGA-based nanoparticles. Heliyon. 6(2): e03451.

Rafael, J., Amado, R., Prada, A.L., Diaz, J.G., Nonato, R., Souto, P., Cesar, J., Arranz, E., Souza, T.P. De, 2020. Development, larvicide activity, and toxicity in nontarget species of the *Croton linearis* Jacq essential oil nanoemulsion 9410–9423.

Rocha, A., Melo, D., Pereira, I.J., Eduardo, J., Lima, H., 2018. Ecotoxicology and Environmental Safety Toxicity of di ff erent fatty acids and methyl esters on *Culex quinquefasciatus* larvae. Ecotoxicol. Environ. Saf. 154, 1–5.

Sarquis, S.F.R., Marinho, V.H.S., Neves, F.B., Sarquis, I.R., Araújo, I.F., Damasceno, L.F., Ferreira, R.M.A., Souto, R.N.P., Carvalho, C.T., Ferreira, I.M., 2020. Industrial Crops & Products *Carapa guianensis* Aubl. (Meliaceae) oil associated with silk fibroin, as alternative to traditional surfactants, and active against larvae of the vector *Aedes aegypti* 157.

Schaffazick, S.R., Guterres, S.S., Freitas, L. de L., Pohlmann, A.R., 2003. Caracterização e estabilidade físico-química de sistemas poliméricos nanoparticulados para administração de fármacos. Quim. Nova 26, 726–737.

Schroën, K., 2020. Microtechnological tools to achieve sustainable food processes , products, and ingredients. Food Eng. Ver. 12, 101–120

Shi, X., Cao, Y., Li, N., Zhu, N., Chen, Y., Ma, B., 2021. Composition , physicochemical properties , preparation methods and application research status on Functional oils and fats of nanoemulsion: a comprehensive review 792, 1–7.

Silva, S., Cocenza, D.S., Ferreira, N., Melo, S. De, Grillo, R., Rosa, A.H., 2010. Nanopartículas de alginato como sistema de liberação para o herbicida clomazone. Quim. Nova, 33, 1868–1873.

Silveira, M., Silva, E. da, Lima, R.A., 2020. Biodiversidade e Biotecnologia no Brasil. Stricto Sensu. 2, 1-313.

Singh, L., Kruger, H.G., Maguire, G.E.M., Govender, T., Parboosing, R., 2017. The role of nanotechnology in the treatment of viral infections. Ther. Adv. Infect. Dis. 4, 105–131.

Song, D., Forciniti, D., 2000. Effects of Cosolvents and pH on Protein Adsorption on Polystyrene Latex: a dynamic light scattering study. 37, 25–37.

Sukhralia, S., Verma, M., Gopirajan, S., Dhanaraj, P.S., Lal, R., Mehla, N., Kant, C.R., 2019. From dengue to Zika: the wide spread of mosquito-borne arboviruses. Eur. J. Clin. Microbiol. Infect. Dis. 38, 3–14.

Tang, X., Qiao, X., Sun, K., 2015. Colloids and Surfaces A: Physicochemical and Engineering Aspects Effect of pH on the interfacial viscoelasticity and stability of the silk fibroin at the oil/water interface. Colloids Surfaces A Physicochem. Eng. Asp. 486, 86–95.

Tavares Carvalho, J.C., 2016. Obtainment and Study of the Toxicity of Perillyl Alcohol Nanoemulsion on Zebrafish (*Danio rerio*). J. Nanomedicine Res. 4, 18–20.

Vergallo, C., 2020. Nutraceutical vegetable oil nanoformulations for prevention and management of diseases. Nanomaterials 10, 1–30.

Verma, S.K., Nandi, A., Sinha, A., Patel, P., Jha, E., 2021. Zebrafish (*Danio rerio*) as an ecotoxicological model for Nanomaterial induced toxicity profiling 4, 750–781.

Vilhena, A.E.G., Sehwartz, R.L. da C., Bezerra, P.T. da S., Brasil, D. do S.B., 2020. Caracterização físico-química do óleo de castanha do Pará extraído por prensagem hidráulica. Brazilian Appl. Sci. Rev. 4, 859–865.

Vranic, S., Shimada, Y., Ichihara, S., Kimata, M., 2019. Toxicological evaluation of SiO_2 nanoparticles by zebrafish embryo toxicity test. Int. J. Mol. Sci. 20: 882.

Walker, R.M., Gumus, C.E., Decker, E.A., McClements, D.J., 2017. Improvements in the formation and stability of fish oil-in-water nanoemulsions using carrier oils: MCT, thyme oil, & lemon oil. J. Food Eng. 211, 60–68.

Who, 2018. Cd-56/11 Plan of Action on Entomology andVector Control 2018-2023. Orig. English Plan action Entomol. Vector. 1–23.

Whopes, 2005. Guidelines for laboratory and field testing of mosquito larvicides. World Heal. Organ. 1–41.

Wlastra, P., 1996. Encyclopedia of Emulsion Technology. Marcel Dekker 4.

Yan, S., Xu, J., Liu, G., Du, X., Hu, M., Zhang, S., Jiang, L., Zhu, H., Qi, B., Li, Y., 2022. Emulsions co-stabilized by soy protein nanoparticles and tea saponin: Physical stability, rheological properties, oxidative stability, and lipid digestion. Food Chem. 387, 132891.

Yang, X., Sun, Z., Wang, W., Zhou, Q., Shi, G., Wei, F., Jiang, G., 2018. Developmental toxicity of synthetic phenolic antioxidants to the early life stage of zebrafish. Sci. Total Environ. 643, 559–568.

Young, P.R., 2018. Arboviruses: A Family on the Move. Adv Exp Med Biol 1062, 1–10.

Zaharia, C., Tudora, M.R., Stanescu, P.O., Vasile, E., Cincu, C., 2012. Silk fibroin films for tissue bioengineering applications. J. Optoelectron. Adv. Mater. 14, 163–168.

Zhang, S., Tian, L., Yi, J., Zhu, Z., Decker, E.A., Mcclements, D.J., 2020. Mixed plant-based emulsifiers inhibit the oxidation of proteins and lipids in walnut oil-in-water emulsions: Almond protein isolate-camellia saponin. Food Hydrocoll. 106136.

Zhang, Y.Q., Shen, W. De, Xiang, R.L., Zhuge, L.J., Gao, W.J., Wang, W.B., 2007. Formation of silk fibroin nanoparticles in water-miscible organic solvent and their characterization. J. Nanoparticle Res. 9, 885–900.

Zhao, Z., Chen, A., Li, Y., Hu, J., Liu, X., Li, J., Zhang, Y., Li, G., Zheng, Z., 2012. Fabrication of silk fibroin nanoparticles for controlled drug delivery. J. Nanoparticle Res. 14.

Artigo 3

Artigo será submetido no periódico **Biocatalysis and Agricultural Biotechnology** (ISSN 1878-8181) Qualis A3 em biotecnologia, segundo a classificação do quadriênio 2017-2020 da plataforma
Sucupira – CAPES

Potencial controle ecológico de nanopartículas de fibroína de seda e óleos amazônicos contra *Spodoptera frugiperda*

Victor H. S. Marinho[a], Donald Manigat[b], Jéssica C. E. Vilhena[c,d], Silvia M. M. Faustino[c], Raimundo N. P. Souto[b], Irlon M. Ferreira[a,*]

[a]*Laboratório de Biocatálise e Síntese Orgânica Aplicada, Universidade Federal do Amapá, Campus Universitário Marco Zero do Equador, Rodovia Josmar Chaves Pinto, Km 02, Bairro Zerão, 68903-419, Macapá, AP, Brasil.*
[b]*Laboratório de Artrópodes, Universidade Federal do Amapá, Campus Universitário Marco Zero do Equador, Rodovia Josmar Chaves Pinto, Km 02, Bairro Zerão, 68903-419, Macapá, AP, Brasil.*
[c]*Laboratorio de Cultivo de Algas, Curso de Farmacia, Universidade Federal do Amapá, Campus Universitário Marco Zero do Equador, Rodovia Josmar Chaves Pinto, Km 02, Bairro Zerão, 68903-419, Macapá, AP, Brasil.*
[d]*Programa de Pós-Graduação em Ciências Ambientais, Universidade Federal do Amapá, Marco Zero do Equador, Rodovia Josmar Chaves Pinto, Km 02, Bairro Zerão, 68903-419, Macapá, AP, Brasil.*
*Corresponding author: irlon.ferreira@gmail.com /Orcid.org/0000-0002-4517-0105

Resumo

Fibroína de seda (SF) vem sendo aplicada como um biopolímero promissor na produção de sistemas "drug delivery", com vasta aplicação na área médica e ambiental. Neste sentido, o presente estudo teve por objetivo avaliar nanopartículas de fibroína de seda combinadas com ésteres butílicos semissintetizados a partir de óleos amazônicos [(*Astrocaryum murumuru* Mart. (Am-SF-NPs), *Bertolletia excelsa* (Be-SF-NPs) e *Carapa guianensis* (Cg-SF-NPs)] contra as larvas de 3º instar de *Spodoptera frugiperda*, bem como seu o efeito ovicida. As nanopartículas foram monitoradas por 50 dias em diferentes temperaturas (4º C e 32º C), apresentando tamanhos de partículas que variaram de 187.6 (±0.8) nm a 540.8 (±23.8) nm, com índice de polidispersidade de 0.238 a 0.560 e potencial zeta de -39.7 (±1.4) mV a -62.9 (±0.7) mV. As microimagens por TEM mostraram que as nanopartículas apresentaram distribuição uniforme e formato esférico. O método de imersão alimentar foi utilizado para avaliar a atividade larvicida das nanopartículas em diferentes concentrações (5000-292 µg.mL^{-1}). As Be-SF-NPs apresentaram maior taxa de mortalidade larval, cerca de 100%, com valor de LC_{50} de 563.03 µg.mL^{-1}, após 96 h de exposição. As Be-SF-NPs ainda foram capazes de inibir a eclosão dos ovos de *S. frugiperda* em 87% com valor de LC_{50} de 341.03 µg.mL^{-1}. Este é o primeiro registro da atividade larvicida de óleos vegetais amazônicos combinados a nanopartículas de fibroína de seda contra *S. frugiperda*. Este trabalho demostrou que as nanopartículas de fibroína de seda apresentam grande potencial como agentes de biocontrole contra *S. frugiperda* e são promissoras para uma gestão bem sucedida no manejo de insetos-praga.

Palavras-chave: Lagarta-do-Cartucho; Nanomateriais, Biopesticida; Óleos amazônicos; Fibroína de seda.

4.1 INTRODUÇÃO

Spodoptera frugiperda, também conhecida como lagarta-do-cartucho, é um lepidóptero migratório altamente polífago. A espécie causa infestação em uma vasta gama de culturas, incluindo trigo, soja, milho, amendoim, cana-de-açúcar e outras, levando a graves perdas de colheitas (Assefa and Ayalew, 2019). É nativa das Américas, mas relatórios recentes mostram que sua presença na Europa, África e no Sudeste Asiático está cada vez mais comum (Harrison et al., 2018; Togola et al., 2018). No Sudeste Asiático, a espécie tornou-se um importante inseto-praga causando danos significativos às culturas, se o crescimento populacional continuar seguindo neste ritmo, estima-se que num curto período de tempo ela poderá passar de uma praga importada para uma praga endêmica (Elizalde et al., 2020).

A *S. frugiperda* é capaz de reproduzir-se rapidamente, migrar e alimentar-se de uma ampla variedade de plantas hospedeiras, tornando difícil o seu controle (Deshmukh et al., 2020; Maruthadurai and Ramesh, 2020). Por não possui predadores naturais, os inseticidas sintéticos tornam-se o principal método de controle desta espécie. Entretanto, a utilização desses inseticidas não estão sendo capazes de reduzir sua reincidência nas lavouras, e ainda causam danos ao meio ambiente e a organismos não-alvo (Kumaravel et al., 2021).

Nesse contexto, como forma de aumentar a eficiência e seletividade em organismo alvo, uma abordagem alternativa à utilização de inseticidas sintéticos tem surgido a partir de nanoformulações, como as nanopartículas lipídicas (Carvalho et al., 2010). Nanopartículas, como “drug delivery”, já possuem várias aplicações na agricultura, medicina, indústria farmacêutica, setor energético e algumas outras ciências (Kathiravan et al., 2015). Nanoformulações comuns ao manejo de pragas incluem os nanogéis, nanoesferas e nanosuspensão (Pittarate et al., 2023), a partir de polímeros orgânicos ou óxidos metálicos inorgânicos que estão sendo utilizados para o controle de insetos-praga (Raju et al., 2019). Os principais objetivos desses materiais são: (a) aumentar a solubilidade de ingredientes ativos pouco solúveis, (b) permitir liberação gradual e orientada e/ou proteger da degradação prematura (Shah and Wani, 2016).

As plantas naturalmente produzem substâncias para se defender de insetos, patógenos e microrganismos (Souza et al., 2017). Geralmente os metabólitos com propriedades inseticidas incluem terpenoides, limonoides, flavonoides, entre outros (Sarria et al., 2011). Estes compostos possuem diferentes modos de ação sobre os insetos, podendo ser agudamente tóxicos, repelente, inibir a alimentação, o crescimento, o desenvolvimento e reprodução.

Inseticidas derivados de plantas geralmente estão disponíveis, comercialmente, como pós, extratos ou óleos (Guerra et al., 2009; Haas et al., 2014).

A floresta amazônica possui uma rica biodiversidade vegetal que se reflete na diversidade de constituintes químicos isolados dessas espécies. Dentre essas, as plantas oleaginosas possuem poucos estudos acerca de sua caracterização, que é restrita a composição das cadeias graxas dos seus óleos e gorduras (Hidalgo et al., 2016). As propriedades químicas das oleaginosas não se restringem apenas a sua composição lipídica, mas também à presença de outras substâncias, como compostos fenólicos e vitaminas, que possuem propriedades biológicas importantes (Souza et al., 2017; Li et al., 2013).

Entre os polímeros de origem natural, a fibroína de seda é um potencial candidato para a administração de inseticidas à base de óleos vegetais (Marinho et al., 2022; Sarquis et al., 2020). A fibroína de seda produzida pelo bicho-da-seda, *Bombyx mori*, tem um grande potencial para a administração de fármacos ou substâncias hidrofóbicas (Holanda et al., 2022), devido a uma rara combinação de propriedades químicas e físicas, tais como a possibilidade de isolamento e purificação em meio aquoso, biodegradabilidade, alta resistência, fácil manipulação mecânica, entre outros (Ferreira et al., 2020; Rockwood et al., 2011). A fibroína é composta por polipeptídios repetidos de glicina, alanina e serina, unidos por ligações de hidrogênio, formando estruturas secundárias β-folha que conferem a seda a sua força e estabilidade (Cheng et al., 2014). Os sistemas de entrega de fármacos baseados em fibroína de seda são influenciados por suas propriedades mecânicas, sua estrutura secundária e cristalinidade (Rockwood et al., 2011).

Diante do exposto, o presente trabalho teve por objetivo avaliar a eficácia da ação larvicida e ovicida de nanopartículas de fibroína de seda combinadas com ésteres graxos de óleos e gordura de três espécies vegetais da Amazônia (*Astrocaryum murumuru, Bertholletia excelsa e Carapa guianensis)* frente as larvas de 3º instar de *S. frugiperda*.

4.2. MATERIAIS E MÉTODOS

4.2.1 Reagentes e solventes

A gordura de *A. murumuru* Mart. (murumuru) foi adquirida da Aspacs (Amazonas, Brasil), o óleo de *B. excelsa* (castanha-da-Amazônia) foi obtido da Cooperativa Mista dos Agricultores do Jari (Laranjal do Jari, Amapá, Brasil), o óleo de *C. guianensis* (andiroba) foi obtido da Embrapa (Macapá, Amapá, Brasil). O álcool butílico (99.5%) foi adquirido da Cromato Chemicals (São Paulo, Brasil). Os solventes utilizados na purificação dos ésteres por

cromatografia em coluna (*n*-hexano 98.5%, acetato de etila 98% e sílica gel 60 [70-230 mesh]) foram adquiridos da Synth (São Paulo, Brasil). A lipase Amano AK de *Pseudomonas fluorescens* (20.000 U/g) foi adquirida da Sigma-Aldrich (São Paulo, Brasil).

4.2.2 Síntese de ésteres butílicos da gordura de murumuru e dos óleos de castanha-do-Brasil e andiroba, catalisada pela lipase Amano AK de *Pseudomonas fluorescens*

A reação de transesterificação enzimática foi realizada separadamente para a gordura de *murumuru* e para os óleos de andiroba e castanha-da-Amazônia, gerando os respectivos ésteres butílicos (FABE-Am, FABE-Cg e FABE-Be), conforme metodologia adaptada por Ferreira et al., (2017). As reações foram realizadas em um balão de reação de 50 mL contendo 1.0 g da gordura e dos respectivos óleos, 3 mL de álcool butílico e 0.1 g (10%) de lipase Amano AK de *Pseudomonas fluorescens*. As misturas de reação foram agitadas magneticamente durante 24 h à temperatura ambiente. Em seguida, as soluções reacionais foram filtradas, as fases orgânicas foram secas com sulfato de sódio anidro e filtradas, e os solventes foram removidos sob vácuo a pressão reduzida. Os ésteres butílicos foram purificados por cromatografia em coluna de gel de sílica, utilizando uma mistura de *n*-hexano e acetato de etila (9:1) como fase móvel. Os produtos isolados foram caracterizados de acordo com os seus dados espectroscópicos (utilizando GC-MS e FTIR, como descrito abaixo).

4.2.3 Cromatografia gasosa-espectrometria de massas (GC-MS)

As amostras de gordura e óleos vegetais transesterificadas com *n*-butanol foram analisadas por cromatografia gasosa acoplada a espectrometria de massas (GC-MS). Estas análises foram realizadas num sistema Shimadzu GC2010 com um detetor de massa seletivo (Shimadzu MS2010plus) em modo de ionização de electrões (EI, 70 eV). O sistema estava equipado com uma coluna RTX-5MS (30 m × 0.25 mm × 0.25 µm). As condições do GC-MS começaram com uma temperatura de forno de 130 ºC, que foi mantida durante 2 min e depois aumentada para 290 ºC a uma taxa de 5 ºC.min^{-1}. A temperatura final foi mantida durante 2 min. O tempo total de análise foi de 36 min. As temperaturas do injetor e do detetor foram mantidas a 210 ºC; foi injetado 1 µL de amostra com divisão 1:15; e utilizou-se hélio como gás de arrastamento a um caudal de 1.0 mL.min^{-1}. Os íons foram monitorizados de 3 a 36 min para m/z 40-500. Os componentes presentes nas amostras foram identificados por comparação dos dados espectrais com os descritos na biblioteca Wiley (Ferreira et al., 2017).

4.2.4 Análise de FT-IR

Um espectrofotômetro de infravermelho com transformada de Fourier (Spectrum Two FT; PerkinElmer, Inc., Waltham, MA, EUA), com um acessório de amostragem de reflexão total atenuada (ATR), uma placa de diamante e um detetor de sulfato de triglicina deuterado, foi utilizado para registar os espectros da gordura e dos óleos vegetais transesterificados com álcool *n*-butílico. A gama espectral foi fixada entre 350 e 4.000 cm^{-1} e a resolução foi fixada em 0.5 cm^{-1} (de Oliveira Penido et al., 2017).

4.2.5 Preparação de nanopartículas poliméricas de fibroína de seda com os ésteres sintetizados Am-SF-NPs, Be-SF-NPs e Cg-SF-NPs

10 mL de nanopartículas foram produzidas através da homogeneização da solução de fibroína de seda com os ésteres butílicos sintetizados (Secção 2.2). As nanopartículas foram desenvolvidas adicionando 1% (v/v) de cada conjunto de ésteres a uma mistura de etanol e isopropanol (1:1) a 5% (v/v) e agitados vigorosamente por 30 min em agitador magnético. Em seguida, 94% (v/v) de solução de fibroína de seda (2% de concentração) foi adicionada lentamente à cada mistura de ésteres (FABE-Am, FABE-BE e FABE-Cg). Por fim, a formulação foi agitada em vórtex a 300 G durante 1 h, conforme descrito por Sarquis et al., (2020). As nanopartículas poliméricas de fibroína da seda combinadas com ésteres butílicos foram denominadas com os códigos: Am-SF-NPs (nanopartículas de fibroína de seda com *A. murumuru*), Be-SF-NPs (nanopartículas de fibroína de seda com *B. excelsa*) e Cg-SF-NPs (nanopartículas de fibroína de seda com *C. guianensis*).

4.2.6 Caracterização das nanopartículas de fibroína de seda (Am-SF-NPs, Be-SF-NPs e Cg-SF-NPs)

Todas as nanopartículas (Am-SF-NPs, Be-SF-NPs e Cg-SF-NPs) foram previamente caracterizadas quanto ao seu tamanho de partícula, índice de polidispersidade e potencial Zeta, através da técnica de dispersão dinâmica de luz utilizando um Zetasizer Nano ZS (Malvern Pananalytical, Malvern, Reino Unido). A morfologia externa das nanopartículas foi determinada através da técnica de microscopia eletrônica de transmissão utilizando um microscópio JEM 2100-FS (JEOL Ltd., Tokyo, Japan) (Marinho et al., 2023, 2022).

4.2.7 Atividade larvicida e ovicida das nanopartículas de fibroína de seda (Am-SF-NPs, Be-SF-NPs e Cg-SF-NPs) em *S. frugiperda*

A população de *S. frugiperda* utilizada no estudo foi fornecida pela estação de Pesquisa do DU PONT DO BRASIL S.A. da cidade de Toledo – PR.

A atividade larvicida por ingestão das nanopartículas (Am-SF-NPs, Be-SF-NPs e Cg-SF-NPs) sobre as larvas de *S. frugiperda* foi realizada conforme metodologia adaptada de (Knaak et al., 2013). Nas dietas dos tratamentos foram aplicados 100 µL das nanopartículas de fibroína de seda em diferentes concentrações (5000-292 $\mu g.mL^{-1}$), e 100 µL da solução de fibroína de seda 2% como controle negativo, além de 100 µL dos controles positivos Karate zeon® (0.5 $\mu g.mL^{-1}$) e Neem® (30 $\mu g.mL^{-1}$). As dietas, após remoção do excesso de umidade à temperatura ambiente, foram colocadas individualmente em câmaras de bioensaio (9x5x4 cm^3) juntamente com 18 lagartas de 3º instar por tratamentos e grupos controles. As câmaras de ensaio foram vedadas e incubadas a 25 ± 2 ºC com 70 ± 10% de umidade relativa e 12 h de fosfatase. O delineamento experimental foi inteiramente casualizado, com 6 repetições, totalizando 144 larvas de *S. frugiperda*. A mortalidade foi registrada após 96 h, após exposição.

Para avaliar a atividade ovicida das nanopartículas de fibroína de seda, foram retiradas posturas de *S. frugiperda* com até 48 h de idade. O método utilizado baseou-se na imersão dos ovos nas soluções das nanopartículas e na solução de fibroína de seda 2% como grupo controle negativo, além dos controles positivos Dimilin® (2.5 $\mu g.mL^{-1}$) e óleo de Neem® (25 $\mu g.mL^{-1}$), conforme metodologia adaptada de (Mink and Luttrell, 1989). Foram utilizados 30 ovos por concentração de nanopartículas, as concentrações variaram de 2222-292 $\mu g.mL^{-1}$. Após remoção do excesso de umidade à temperatura ambiente, as câmaras de bioensaio foram vedadas e incubadas a 25 ± 2 ºC com 70 ± 10% de umidade relativa e 12 h de fosfatase. O delineamento experimental foi inteiramente casualizado, com 3 repetições, totalizando 540 ovos. A atividade de eclosão dos ovos foi registrada após 96 h, após exposição.

4.2.8 Ensaio de toxicidade ambiental

Para o ensaio de toxicidade ambiental das nanopartículas (Am-SF-NPs, Be-SF-NPs e Cg-SF-NPs) foi utilizado a alga verde *Chlorella vulgaris*, conforme metodologia descrita por (Oliveira et al., 2017) com modificações. Alíquotas de 10 mL de *C. vulgaris* foram cultivadas em solução aquosa de nitrogênio, potássio e fósforo (NPK 08:08:08). A densidade celular inicial foi de $1x10^4$ células mL^{-1} para todos os grupos. As concentrações das nanopartículas, utilizadas no ensaio, foram baseadas nos valores de CL_{50} obtidos do ensaio larvicida. Para as

Am-SF-NPs (1117.49 µg.mL^{-1}), Be-SF-NPs (563.03 µg.mL^{-1}) e Cg-SF-NPs (914.59 µg.mL^{-1}). Além dos grupos controles: um contendo somente fibroína de seda 2% e outro contendo uma dispersão de *C. vulgaris* (1x10^{4} células mL^{-1}) em solução aquosa de NPK. A densidade das células foi quantificada usando uma câmara de Neubauer após 1, 5, 10, 15, 20 e 30 dias. A porcentagem de células viáveis (%VC) foi calculada da seguinte forma: %VC = (D/DO) x 100, onde: D0 é a densidade celular antes da adição das soluções; D e a densidade celular em cada dia específico. Todos os ensaios foram realizados em triplicata.

4.2.9 Análise morfológica das larvas de *S. frugiperda*

Após o teste larvicida, as larvas mortas foram fixadas em formalina a 10%. A sua morfologia externa foi então analisada num microscópio ótico e fotografada com uma câmera digital (MDCE - SC USB 2.0) utilizando o software ScopeImage 9.0, tal como descrito por Araújo et al., (2022).

4.2.10 Análises estatística

As concentrações letais (LC_{50} e LC_{90}) foram determinadas pelo modelo Probit através do Polo-Plus software (LeOra Software Co., Petaluma, CA, USA), com intervalos de confiança de 95%, também por ANOVA com teste de comparações de médias e teste de Tukey com intervalos de confiança a 95% por meio do Sistema SAS para Windows versão 9.00 (SAS Institute, 2001).

4.3 RESULTADOS E DISCUSSÕES

4.3.1 Análise de CG-MS da gordura de *A. murumuru* e dos óleos de *C. guianensis e B. excelsa*

A reação de transesterificação da gordura de *A. murumuru* e dos óleos de castanha-da-Amazônia e andiroba foi realizada utilizando a lipase *P. fluorescens* e analisada através da técnica de CG-MS. A análise de CG-MS revelou que a gordura de *A. murumuru* apresentou predominantemente a presença de ácidos graxos saturados com destaque para o ácido láurico (C12:0) e o ácido mirístico (C14:0), com 53.5% e 25.8%, respectivamente. Enquanto, que os óleos de castanha-da-Amazônia e andiroba esterificados apresentaram alta similaridade entre seus principais derivados de ácidos graxos, com destaque para o ácido oleico (C18:1, ω-9) 31.8% e 43.61%, respectivamente. Além do ácido palmítico (C16:0) 19% e 40.5%, para a castanha-da-Amazônia e andiroba, respectivamente Tabelas S1, S2; Figuras S1, S2 (Material suplementar). Dados obtidos dos trabalhos anteriores de Marinho et al., (2022, 2023).

4.3.2 Análise de FT-IR dos ésteres graxos FABE-Am, FABE-Be e FABE-Cg

A figura 4.1 exibi os espectros de FT-IR para os três ésteres obtidos do murumuru, castanha-da-Amazônia e andiroba. Os espectros revelaram evidências da formação dos ésteres, incluindo uma vibração de estiramento C-H na região 2950-2853 cm^{-1} para a presença de ligações alifáticas. As bandas de estiramento C=O a 1740 cm^{-1} estão relacionadas com a vibração do grupo carbonila, e foram observadas bandas características de ésteres insaturados, tais como C-C-O a 1164 cm^{-1}. Uma vibração de estiramento C=C na região de 1655-1686 cm^{-1} evidenciou a presença de carbonos insaturados. Foram observadas bandas de estiramento angular assimétrico C-H a 1466-1371 cm^{-1} e bandas de estiramento O-C-C na região de 1113-1111 cm^{-1}. Resultados semelhantes foram relatados por Enumo et al., (2020).

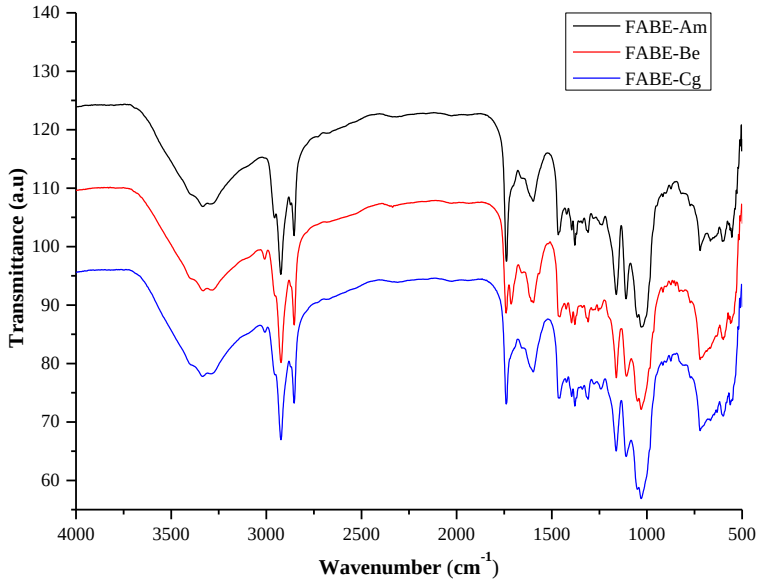

Fig. 4.1. Espectro de FT-IR dos ésteres butílicos (FABE-Am, FABE-Be e FABE-Cg).

4.3.3 Caracterização das nanopartículas de fibroína de seda (Am-SF-NPs, Be-SF-NPs e Cg-SF-NPs)

As nanopartículas de fibroína de seda combinadas aos ésteres graxos da gordura de *A. murumuru* e dos óleos de *C. guianensis* e *B. excelsa* tiveram seus tamanhos de partículas, índice de polidispersidade e potencial zeta determinados através da técnica de dispersão dinâmica da luz DLS. A estabilidade temporal das nanopartículas foi avaliada até o 50º dia em diferentes temperaturas a 4 ºC e a 32 ºC, após o preparo (Tabela 4.1).

O perfil das nanopartículas por DLS mostrou que as Am-SF-NPs apresentaram tamanhos que variaram de 190.3 ± 1.5 nm a 187.6 ± 0.8 nm, quando estocadas a 4 ºC, enquanto foram estocadas a 32 ºC o tamanho de partículas variou de 190.3 ± 1.5 nm a 221.5 ± 1.9 nm. Já as nanopartículas Be-SF-NPs quando estocadas a 4 ºC o tamanho das partículas variou de 383.2 ± 36.8 nm a 239.9 ± 4.8 nm e quando estocadas a 32 ºC apresentou tamanho de 383.2 ± 36.8 nm a 540.8 ± 23.8 nm. Enquanto que, as nanopartículas Cg-SF-NPs exibiram tamanhos entre 330.7 ± 1.8 nm a 207 ± 2.3 nm, durante os 50 dias de monitoramento (Tabela 4.1).

As Am-SF-NPs exibiram valores de índice de polidispersidade (PdI) variando de 0.288 a 0.248 a 4 ºC, e variando de 0.288 a 0.286 quando estocadas a 32 ºC. As Be-SF-NPs exibiram valores de PdI variando de 0.484 a 0.278 quando estocadas a 4 ºC, e quando estocadas a 32 ºC apresentaram valores entre 0.484 e 0.486, e as Cg-SF-NPs apresentaram valores de PdI entre 0.315 e 0.294 quando estocadas a 4 ºC, e a 32 ºC os valores variam entre 0.315 a 0.308, durante os 50 dias de monitoramento (Tabela 4.1).

O potencial zeta (PZ) para as Am-SF-NPs apresentou valores de -49.0 ± 0.37 mV a -41.0 ± 1.7 mV quando foram mantidas a 4 ºC, e com baixa variação de -49.0 ± 0.37 mV a -48.2 ± 1.6 quando mantidas a 32 ºC. As Be-SF-NPs exibiram valores de PZ entre -50.7 ± 2.1 mV e de -47.0 ± 0.9 mV quando mantidas a 4 ºC, e entre -50.7 ± 2.1 mV a -51.0 ± 0.6 mV quando mantidas a 32 ºC, e as Cg-SF-NPs exibiram valores de ZP quanto mantidas a 4 ºC entre 46.8 ± 0.7 mV e -41.0 ± 0.5 mV, e quando mantidas a 32 ºC apresentaram valores entre -46.8 ± 0.7 mV e -62.9 ± 0.7 mV. Durante os 50 dias de monitoramento (Tabela 4.1).

As micrografias de microscopia eletrônica de transmissão mostraram que as nanopartículas Am-SF-NPs, Be-SF-NPs e Cg-SF-NPs apresentaram distribuição uniforme e formato esférico (Figura 4.2). A estrutura compacta que as nanopartículas exibiram pode ter sido induzida pelo efeito de reticulação das cadeias da fibroína de seda quando elas se aproximam para a formação de ligações amídicas (Pham et al., 2018).

Tabela 4.1 Tamanho de partículas, PdI e zeta potencial das nanopartículas poliméricas de fibroína de seda (Am-SF-NPs, Be-SF-NPs e Cg-SF-NPs).

	4ºC				32ºC			
	Tempo (dias)	**Tamanho (nm)**	**PDI**	**Zeta (mV)**	**Tempo (dias)**	**Tamanho (nm)**	**PDI**	**Zeta (mV)**
Am-SF-NPs	0	190.3 (±1.5)	0.288	-49.0 (±0.37)	0	190.3 (±1.5)	0.288	-49.0 (±0.37)
	7	211.1 (±4.1)	0.407	-40.7 (±3.3)	7	202.1 (±0.2)	0.238	-44.2 (±1.6)
	14	200.2 (±2.9)	0.290	-47.2 (±1.2)	14	211.7 (±2.9)	0.324	-39.7 (±1.4)
	21	195.2 (±3.6)	0.282	-46.5 (±0.7)	21	211.2 (±1.6)	0.275	-41.3 (±1.1)
	28	189.8 (±2.8)	0.258	-39.0 (±0.5)	28	217.3 (±1.7)	0.250	-41.2 (±1.7)
	50	187.6 (±0.8)	0.248	-41.0 (±1.7)	50	221.5 (±1.9)	0.286	-48.2 (±1.6)
Be-SF-NPs	0	383.2 (±36.8)	0.484	-50.7 (±2.1)	0	383.2 (±36.8)	0.484	-50.7 (±2.1)
	7	334.5 (±11.6)	0.451	-42.9 (±1.1)	7	381.8 (±26.8)	0.449	-50.2 (±1.1)
	14	301.6 (±2.1)	0.413	-42.4 (±1.6)	14	361.4 (±16.8)	0.430	-44.9 (±0.2)
	21	274.3 (±3.7)	0.374	-43.2 (±4.5)	21	334.1 (±9.3)	0.505	-49.7 (±1.6)
	28	255.6 (±7.4)	0.271	-37.9 (±0.3)	28	363.7 (±41.3)	0.560	-43.4 (±1.5)
	50	239.9 (±4.8)	0.278	-47.0 (±0.9)	50	540.8 (±23.8)	0.486	-51.0 (±0.6)
Cg-SF-NPs	0	330.7 (±1.8)	0.315	-46.8 (±0.7)	0	330.7 (±1.8)	0.315	-46.8 (±0.7)
	7	305.1 (±13.0)	0.439	-46.7 (±4.8)	7	329.1 (±12.2)	0.359	-45.5 (±3.4)
	14	267.3 (±7.2)	0.477	-42.7 (±4.8)	14	334.5 (±6.6)	0.350	-43.1 (±2.3)
	21	229 (±6.5)	0.348	-44.5 (±0.2)	21	328.4 (±2.2)	0.323	-46.7 (±0.8)
	28	226.3 (±2.6)	0.320	-38.1 (±0.4)	28	323.2 (±14.6)	0.343	-45.3 (±1.4)
	50	207 (±2.3)	0.294	-41.0 (±0.5)	50	306.5 (±3.9)	0.308	-62.9 (±0.7)

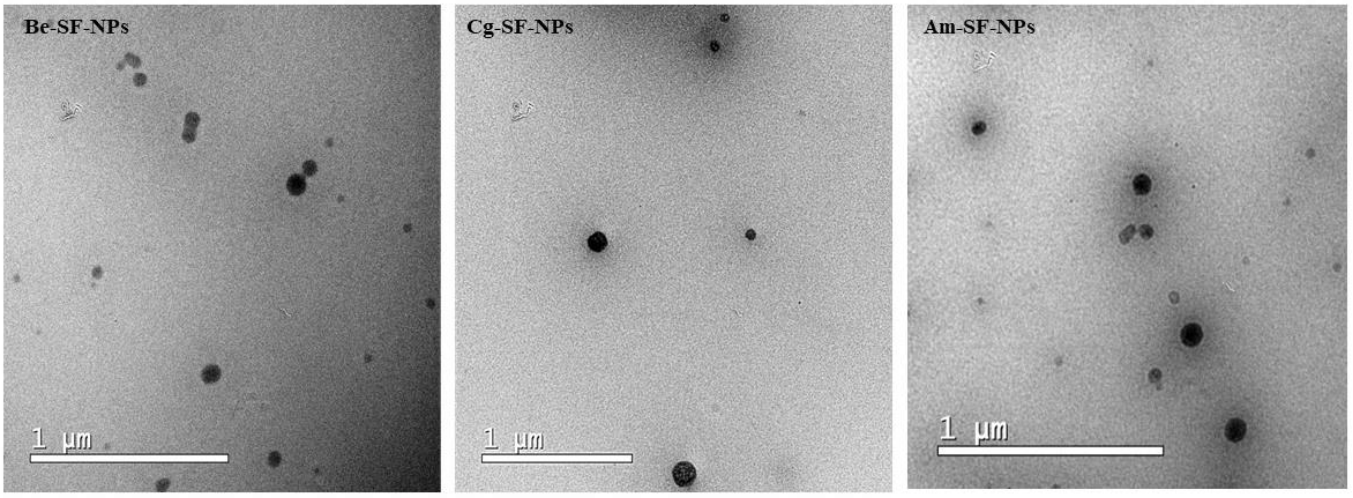

Fig. 4.2. Micrografias de TEM das nanopartículas de fibroína de seda (Be-SF-NPs, Cg-SF-NPs e Am-SF-NPs).

4.3.4 Atividade larvicida e ovicida das nanopartículas de fibroína de seda (Am-SF-NPs, Be-SF-NPs e Cg-SF-NPs) em *S. frugiperda*.

Os resultados da atividade larvicida mostraram que as nanopartículas de fibroína de seda (Am-SF-NPs, Be-SF-NPs e Cg-SF-NPs) foram altamente tóxicas para as larvas de 3º instar de *S. frugiperda*, através do método de imersão alimentar. A atividade larvicida entre as nanopartículas variaram aproximadamente de 85 a 100%, após 96 h de tratamento. As nanopartículas Be-SF-NPs foram mais eficientes, apresentando taxa de mortalidade de 100%, na concentração de 5000 $\mu g.mL^{-1}$ contra as larvas de *S. frugiperda*, exibindo uma atividade larvicida ligeiramente superior aos controles positivos Karate zeon® e o óleo de Neem®, inseticidas comerciais já bem utilizados no manejo desses insetos (Figura 4.3). Todas as nanopartículas apresentaram efeito larvicida quando comparadas a solução de fibroína de seda 2%, utilizada como controle negativo.

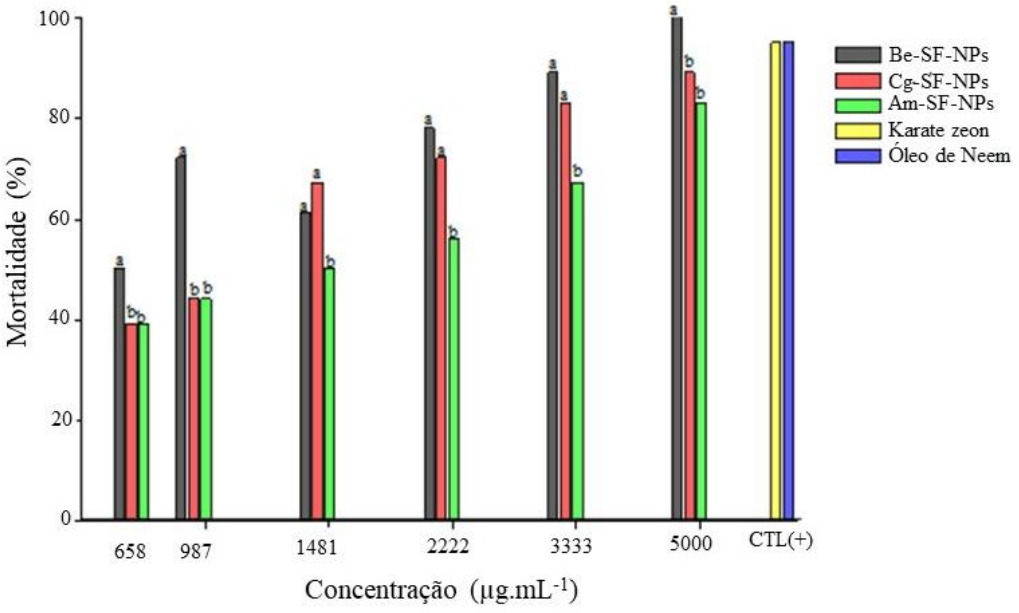

Fig. 4.3. Porcentagem de mortalidade de *S. frugiperda* após 96 h de exposição às nanopartículas (Am-SF-NPs, Be-SF-NPs e Cg-SF-NPs) em diferentes concentrações. CLT (+): solução de Karate zeon [0.5 µg.mL^{-1}], Neem [30 µg.mL^{-1}]. Cada valor na figura é a média de três repetições ± desvio padrão e representa a taxa de mortalidade das três nanoformulações. A significância estatística é mostrada por letras minúsculas diferentes, com base no teste ANOVA ($p < 0,05$).

A atividade larvicida das nanopartículas (Am-SF-NPs, Be-SF-NPs e Cg-SF-NPs) está intrinsicamente ligada à sua composição lipídica. A literatura já noticia que vários ácidos graxos, como o ácido láurico, mirístico, palmítico, oleico e linoleico são compostos bioativos a uma variedade de insetos artrópodes, agindo por contato bloqueando a respiração e afetando as funções da membrana celular, além de reduzir sua movimentação e alimentação (Bernklau et al., 2016; Fenigstein et al., 2001; Sims et al., 2014). Outrossim, alguns óleos vegetais podem conter outros compostos bioativos a insetos, a exemplo o óleo de andiroba que contêm vários limonoides, terpenos e outros compostos com atividade bioinseticida (Santos et al., 2012).

Foram determinados os valores de LC_{50} e LC_{90} para as nanopartículas após 96 h de tratamento (Tabela 4.2). Após exposição das larvas por 96h, as Be-SF-NPs foram mais eficientes quando comparadas as demais nanopartículas, apresentando LC_{50} 563.03 µg.mL^{-1} e LC_{90} de 3685.98 µg.mL^{-1}. Já as nanopartículas Cg-SF-NPs apresentaram LC_{50} de 914.59 µg.mL^{-1} e LC_{90} de 5831.98 µg.mL^{-1}, após 96 h de exposição. Por fim, as nanopartículas Am-SF-NPs, após 96 h apresentou menor toxicidade para as larvas de *S. frugiperda* com LC_{50} de 1020.46 µg.mL^{-1} e LC_{90} de 1117.49 µg.mL^{-1}.

Pittarate et al., (2023) relataram que nanopartículas metálicas de iodeto de potássio, disponíveis comercialmente, apresentaram alta susceptibilidade contra larvas de 4º instar de *S.*

frugiperda pelo método de imersão alimentar com taxa de mortalidade variando de 31 a 83%, após três dias de exposição. Nanoformulação à base de Neem (*Azadirachta indica*) exibiu elevada mortalidade contra larvas de 2º, 3º e 4º insta de *Spodoptera litura* com taxas de mortalidade de variando de 76.56 a 68.43% a 100 μg.mL^{-1}, o método de imersão alimentar da nanoformulação à base de Neem ainda foi capaz de retardar o crescimento dos insetos prologando o período larval em até 4 dias (Kamaraj et al., 2018).

Tabela 4.2 Valores de LC_{50} e LC_{90} para *S. frugiperda* em contato com as nanopartículas poliméricas de fibroína de seda (Am-SF-NPs, Be-SF-NPs e Cg-SF-NPs).

Nanopartículas	**Inclinação±E.P**	**LC_{50} (μg.mL^{-1}) (UCL-LCL)**	**LC_{90} (μg.mL^{-1}) (UCL-LCL)**	**X^2 (df = 6)**
Am-SF-NPs	1.33±0.5	1020.46 (4739.72-7841.70)	1117.49 (488.64-1944.34)	1.38
Be-SF-NPs	1.57±0.31	563.03 (326.28-793.99)	3685.98 (2293.37-9658.02)	4.19
Cg-SF-NPs	1.59±0.29	914.59 (623.58-1263.47)	5831.98 (3464.71-6415.11)	1.1

*LC - concentração letal (50% e 90%); LCL - limite inferior de confiança; UCL - limite superior de confiança; X2 - qui-quadrado; df - grau de liberdade; significativo a P < 0,05.

O presente estudo ainda demonstrou que os ovos de *S. frugiperda* foram susceptíveis as nanopartículas de fibroína de seda (Am-SF-NPs, Be-SF-NPs e Cg-SF-NPs). As nanopartículas Be-SF-NPs inibiram a eclosão de aproximadamente 87% dos ovos de *S. frugiperda,* na maior concentração testada. Já as nanopartículas Am-SF-NPs inibiram a eclosão de 65% dos ovos. Enquanto, que as nanopartículas Cg-SF-NPs inibiram cerca de 62% a eclosão dos ovos de *S. frugiperda* (Figura 4.4).

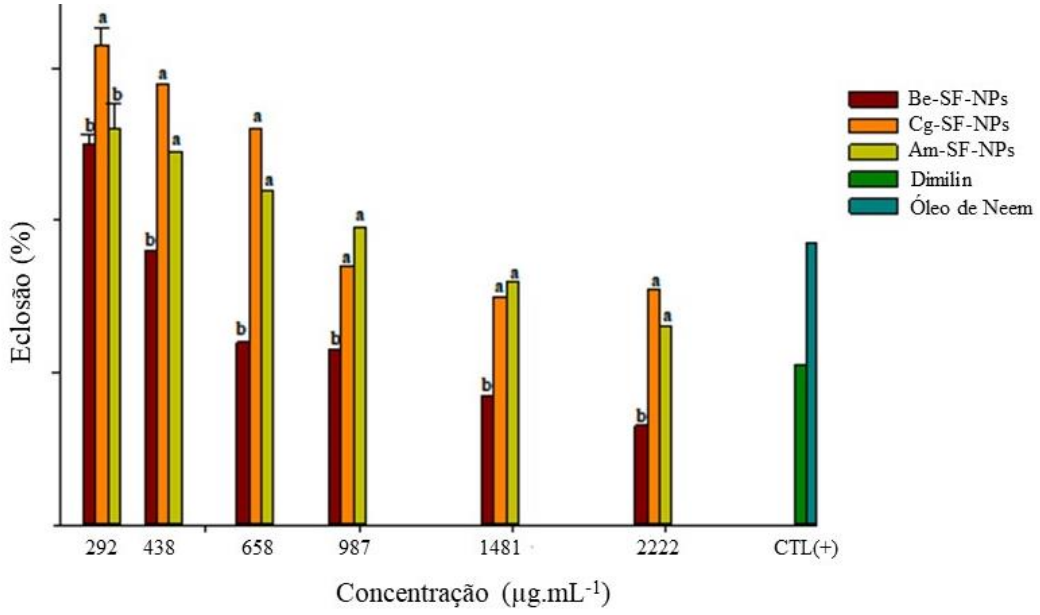

Fig. 4.4. Porcentagem de eclosão de ovos de *S. frugiperda* após 96 h de exposição às nanopartículas (Am-SF-NPs, Be-SF-NPs e Cg-SF-NPs) em diferentes concentrações. CLT (+): solução de Dimillin [2.5 µg.mL^{-1}], Neem [25 µg.mL^{-1}]. Cada valor na figura é a média de três repetições ± desvio padrão e representa a taxa de mortalidade das três nanoformulações. A significância estatística é mostrada por letras minúsculas diferentes, com base no teste ANOVA ($p < 0,05$).

As nanopartículas Be-SF-NPs mostraram atividade ovicida contra a eclosão de ovos de *S. frugiperda* com LC_{50} de 341.03 µg.mL^{-1} e LC_{90} de 3901.22 µg.mL^{-1}, após 96 h de exposição. As Am-SF-NPs inibiram a eclosão de ovos de *S. frugiperda* com valores de LC_{50} de 781.07 µg.mL^{-1} e LC_{90} de 1516.07 µg.mL^{-1}, após 96 h de exposição. As Cg-SF-NPs apresentaram atividade ovicida frente aos ovos de *S. frugiperda* com valores de LC_{50} de 1046.88 µg.mL^{-1} e LC_{90} de 8806.45 µg.mL^{-1}, após 96 h de exposição (Tabela 4.3).

Tabela 4.3 Valores de LC_{50} e LC_{90} para a atividade ovicida das nanopartículas poliméricas de fibroína de seda (Am-SF-NPs, Be-SF-NPs e Cg-SF-NPs) em ovos de *S. frugiperda*.

Nanopartículas	Inclinação±E.P	LC_{50} (µg.mL^{-1}) (UCL-LCL)	LC_{90} (µg.mL^{-1}) (UCL-LCL)	X^2 (df = 4)
Am-SF-NPs	1.01±0,22	781.07 (257.11-1585.06)	1516.07 (4400.28-9433.66)	5.09
Be-SF-Nps	1.34±0.22	341.03 (201.38-468.23)	3091.22 (2059.16-6451.61)	2.38
Cg-SF-NPs	1.39±0.26	1046.88 (729.05-1466.36)	8806.45 (4763.25-0472.44)	3.89

*LC - concentração letal (50% e 90%); LCL - limite inferior de confiança; UCL - limite superior de confiança; X2 - qui-quadrado; df - grau de liberdade; significativo a $P < 0,05$.

A literatura ainda é carente de dados que relacionam nanopartículas lipídicas no controle das larvas de *S. frugiperda*, bem como para o controle da eclosão de seus ovos. Pinheiro et al., (2022) observaram que o óleo essencial das folhas e frutos de *Piper fuligineum* foi capaz de reduzir a viabilidade de 84% dos ovos de *S. frugiperda*. Segundo Machado et al., (2011) o extrato aquoso das folhas de neem inibiu cerca de 86.2% da eclosão dos ovos de *S. frugiperda*.

Don-Pedro (1989) observou que óleos fixos foram capazes de inibir a eclosão de ovos de *Callosobruchus maculatus* e atribui o efeito ovicida a acumulação de metabolitos tóxicos na superfície dos ovos, como resultado de um efeito barreira. Além do efeito tóxico direto da penetração do óleo ou de seus constituintes no interior dos ovos através do cório, membrana serosa que permite a troca gasosa entre o embrião e o meio externo. O grau de saturação de óleos fixos também pode influenciar na eficácia do efeito ovicida, pois segundo Hall & Harman (1991), os ácidos graxos altamente insaturados aderem mais facilmente para o interior dos ovos através do cório que os ácidos graxos saturados que normalmente solidificam formando uma película mais espessa sobre os ovos. Deste modo, o efeito ovicida provavelmente pode decorrer das propriedades físicas ou químicas do composto testado (Krinski et al., 2018). Diante do exposto, o efeito ovicida das nanopartículas (Am-SF-NPs, Be-SF-NPs e Cg-SF-NPs podem estar relacionados tanto pela toxicidade dos seus componentes, bem como com as propriedades físicas dos óleos.

4.3.5 Análise morfológica das larvas de *S. frugiperda* expostas as nanopartículas Am-SF-NPs, Be-SF-NPs e Cg-SF-NPs

As nanopartículas Am-SF-NPs, Be-SF-NPs e Cg-SF-NPs causaram danos na morfologia externa das larvas de 3º instar de *S. frugiperda*. As larvas expostas as Am-SF-NPs apresentaram ausência de pigmentação, encurtamento do tórax e diminuição da cabeça. As Be-SF-NPs causou inchaço no tórax e na cabeça, além de deformação no segmento final do abdome das larvas expostas a elas. As Cg-SF-NPs causou deformação no tórax e no segmento inicial do abdome das larvas, em contraste as larvas submetidas ao controle contendo somente fibroína de seda 2% não apresentou alterações morfológicas (Figura 4.5). Os efeitos obtidos com as nanopartículas de fibroína de seda podem estar sendo induzidos a uma inibição na produção dos hormônios ecdisteróides, que são os hormônios encontrados em artrópodes, responsáveis

pela muda, desenvolvimento e em menor grau a reprodução (Matos et al., 2009; Roel and Vendramim, 2006).

Segundo Magrini et al., (2015) os extratos de frutos e sementes de *Cabralea canjerana canjerana* (Vell.), quando testados em estágios imaturos de *S. frugiperda,* impediu que as larvas realizassem a ecdise para estágios intermediários de desenvolvimento. Além disso, foi observado o aparecimento de tumores nas larvas tratadas. O extrato aquoso de *Melia azedarach* promoveu a morte de larvas de *S. frugiperda* durante a ecdise, sem que ocorresse a liberação total de exúvia e da cápsula cefálica. Ainda de acordo com o estudo, os extratos utilizados diminuíram os níveis de ecdisônios das larvas utilizadas nos testes (Maroneze and Gallegos, 2009).

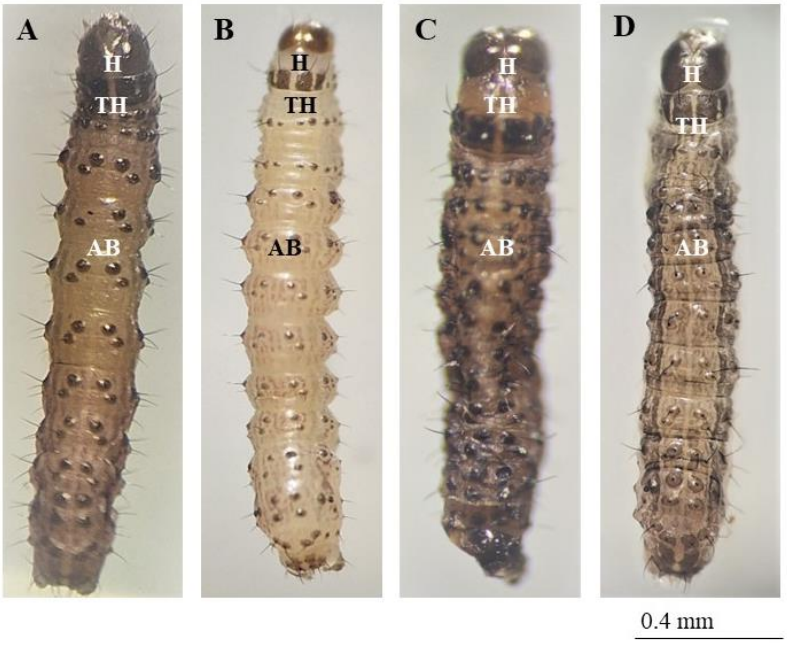

Fig. 4.5. (A) Larva exposta ao controle contendo fibroína de seda 2%. (B) Larva exposta a Am-SF-NPs. (C) Larva exposta a Be-SF-NPs. (D) Larva exposta a Cg-SF-NPs.

4.4 CONCLUSÕES

Em resumo, este estudo avaliou a atividade bioinseticida das nanopartículas de fibroína de seda (Am-SF-NPs, Be-SF-NPs e Cg-Be-NPs) contra as larvas de 3º instar de *S. frugiperda*. As nanopartículas apresentaram boa estabilidade temporal durante os 50 dias de monitoramento nas temperaturas de 4 ºC e 32 ºC. As nanopartículas apresentaram distribuição uniforme e formato esférico. Todas as nanopartículas apresentaram boa atividade larvicida e ovicida contra

S. frugiperda, com destaque para a Be-SF-NPs que apresentou taxa de mortalidade larval de 100% com LC_{50} de 563.03 µg.mL^{-1}. A Be-SF-NPs também foi capaz de inibir em 87% a eclosão dos ovos de *S. fugiperda,* apresentando valor de LC_{50} de 341.03 µg.mL^{-1}. As nanopartículas ainda foram capazes de causar deformações na morfologia externa das larvas. Em conjunto, esses resultados sugerem que as nanopartículas obtidas a partir da fibroína de seda e derivados de óleos amazônicos podem tornar-se uma alternativa sustentável para futuras aplicações na nanotecnologia agro-ambiental.

Declaração de contribuição de autoria do Credito

Victor H. S. Marinho, Donald Manigat, Irlon M. Ferreira: Conceitualização, Metodologia, Validação, Software, Análise formal, Investigação, Curadoria de dados, Redação - rascunho original. **Jéssica C. E. Vilhena, Silvia M. M. Faustino**: Metodologia, Investigação, Redação - rascunho original, Redação - revisão e edição, Visualização. **Irlon M. Ferreira, Raimundo N. P. Souto**: Conceitualização, Supervisão, Administração do projeto, Obtenção de financiamento.

Declaração de Interesse Concorrente

Os autores declaram que não têm quaisquer interesses financeiros ou relações pessoais que possam parecer influenciar o trabalho relatado neste artigo.

Agradecimentos

Os autores gostariam de agradecer à Fundação de Amparo à Pesquisa do Estado do Amapá, (Fundação de Amparo à Pesquisa do Estado do Amapá, FAPEAP; bolsa nº. 34568.515.22257.28052017) e a Coordenação de Aperfeiçoamento do Ensino Superior, pelas bolsas de estudo financiadas.

4.5 REFERÊNCIAS

Araújo, I.F., Marinho, V.H. de S., Sena, I. da S., Curti, J.M., Ramos, R. da S., Ferreira, R.M.A., Souto, R.N.P., Ferreira, I.M., 2022. Larvicidal activity against *Aedes aegypti* and molecular docking studies of compounds extracted from the endophytic fungus

Aspergillus sp. isolated from *Bertholletia excelsa* Humn. & Bonpl. Biotechnol. Lett. 44, 439–459.

Assefa, F., Ayalew, D., 2019. Status and control measures of fall armyworm (*Spodoptera frugiperda*) infestations in maize fields in Ethiopia: A review. Cogent Food Agric. 5: 1641902.

Bernklau, E.J., Hibbard, B.E., Bjostad, L.B., 2016. Toxic and behavioural effects of free fatty acids on western corn rootworm (Coleoptera: Chrysomelidae) larvae. J. Appl. Entomol. 140, 725–735.

Carvalho, K.C.C., Mulinari, D.R., Voorwald, H.J.C., Cioffi, M.O.H., 2010. Chemical modification effect on the mechanical properties of hips/coconut fiber composites. BioResources 5, 1143–1155.

Cheng, Y., Koh, L.D., Li, D., Ji, B., Han, M.Y., Zhang, Y.W., 2014. On the strength of β-sheet crystallites of *Bombyx mori* silk fibroin. J. R. Soc. Interface 11: 20140305.

de Oliveira Penido, C.A.F., Pacheco, M.T.T., Novotny, E.H., Lednev, I.K., Silveira, L., 2017. Quantification of cocaine in ternary mixtures using partial least squares regression applied to Raman and Fourier transform infrared spectroscopy. J. Raman Spectrosc. 48, 1732–1743.

Deshmukh, S., Pavithra, H.B., Kalleshwaraswamy, C.M., Shivanna, B.K., Maruthi, M.S., Mota-Sanchez, D., 2020. Field Efficacy of Insecticides for Management of Invasive fall Armyworm, *Spodoptera frugiperda* (J. E. Smith) (Lepidoptera: Noctuidae) on Maize in India. Florida Entomol. 103, 221–227.

Don-pedro, K. N., 1989. Mode of action of fixed oils against eggs of Callosobruchus maculatus (F.). Pest. Sci. 26 (1989): 107-115.

Elizalde, L., Arbetman, M., Arnan, X., Eggleton, P., Leal, I.R., Lescano, M.N., Saez, A., Werenkraut, V., Pirk, G.I., 2020. The ecosystem services provided by social insects: traits, management tools and knowledge gaps. Biol. Rev. 95, 1418–1441.

Enumo, A., Gross, I.P., Saatkamp, R.H., Pires, A.T.N., Parize, A.L., 2020. Evaluation of mechanical, thermal and morphological properties of PLA films plasticized with maleic acid and its propyl ester derivatives. Polym. Test. 88, 106552.

Fenigstein, A., Eliyahu, M., Gan-Mor, S., Veierov, D., 2001. Effects of five vegetable oils on the sweetpotato whitefly *Bemisia tabaci*. Phyto. 29, 197–206.

Ferreira, I.M., Fiamingo, A., Campana-Filho, S.P., Porto, A.L.M., 2020. Biotransformation of (E)-2-methyl-3-phenylacrylaldehyde using mycelia of Penicillium citrinum CBMAI 1186, both free and immobilized on chitosan. Mar. Biotechnol. 22, 348–356.

Ferreira, I.M, Ganzeli, L.D.S., Rosset, I.G., Yoshioka, S.A., 2017. Ethylic biodiesel production using lipase immobilized in silk fibroin-alginate spheres by encapsulation. Catal. Letters 147, 269–280.

Ferreira, I.M., Yoshioka, S.A., Comasseto, J. V., Porto, A.L.M., 2017. Immobilization of Amano lipase from *Pseudomonas fluorescens* on silk fibroin spheres: an alternative protocol for the enantioselective synthesis of halohydrins. RSC Adv. 7, 12650–12658.

Guerra, A.M.N. de M., Maracajá, P.B., Freitas, R. da S. de, Sousa, A.H., Sousa, C.S.M., 2009. Atividade inseticida de plantas medicinais sobre o *Callosobruchus maculatus* (Coleoptera: Bruchidae). Rev. Caatinga (UFERSA. Impresso) 22, 146–150.

Haas, J., Garcia, B.C., Francisco, L., Alves, A., Haida, K.S., 2014. Efeito de extratos aquosos vegetais sobre a lagarta-do-cartucho Effect of aqueous plant extracts on the fall armyworm. Arq. Inst. Biol 81, 79–82.

Hall, J.S., Harman, G.E., 1991. Protection of stored legume seeds against attack by storage fungi and weevils: Mechanism of action of lipoidal and oil seed treatments. Crop Prot. 10, 375–380.

Harrison, M.C., Arning, N., Kremer, L.P.M., Ylla, G., Belles, X., Bornberg-Bauer, E., Huylmans, A.K., Jongepier, E., Piulachs, M.D., Richards, S., Schal, C., 2018. Expansions of key protein families in the German cockroach highlight the molecular basis of its remarkable success as a global indoor pest. J. Exp. Zool. Part B Mol. Dev. Evol. 330, 254–264.

Hidalgo, P.S.P., Nunomura, R.D.C.S., Nunomura, S.M., 2016. Amazon oil seeds: Chemistry and antioxidant activity of patawa (*Oenocarpus bataua* Mart.). Rev. Virtual Quim. 8, 130–140.

Holanda, F.H., Ribeiro, A.N., Sánchez-Ortiz, B.L., de Souza, G.C., Borges, S.F., Ferreira, A.M., Florentino, A.C., Yoshioka, S.A., Moraes, L.S., Carvalho, J.C.T., Ferreira, I.M., 2022. Anti-inflammatory potential of baicalein combined with silk fibroin protein in a zebrafish model (*Danio rerio*). Biotechnol. Lett. 45, 235–253.

Kamaraj, C., Gandhi, P.R., Elango, G., Karthi, S., Chung, I.M., Rajakumar, G., 2018. Novel

and environmental friendly approach; Impact of Neem (*Azadirachta indica*) gum nano formulation (NGNF) on *Helicoverpa armigera* (Hub.) and Spodoptera litura (Fab.). Int. J. Biol. Macromol. 107, 59–69.

Kathiravan, V., Ravi, S., Ashokkumar, S., Velmurugan, S., Elumalai, K., Khatiwada, C.P., 2015. Green synthesis of silver nanoparticles using croton sparsiflorus morong leaf extract and their antibacterial and antifungal activities. Spectrochim. Acta - Part A Mol. Biomol. Spectrosc. 139, 200–205.

Knaak, N., Wiest, S.L.F., Andreis, T.F., Fiuza, L.M., 2013. Toxicity of essential oils to the larvae of *Spodoptera frugiperda* (Lepidoptera: Noctuidae). J. Biopestic. 6, 49–53.

Krinski, D., Foerster, L.A., Deschamps, C., 2018. Efeito ovicida de óleos essenciais de 18 espécies Brasileiras de piper: Controlando Anticarsia gemmatalis (Lepidoptera, Erebidae) no estágio inicial de desenvolvimento. Acta Sci. - Agron. 40, 35273.

Kumaravel, J., Lalitha, K., Arunthirumeni, M., Shivakumar, M.S., 2021. Mycosynthesis of bimetallic zinc oxide and titanium dioxide nanoparticles for control of *Spodoptera frugiperda*. Pestic. Biochem. Physiol. 178, 104910.

Li, P., Chen, Z., Gu, Y., Si, Y., 2013. Spacecrafts navigation signal research based on GNSS constellation. Lect. Notes Electr. Eng. 244 LNEE, 35–48.

Machado, Keneson, Lemos, R., Pinto, F., Machado, Kedma, Cardoso, S., 2011. Potencial inseticida do extrato aquoso de nim sobre os ovos de Spodoptera frugiperda, in: VII Congresso Brasileiro de Agroecologia. 6, 11863.

Magrini, F.E., Specht, A., Gaio, J., Girelli, C.P., Migues, I., Heinzen, H., Saldaña, J., Sartori, V.C., Cesio, V., 2015. Antifeedant activity and effects of fruits and seeds extracts of *Cabralea canjerana canjerana* (Vell.) Mart. (Meliaceae) on the immature stages of the fall armyworm *Spodoptera frugiperda* (J.E Smith) (Lepidoptera: Noctuidae). Ind. Crops Prod. 65, 150–158.

Marinho, V.H.S., Holanda, F.H., Araújo, I.F., Jimenez, D.E.Q., Pereira, R.R., Porto, A.L.M., Ferreira, A.M., Carvalho, J.C.T., Albuquerque de Freitas, A.C.G., Fernandes, C.P., Souto, R.N.P., Ferreira, I.M., 2023. Nanoparticles from silk fibroin and Amazon oils: Potential larvicidal activity and oviposition deterrence against *Aedes aegypti*. Ind. Crops Prod. 203.

Marinho, V.H.S., Neves, F.B., Jimenez, D.E.Q., Oliveira, F.R., Santos, A.V.T.L.T., Ferreira, R.M.A., Souto, R.N.P., Carvalho, J.C.T., Yoshioka, S.A., Ferreira, I.M., 2022.

Development of an environmentally friendly formulation of silk fibroin combined with fatty acid from *Astrocaryum murumuru* Mart. effective against *Aedes aegypti* larvae. J. Drug Deliv. Sci. Technol. 75.

Maroneze, D.., Gallegos, D.M.., 2009. Efeito de extrato aquoso de Melia azedarach no desenvolvimento das fases imatura e reprodutiva de Spodoptera frugiperda (J. E. Smith, 1797) (Lepidoptera: Noctuidae). Sem. Cien. Agra 30, 537–550.

Maruthadurai, R., Ramesh, R., 2020. Occurrence, damage pattern and biology of fall armyworm, *Spodoptera frugiperda* (J.E. smith) (Lepidoptera: Noctuidae) on fodder crops and green amaranth in Goa, India. Phytoparasitica 48, 15–23.

Matos, A.P., Nebo, L., Vieira, P.C., Fernandes, J.B., Silva, M.F. das G. F. da., Rodrigues, R.R., 2009. Constituintes químicos e atividade inseticida dos extratos de frutos de Trichilia elegans E T. catigua (Meliaceae). Química Nova, 32(6), 1553–1556.

Mink, J.S., Luttrell, R.G., 1989. Mortality of fall army worm, *Spodoptera frugiperda* (Lepidoptera: Noctuidae) eggs, larvae and adults exposed to several insecticides on cotton. J. Entomol. Sci 24: 563-57.

Oliveira, A.E.M.F.M., Duarte, J.L., Cruz, R.A.S., Souto, R.N.P., Ferreira, R.M.A., Peniche, T., Conceição, E.C., Oliveira, L.A.R., Faustino, S.M.M., Florentino, A.C., Carvalho, J.C.T., Fernandes, C.P., 2017. *Pterodon emarginatus* oleoresin-based nanoemulsion as a promising tool for *Culex quinquefasciatus* (Diptera: Culicidae) control. J. Nanobiotechnology 15, 1–11.

Pham, D.T., Saelim, N., Tiyaboonchai, W., 2018. Crosslinked fibroin nanoparticles using EDC or PEI for drug delivery: physicochemical properties, crystallinity and structure. J. Mater. Sci. 53, 14087–14103.

Pinheiro, K.D., Rezende, K.F., Krinski, D., 2022. EFeito ovicida de óleo essencial de folhas e frutos de Piper fuligineum (Piperaceae) sobre ovos de *Spodoptera frugiperda* (Lepidoptera). J. Educ. Sci. Heal. 2, 2763-6119.

Pittarate, S., Perumal, V., Kannan, S., Mekchay, S., Thungrabeab, M., Suttiprapan, P., Sengottayan, S.N., Krutmuang, P., 2023. Insecticidal efficacy of nanoparticles against *Spodoptera frugiperda* (J.E. Smith) larvae and their impact in the soil. Heliyon 9, e16133.

Raju, I.M., Rao, T.S., Lakshmi, K.V.Di., Chandra, M.R., Padmaja, J.S., DIvya, G., 2019. Poly 3-Thenoic acid sensitized, copper doped anatase/brookite TiO_2 nanohybrids for enhanced

photocatalytic degradation of an organophosphorus pesticide. J. Environ. Chem. Eng. 7, 103211.

Rockwood, D.N., Preda, R.C., Yücel, T., Wang, X., Lovett, M.L., Kaplan, D.L., 2011. Materials fabrication from *Bombyx mori* silk fibroin. Nat. Protoc. 6, 1612–1631.

Roel, A.R., Vendramim, J.D., 2006. Efeito residual do extrato acetato de etila de Trichilia pallida Swartz (Meliaceae) para lagartas de diferentes idades de *Spodoptera frugiperda* (J.E. Smith, 1797) (Lepidoptera: Noctuidae). Cienc. Rural 36, 1049–1054.

Santos RC, dos Santos Alves CF, Schneider T, Lopes LQ, Aurich C, Giongo JL, Brandelli A, de Almeida Vaucher R. 2012 Antimicrobial activity of Amazonian oils against *Paenibacillus* species. J Invertebr Pathol. 109(3):265-8.

Sarquis, S.F.R., Marinho, V.H.S., Neves, F.B., Sarquis, I.R., Araújo, I.F., Damasceno, L.F., Ferreira, R.M.A., Souto, R.N.P., Carvalho, C.T., Ferreira, I.M., 2020. Industrial Crops & Products *Carapa guianensis* Aubl. (Meliaceae) oil associated with silk fibroin , as alternative to traditional surfactants , and active against larvae of the vector *Aedes aegypti* 157.

Sarria, A.L.F., Soares, M.S., Matos, A.P., Fernandes, J.B., Vieira, P.C, da Silva, M. F. G. F., 2011. Effect of Triterpenoids and Limonoids Isolated from *carapa*. Verlag der Zeitschrift für Naturforsch. 66, 245–250.

Souza, B.S.F., Carvalho, H.O., Ferreira, I.M., da Cunha, E.L., Barros, A.S., Taglialegna, T., Carvalho, J.C.T., 2017. Effect of the treatment with *Euterpe oleracea* Mart. oil in rats with triton-induced dyslipidemia. Biomed. Pharmacother. 90, 542–547.

Shah, M.A., Wani, S.H., 2016. Nanotechnology and insecticidal formulations. J. Food Bioeng. Nanoprocessing 1, 285–310.

Sims, S.R., Balusu, R.R., Ngumbi, E.N., Appel, A.G., 2014. Topical and vapor toxicity of saturated fatty acids to the *German Cockroach* (Dictyoptera: Blattellidae). J. Econ. Entomol. 107, 758–763.

Togola, A., Meseka, S., Menkir, A., Badu-Apraku, B., Boukar, O., Tamò, M., Djouaka, R., 2018. Measurement of pesticide residues from chemical control of the invasive *Spodoptera frugiperda* (Lepidoptera: Noctuidae) in a maize experimental field in Mokwa, Nigeria. Int. J. Environ. Res. Public Health 15.

CONSIDERAÇÕES FINAIS

O presente trabalho teve por objetivo desenvolver e caracterizar nanopartículas de fibroína de seda combinadas a óleos amazônicos como promissor agente larvicida frente às larvas do mosquito *Ae. aegypti* e da lagarta *S. frugiperda*. Insetos de grande importância na atualidade, pois um atua como vetor de transmissão de doenças ao homem e o outro vem causando grandes perdas na agricultura.

As nanopartículas produzidas a partir da solução fibroína de seda combinadas com gordura de *A. murumuru* e dos óleos de *B. excelsa* e *C. guianensis* foram caracterizadas através das técnicas de espalhamento dinâmico da luz, microscopia eletrônica de transmissão, infravermelho. Em conjunto essas análises mostraram que as nanopartículas produzidas apresentaram tamanhos de partículas variando de 207 ± 2.3 nm a 540.8 ± 23.8 nm, valores de PdI variando de 0.294 a 0.560 e potencial zeta variando de -37.9 ± 0.3 mV a -62.9 ± 0.7 mV. A microscopia eletrônica de transmissão mostrou que as nanopartículas apresentaram distribuição uniforme e formato esférico. Os espectros de infravermelho das nanopartículas obtidas foram semelhantes ao espectro de infravermelho da fibroína de seda, deste modo, pode-se inferir que a solução de fibroína de seda forma a parede das nanopartículas armazenando em seu núcleo os óleos.

Todas as nanopartículas apresentaram boa atividade larvicida frente as larvas de *Ae. aegypti*, com destaques para as nanopartículas combinadas a ésteres butílicos oriundos dos diferentes óleos. As nanopartículas de fibroína de seda combinadas ao éster butílico de *A. murumuru* (FABE-SF) exibiu taxa de mortalidade de 100% (LC_{50} de 21.35 $\mu g.mL^{-1}$), após 48 h de tratamento. As nanopartículas em combinação com o éster butílico de *B. excelsa* (FABE-Be-SF-NPs) apresentou taxa de mortalidade de 100% (LC_{50} de 21.14 $\mu g.mL^{-1}$), após 48 h de tratamento. As nanopartículas combinadas com o éster butílico de *C. guianensis* (FABE-Cg-SF-NPs) exibiu taxa de mortalidade de 98% (LC_{50} de 27.45 $\mu g.mL^{-1}$), após 48 h de tratamento. As nanopartículas FABE-Be-SF-NPs e FABE-Cg-SF-NPs ainda foram capazes de inibir a oviposição de fêmeas de *Ae. aegypti*. Além disso, as nanopartículas causaram danos em vários segmentos do corpo das larvas. Entretanto, as nanopartículas FABE-Be-SF-NPs e FABE-Cg-SF-NP não causaram efeitos teratogênicos significativos em embriões de zebrafish, até 96 h pós fertilização.

Por fim, foi avaliada a atividade larvicida de todas as nanopartículas frente as larvas de *S. frugiperda,* após 96 h de tratamento. As nanopartículas de fibroína de seda combinadas com o éster butílico de *B. excelsa* (Be-SF-NPs) apresentou melhor taxa de mortalidade, cerca de 100% (LC_{50} de 563.03 $\mu g.mL^{-1}$), ligeiramente maior que os controles positivos Karate zeon® e o óleo de Neem® já bem utilizados contra a *S. frugiperda*. As nanopartículas Be-SF-NPs inibiram a eclosão de ovos de *S. frugiperda* em 87% (LC_{50} de 341.03 $\mu g.mL^{-1}$). As nanopartículas ainda causaram modificações em vários segmentos do corpo das larvas de *S, frugiperda.*

No geral, a produção de nanopartículas de fibroína de seda combinadas a ésteres butílicos de diferentes óleos amazônicos, podem tornar-se uma ferramenta eficaz, sustentável e ecologicamente correta para o controle de larvas de *Ae. aegypti* e *S. frugiperda*.

Como perspectivas futuras este trabalho apresenta as seguintes possibilidades:

- Avaliar o grau de toxicidade ambiental das nanopartículas de *A. murumuru, B. excelsa* e *C. guianensis* em algas verdes (*Chlorella vulgaris*).
- Elucidar os mecanismos de ação dos óleos de *B. excelsa* e *C. guianensis* e da gordura de *A. murumuru,* bem como de suas respectivas nanopartículas.

ANEXO 1

Journal of Drug Delivery Science and Technology 75 (2022) 103626

Contents lists available at ScienceDirect

Journal of Drug Delivery Science and Technology

journal homepage: www.elsevier.com/locate/jddst

Opinion paper

Development of an environmentally friendly formulation of silk fibroin combined with fatty acid from *Astrocaryum murumuru* Mart. effective against *Aedes aegypti* larvae

Victor H.S. Marinho [a], Fernando B. Neves [a], David E.Q. Jimenez [a], Fabio R. Oliveira [b], Abrahão Victor T.L.T. Santos [c], Ricardo M.A. Ferreira [d], Raimundo N.P. Souto [d], José C.T. Carvalho [c], Sérgio A. Yoshioka [e], Irlon M. Ferreira [a,*]

[a] *Biocatalysis and Applied Organic Synthesis Laboratory, Federal University of Amapá, Campus Universitário Marco Zero do Equador, Rodovia Juscelino Kubitschek de Oliveira Km 02, Bairro Zerão, 68902-280, Macapá, AP, Brazil*

[b] *Quality Control and Bromatology Laboratory, Federal University of Amapá, Campus Universitário Marco Zero do Equador, Rodovia Juscelino Kubitschek de Oliveira Km 02, Bairro Zerão, 68902-280, Macapá, AP, Brazil*

[c] *Drug Research Laboratory, Federal University of Amapá, Campus Universitário Marco Zero do Equador, Rodovia Juscelino Kubitschek de Oliveira Km 02, Bairro Zerão, 68902-280, Macapá, AP, Brazil*

[d] *Artropod Laboratory, Federal University of Amapá, Campus Universitário Marco Zero do Equador, Rodovia Juscelino Kubitschek de Oliveira Km 02, Bairro Zerão, 68902-280, Macapá, AP, Brazil*

[e] *Biochemistry and Biomaterials Laboratory, Institute of Chemistry of São Carlos, University of São Paulo, Universidade de São Paulo, Av. Trabalhador São-Carlense 400, 13560-970, São Carlos, SP, Brazil*

ARTICLE INFO

Keywords:
Silkworm cocoon
Larvicidal activity
Biomaterial
Biopesticide
Fatty acid esters
Dengue
Amazon oil

ABSTRACT

The *Aedes aegypti* mosquito is a vector of several diseases, including dengue, yellow fever and the Zika virus. Synthetic insecticides such as chlorpyrifos and chlorothalonil have been used to control this vector, despite causing damage to both the environment and humans. Research into natural active compounds with a low environmental impact is therefore required. The present study developed an environmentally friendly formu- lation of silk fibroin (SF) combined with fatty acid esters [ethyl (FAEE-SF), propyl (FAPE-SF) and butyl (FABE- SF)] from *A. murumuru* fat, which was effective against larvae of the *Ae. aegypti* vector. The FABE-SF nanoparticle induced a higher mortality rate in *Ae. aegypti* larvae after 48 h (LC_{50} = 21.35 μg/mL). The stability of the nano was monitored for 21 days, and FABE-SF exhibited greater stability throughout this period, with average particle,zeta and PDI values of around 217.5 ± 0.85 nm, —25.6 ± 3.24 mV and 0.338 ± 0.01, respectively. This is the first work of its type to identify the larvicidal activity of fatty acid esters from *A. murumuru,* combined with silk fibroin, against *Ae. aegypti.*

1. Introduction

The effective and sustainable control of mosquito population vectors of diseases is a challenging task [1,2]. For many years, the control of such populations has involved the use of various synthetic insecticides, such as organochlorines, organophosphates and pyrethroids [3]. How- ever, the indiscriminate and frequent use of such substances has caused selected populations of mosquitoes to become more resistant, as well as resulting in environmental pollution from their non-selective inhibitory enzymatic actions [4], putting humans and other non-target populations at risk [5]. An effective low-cost insecticide with a lower environmental risk is therefore required [1,2].

There is a growing demand for biopesticides, since certain plant species contain a variety of bioactive compounds with insecticidal

properties [1]. Fat extracted from the fruits of *A. murumuru,* for example, is a potentially effective biopesticide for vector control. *A. murumuru* fat is easily obtained, as the species is widely distributed around the Amazon estuary. Its natural fat is used as a raw material in the cosmetics and food industries, as its composition contains saturated fatty acids such as lauric and myristic acid [6]. Although the larvicidal, insecticidal, and repellent action of fatty acids against mosquitoes has been widely reported in literature [7–9],

* Corresponding author.
E-mail address: irlon.ferreira@gmail.com (I.M. Ferreira).

https://doi.org/10.1016/j.jddst.2022.103626
Received 21 July 2021; Received in revised form 18 July 2022; Accepted 20 July 2022
Available online 31 July 2022

ANEXO 2

Industrial Crops & Products 203 (2023) 117133

Contents lists available at ScienceDirect

Industrial Crops & Products

journal homepage: www.elsevier.com/locate/indcrop

Nanoparticles from silk fibroin and Amazon oils: Potential larvicidal activity and oviposition deterrence against *Aedes aegypti*

Victor H.S. Marinho [a], Fabrício H. Holanda [a], Inana F. Araújo [a], David E.Q. Jimenez [a], Rayanne R. Pereira [b], André L.M. Porto [c], Adriana M. Ferreira [d], José C.T. Carvalho [d], Ana C.G. Albuquerque de Freitas [e], Caio P. Fernandes [d], Raimundo N.P. Souto [f], Irlon M. Ferreira [a,*,1]

[a] Laboratório de Biocatálise e Síntese Orgânica Aplicada, Departamento de Ciências Exatas e Tecnológicas, Universidade Federal do Amapá, Rod. JK, KM 02, 68902- 280, Macapá, Amapá, Brazil

[b] Universidade Federal do Oeste do Pará, Instituto de Saúde Coletiva (Unidade Tapajós), 68035-110, Santarém, Pará, Brazil

[c] Laboratório de Química Orgânica e Biocatálise, Instituto de Química de São Carlos, Universidade de São Paulo, Av. João Dagnone, 1100, Ed. Prof. Dr. Wagner Douglas, J. Santa Angelina, 13563-120, São Carlo, São Paulo, Brazil

[d] Laboratório de Pesquisa em Fármacos, Departamento de Ciências Biológicas e da Saúde, Universidade Federal do Amapá, Rod. JK, KM 02, 68902-280, Macapá, Amapá, Brazil

[e] Laboratório de Planejamento e Desenvolvimento de Fármacos, Instituto de Ciências Exatas e Naturais, Universidade Federal do Pará, Belém, PA, Brazil

[f] Laboratório de Artrópodes, Departamento de Ciências Exatas e Tecnológicas, Universidade Federal do Amapá, Rod. JK, KM 02, 68902-280, Macapá, Amapá, Brazil

ARTICLEINFO

Keywords:
Andiroba
Carapa guianensis
Brazil nuts
Bertholletia excelsa
Dengue
Amazon oils

ABSTRACT

This work reports the preparation of nanoparticles of silk fibroin with esters obtained from the oils of two Amazonian plant species (*Carapa guianensis* Aublet and *Bertholletia excelsa*) with excellent physicochemical properties and activity against the larvae of the vector *Aedes aegypti*. The temporal stability of the nanoparticles was evaluated for 50 days at temperatures of 4 °C and 32 °C. The size of the nanoparticle was satisfactory, with sizes ranging from 207 ± 2.3 nm to 540.8 ± 23.8 nm, and PdI values ranging from 0.294 to 0.560, and zeta potential from − 37.9 ± 0.3 mV to − 62.9 ± 0.7 mV. Study of the morphology of nanoparticles, by transmission electron microscopy analysis, clearly showed spherical shapes. The nanoparticles presented slow and controlled release that induced a high mortality rate in the 3rd larval instar of *Ae. aegypti*, with LC_{50} of 27.45 μg. mL^{-1} for FABE-Cg-SF-NPs and LC_{50} of 21.14 μg.mL^{-1} for FABE-Be-SF-NPs, after 48 h of exposure. In addition, they were able to inhibit oviposition by *Ae. aegypti*. However, the nanoparticles did not present significant teratogenic effects on zebrafish embryos up to 72 h post-fertilization. Thus, the formation of nanoparticles by butyl esters in silk fibroin may become an (eco)alternative and effective in the control of *Ae. aegypti* larvae.

1. Introduction

The World Health Organization states that vector-transmitted infectious diseases such as dengue, yellow fever, Zika fever, chikungunya fever, malaria, filariasis, leishmaniasis and Chagas disease account for more than 17% of infectious diseases worldwide and cause more than 700,000 deaths per year (Who, 2018). Arboviruses are groups of viruses of medical relevance for public health that can be transmitted to vertebrate hosts through several vectors such as hematophagous arthropods, sandflies and ticks, but mosquitoes are the principal vector for this group of viruses (Huang et al., 2019; Sukhralia et al., 2019; Young, 2018).

Dengue is a serious public health problem that affects millions of people worldwide. It is transmitted by mosquitoes that carry arboviruses. Dengue is endemic in more than 129 countries, especially in tropical and subtropical regions, where the climate and environmental conditions favor the breeding of mosquitoes. (Duarte et al., 2021). An estimated 100-400 million cases of dengue occur per year, with 96 million symptomatic cases and 40,000 deaths worldwide (Who, 2018). There is still no specific antiviral treatment for the different dengue

* Corresponding author.
E-mail address: irlon.ferreira@gmail.com (I.M. Ferreira).
[1] Orcid.org/0000-0002-4517-0105

https://doi.org/10.1016/j.indcrop.2023.117133
Received 11 April 2023; Received in revised form 23 June 2023; Accepted 5 July 2023
Available online 18 July 2023

ANEXO 3

Supplementary Information

Development of an environmentally friendly formulation of silk fibroin associated with fatty acid from *Astrocaryum murumuru* Mart. fat, effective against larvae of the *Aedes aegypti* vector

Victor H. S. Marinho[a], Fernando B. Neves[a], David E. Q. Jimenez[a], Fabio R. Oliveira[b], Abrahão Victor T. L. T. Santos[c], Ricardo M. A. Ferreira[d], Raimundo N. P. Souto[d], José C. T. Carvalho[c], Sérgio A. Yoshioka[e], Irlon M. Ferreira[a,*]

[a]Biocatalysis and Applied Organic Synthesis Laboratory, Federal University of Amapá, Campus Universitário Marco Zero do Equador, Rodovia Juscelino Kubitschek de Oliveira Km 02, Bairro Zerão, CEP: 68902-280, Macapá, AP, Brazil.

[b]Laboratory of Quality Control and Bromatology, Federal University of Amapá, Campus Universitário Marco Zero do Equador, Rodovia Juscelino Kubitschek de Oliveira Km 02, Bairro Zerão, CEP: 68902-280, Macapá, AP, Brazil.

[c]Drug Research Laboratory, Federal University of Amapá, Campus Universitário Marco Zero do Equador, Rodovia Juscelino Kubitschek de Oliveira Km 02, Bairro Zerão, CEP: 68902-280, Macapá, AP, Brazil.

[d]Artropod Laboratory, Federal University of Amapá, Campus Universitário Marco Zero do Equador, Rodovia Juscelino Kubitschek de Oliveira Km 02, Bairro Zerão, CEP: 68902-280, Macapá, AP, Brazil.

[e]Biochemistry and Biomaterials Laboratory, Institute of Chemistry of São Carlos, University of São Paulo, Universidade de São Paulo, Av. Trabalhador São-Carlense, 400, 13560-970, São Carlos, SP, Brazil.

*Corresponding autor: irlon.ferreira@gmail.com

Characterization of murumuru fat by GC-MS

Fig. 1. Fatty ethyl ester compositions of *A. murumuru*, determined by GC-MS analysis.

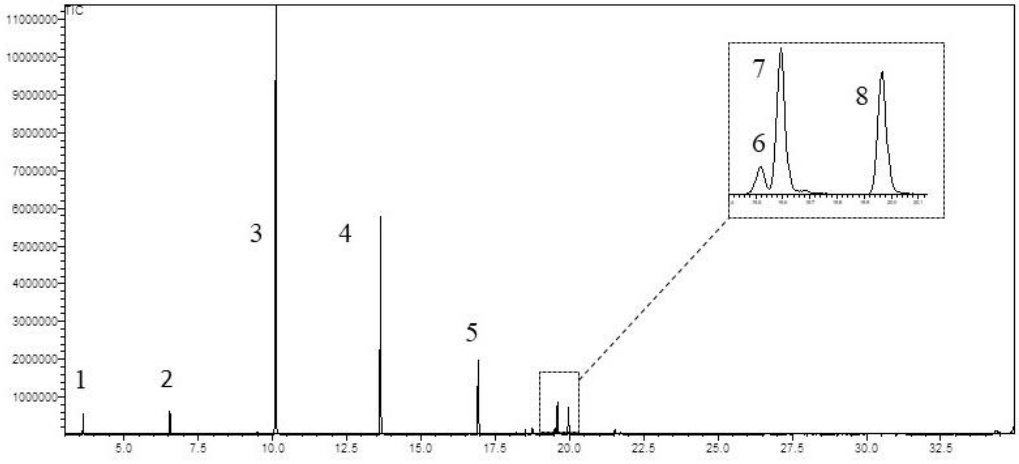

Table 1. Fatty acid composition (%) of *A. murumuru* fat by GC-MS analysis

Fatty acid	Peak	Time (min)	Relative Concentration (%)[c]
Caproic (C6:0)	1	3.63	1.73
Caprylic (C8:0)	2	6.54	2.40
Lauric (C12:0)	3	10.11	53.51
Myristic (C14:0)	4	13.63	25.79
Palmitic (C16:0)	5	16.92	8.59
Linoleic (C18:2)	6	19.51	0.66
Oleic (C18:1)	7	19.59	3.88
Stearic (C18:0)	8	19.96	3.45
Total Saturated	-	-	95.47
Total Monounsaturated	-	-	3.88
Total Polyunsaturated	-	-	0.66

*Percentage of FAEE corresponding fatty acid; [b]MS database (NIST 5.0)

Fig. 1a. Lauric acid ethyl ester profile determined by GC-MS analysis.

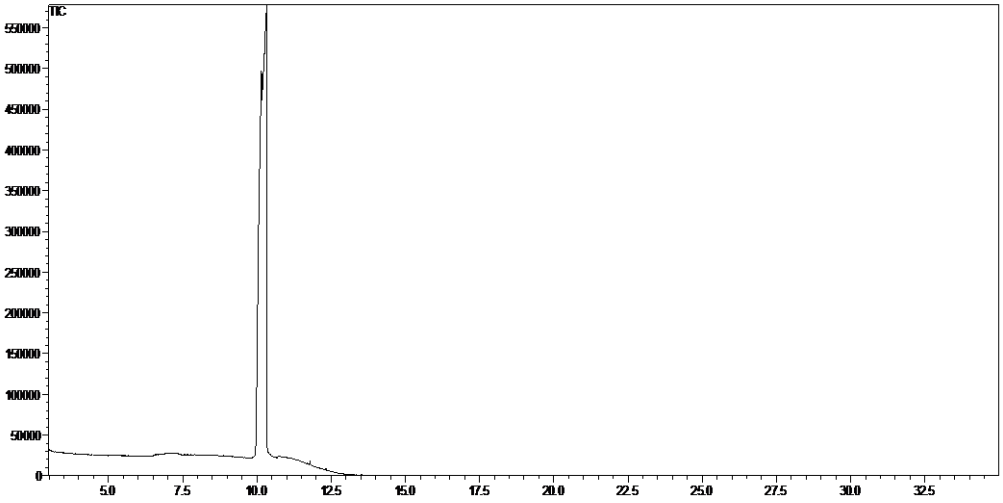

Fig. 1b. GC-MS of Lauric acid ester.

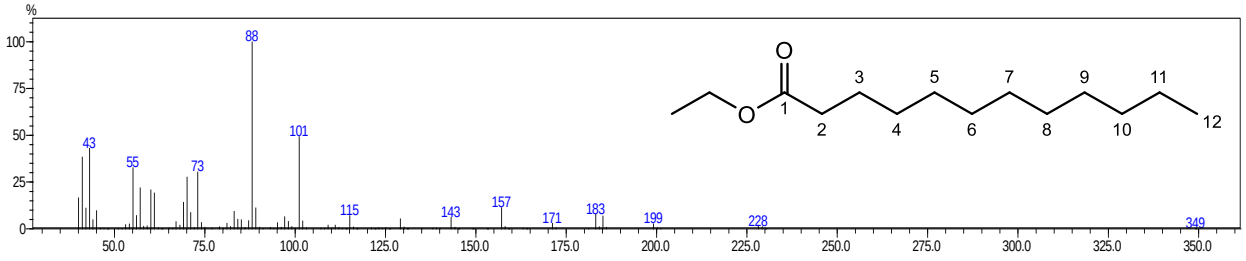

Fig. 1c. Myristic acid ethyl ester profile determined by GC-MS analysis.

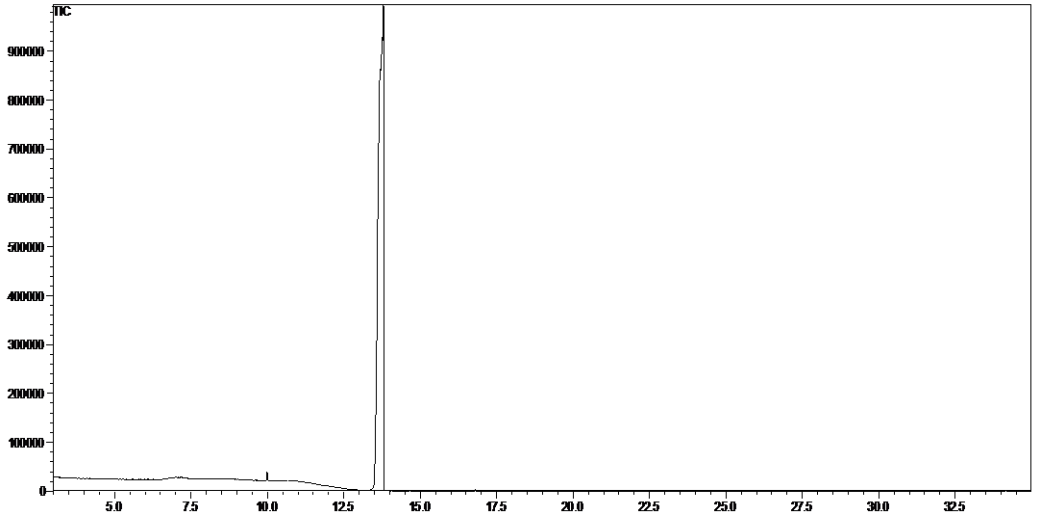

Fig. 1d. GC-MS of Myristic acid ester.

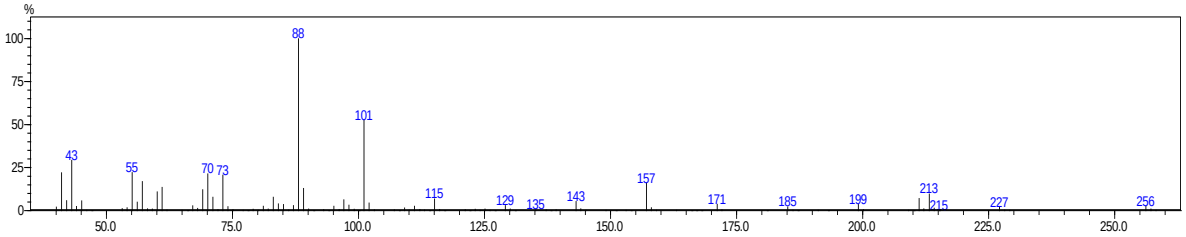

Fig. 1e. Oleic acid ethyl ester profile determined by GC-MS analysis.

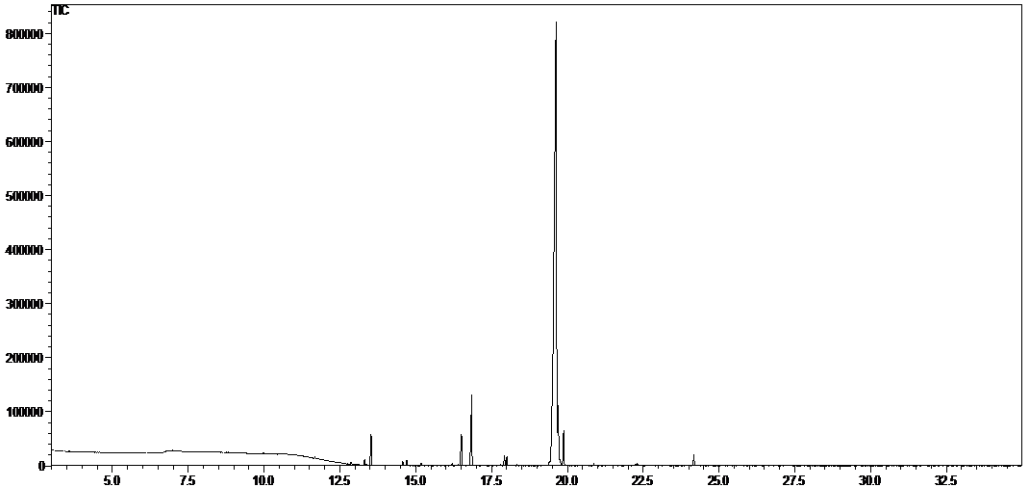

Fig. 1f. GC-MS of Oleic acid ester.

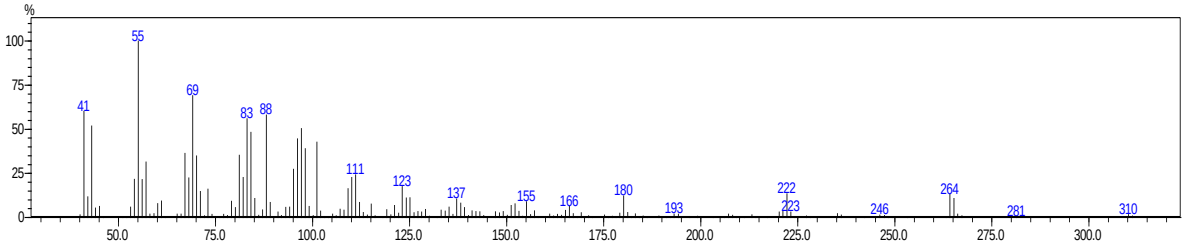

Fig. 1g. Stearic acid ethyl ester profile determined by GC-MS analysis.

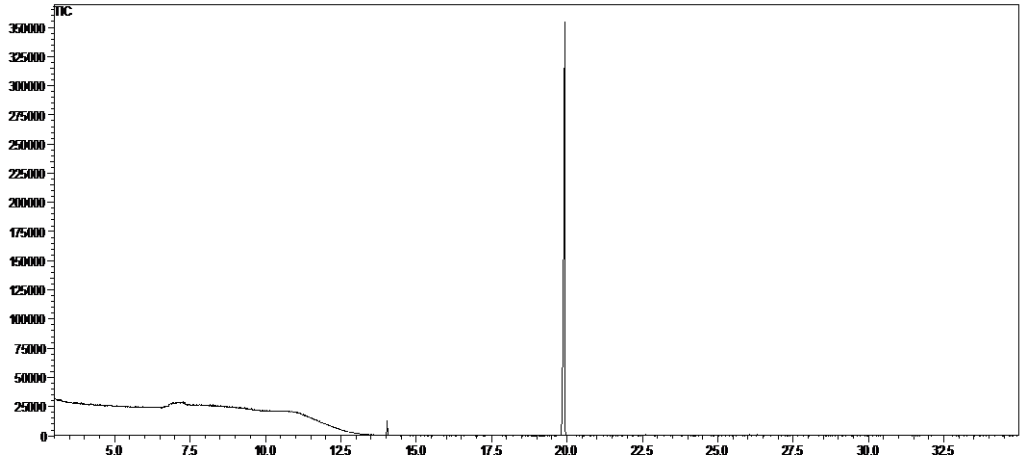

Fig. 1g. GC-MS of Stearic acid ester.

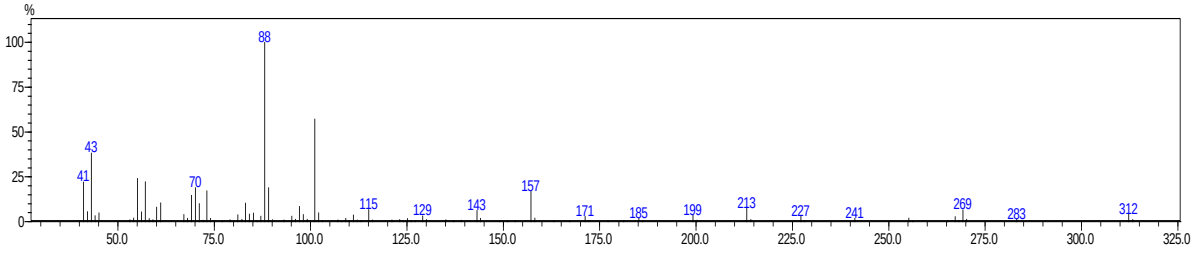

Characterization of murumuru oils and derivatives by FTIR

Murumuru fat

Yellow oil; FTIR ν_{max}(cm^{-1}) (pure) = 2931, 2850, 1740, 1655, 1465, 1371, 1164.

Murumuru FAEE

Yellow oil; FTIR ν_{max}(cm^{-1}) (pure) = 2930, 2853, 1740, 1655, 1462, 1376, 1169.

Murumuru FAPE

Yellow oil; FTIR ν_{max}(cm^{-1}) (pure) = 2923, 2853, 1747, 1653, 1462, 1379, 1169.

Murumuru FABE

Yellow oil; FTIR ν_{max}(cm^{-1}) (pure) = 2950, 2854, 1743, 1686, 1466, 1371, 1164.

Fig. 2. FTIR spectra of Murumuru fat and derivatives.

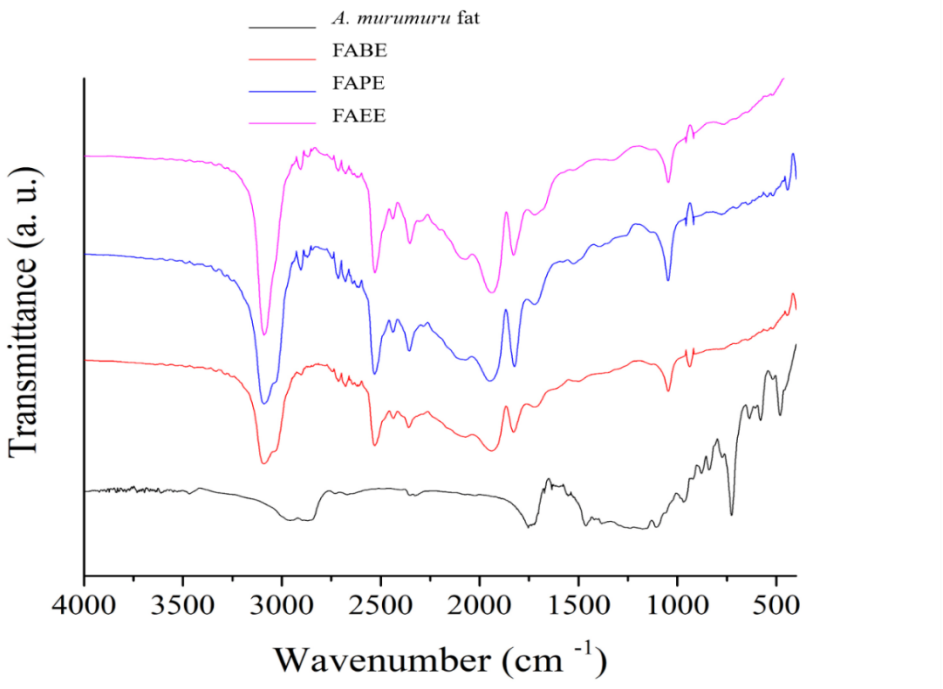

Murumuru FAEE

Fig. 3. GC-MS of Murumuru esterification reaction with ethanol.

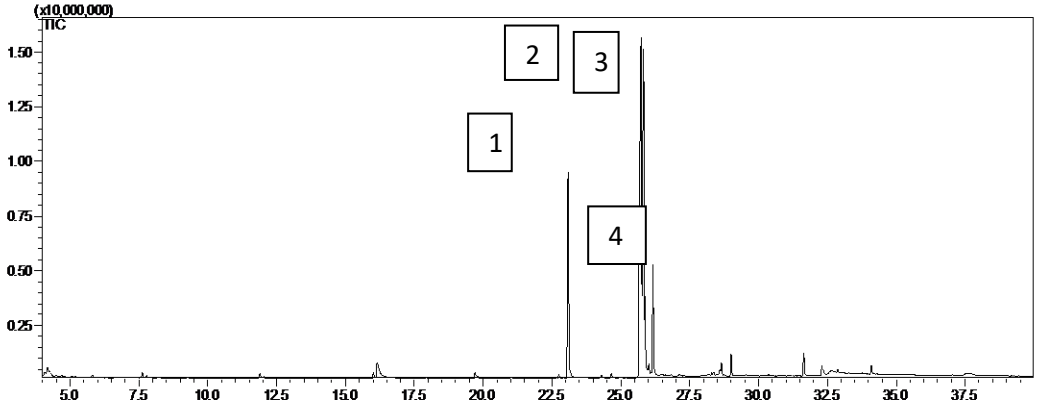

Fig. 3a. GC-MS of Hexadecanoic acid ethyl ester **1** (96% similarity).

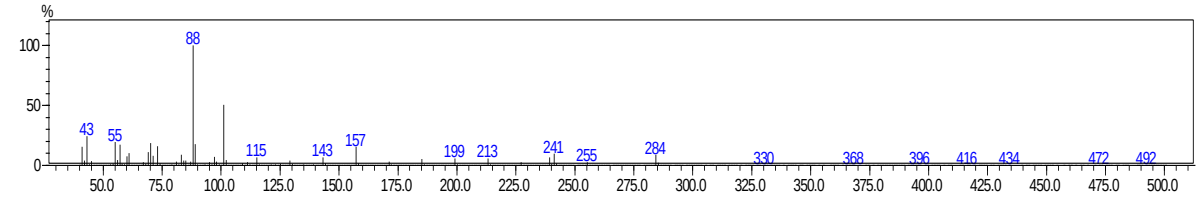

Fig. 3b. GC-MS of ethyl (9*Z*, 12*Z*)-octadeca-9,12-dienoate **2** (94% similarity).

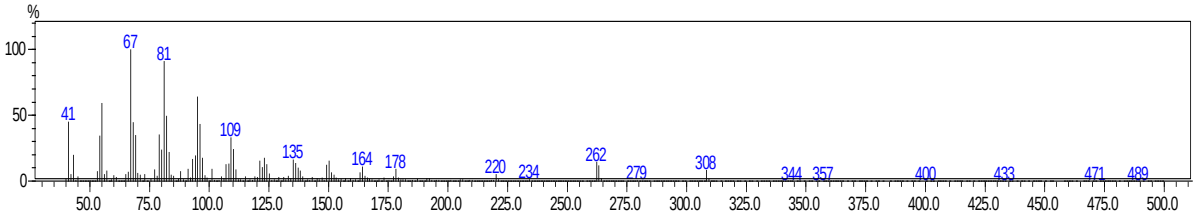

Fig. 3c. GC-MS of Ethyl oleate **3** (93% similarity).

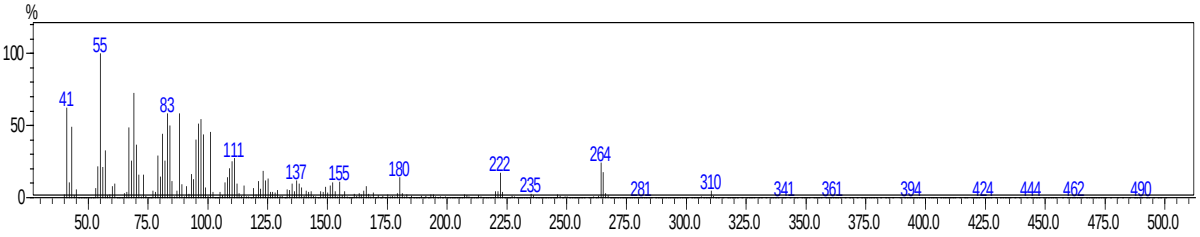

Fig. 3d. GC-MS ethyl (*E*)-octadec-9-enoate **4** (94% similarity).

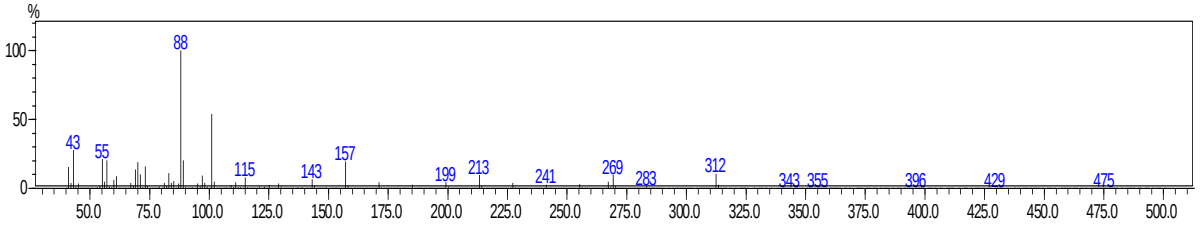

Table 2. GC-MS analyses of Murumuru esterification using Ethanol.

Compounds	Retention tome (min)	Quantity compound (%)	Similarity (%)
Hexadecanoic acid ethyl ester	23.1	22.0	96
ethyl (9*Z*,12*Z*)-octadeca-9,12-dienoate	25.7	37.3	94
Ethyl oleate.	25.8	30.0	93
ethyl (*E*)-octadec-9-enoate	26.1	10.6	94
Total identification (%)		99.9	
Monounsaturated compounds (%)		40.6	
Poly-unsaturated compounds (%)		37.3	
Saturated compounds (%)		22.0	

*MS database (NIST 5.0)

Murumuru FAPE

Fig. 4. GC-MS of Murumuru esterification reaction with propanol.

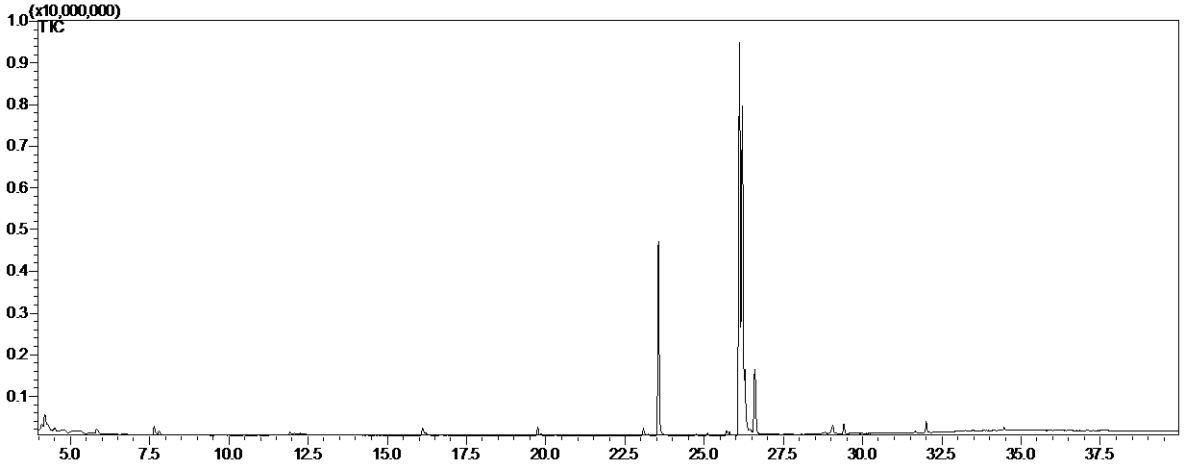

Fig. 4a. GC-MS of Hexadecanoic acid propyl ester **1** (95% similarity).

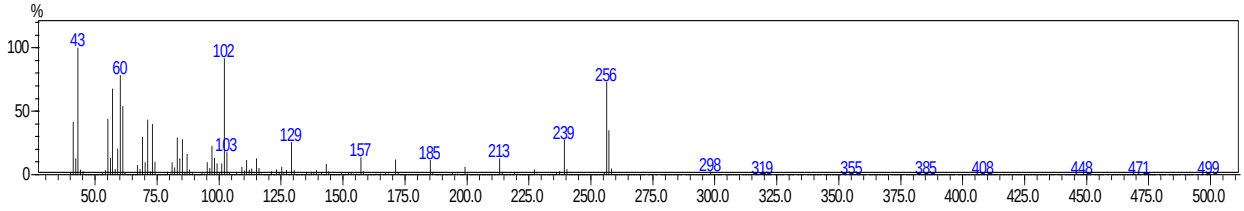

Fig. 4b. GC-MS propyl linoleate **2** (88% similarity).

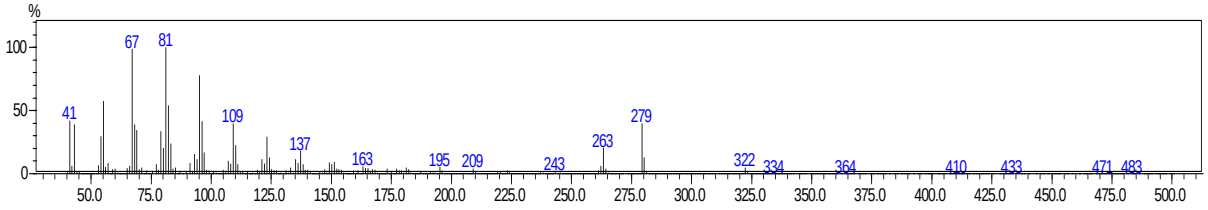

Fig. 4c. GC-MS propyl oleate **3** (89% similarity).

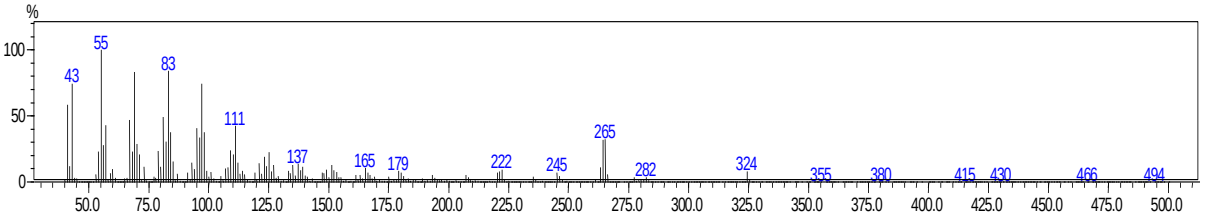

Fig. 4d. GC-MS propyl (*E*)-octadec-9-enoate **4** (92% similarity).

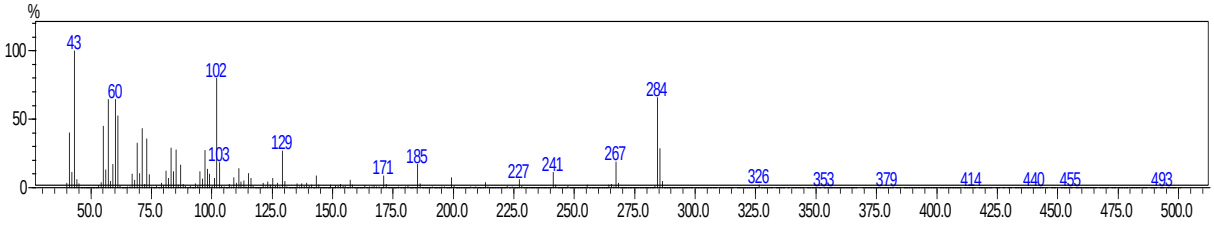

Table 3. GC-MS analyzes of Murumuru esterification using propanol.

Compounds	**retention time (min)**	**Quantity compound (%)**	**Similarity (%)**
Hexadecanoic acid propyl ester	23.5	22.0	95
propyl linoleate	26.1	39.4	88
propyl oleate.	26.2	32.3	89
propyl (*E*)-octadec-9-enoate	26.6	6.25	92
Total identification (%)		99.9	
Monounsaturated compounds (%)		38.5	
Poly-unsaturated compounds (%)		39.4	
Saturated compounds (%)		22.0	

*MS database (NIST 5.0)

Murumuru FABE

Fig. 5. GC-MS of Murumuru esterification reaction with butanol.

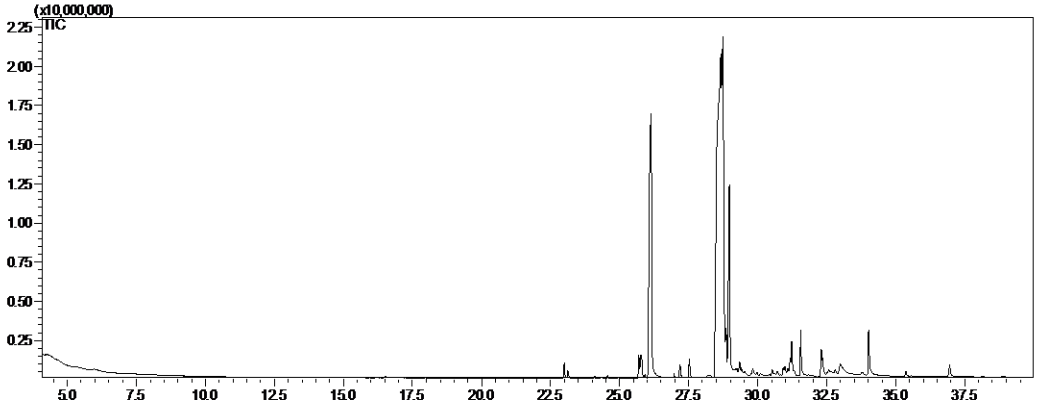

Fig. 5a. GC-MS of Hexadecanoic acid butyl ester **1** (95% similarity).

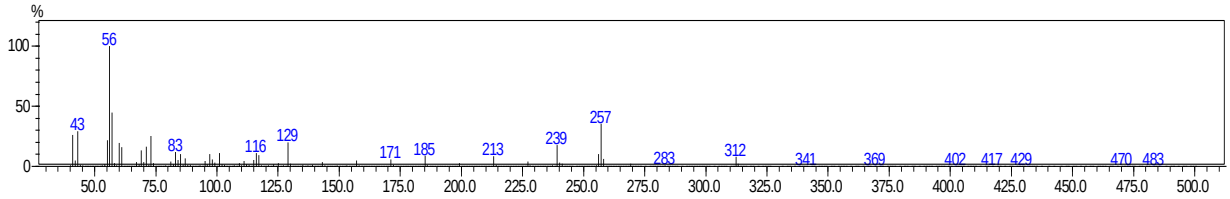

Fig. 5b. GC-MS of butyl linoleate **2** (91% similarity).

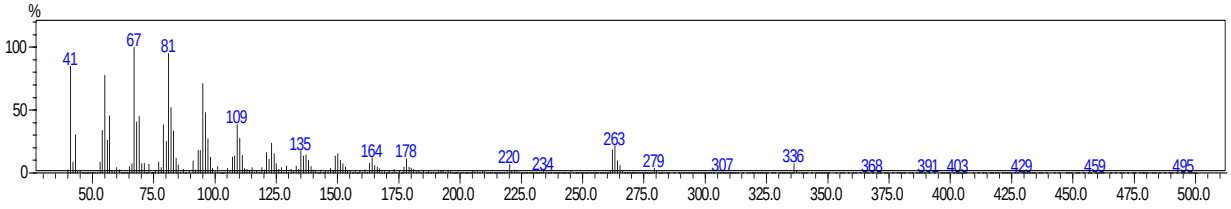

Fig. 5c. GC-MS of butyl oleate **3** (91% similarity).

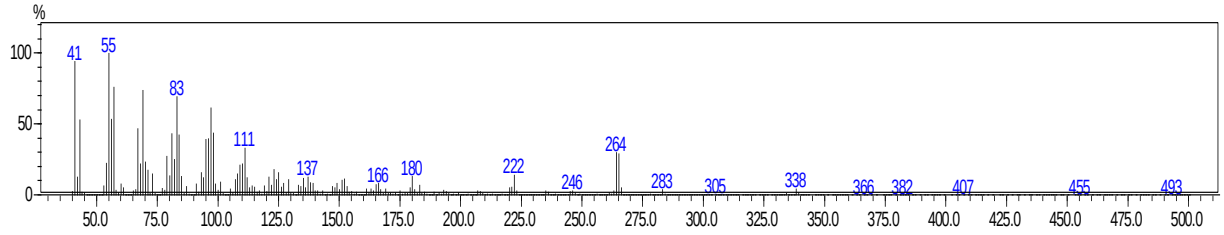

Fig. 5d. GC-MS of butyl (*E*)-octadec-9-enoate **4** (93% similarity).

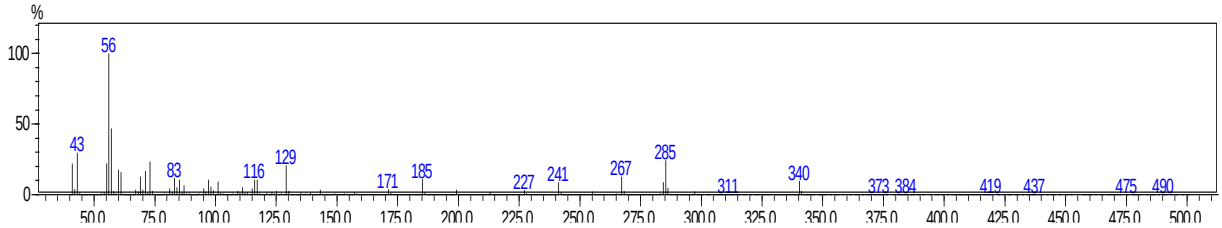

Table 4. GC-MS Analyzes of murumuru esterification using Butanol.

Compounds	**Retention time (min)**	**Quantity compound (%)**	**Similarity (%)**
Hexadecanoic acid butyl ester	26.1	24.7	95
butyl linoleate	28.6	29.3	91
butyl oleate	28.7	31.7	91
butyl (*E*)-octadec-9-enoate	28.9	14.2	93
Total identification (%)		99.9	
Monounsaturated compounds (%)		45.9	
Poly-unsaturated compounds (%)		29.3	
Saturated compounds (%)		24.7	

*MS database (NIST 5.0)

ANEXO 4

Supplementary Information

Polymeric Nanoparticles from Silk Fibroin and Amazon Oils: Potential Larvicidal Activity and Oviposition Deterrence Against *Aedes aegypti*

Victor H. S. Marinho[a], Fabrício H. Holanda[a], Inana F. Araújo[a], David E. Q. Jimenez[a], Rayanne R. Pereira[b], André L.M. Porto[c], Adriana M. Ferreira[d], José C.T. Carvalho[d], Ana C. G. Albuquerque de Freitas[e], Caio P. Fernandes[d], Raimundo N. P. Souto[e], Irlon M. Ferreira[a],*

[a]Biocatalysis and Applied Organic Synthesis Laboratory, Federal University of Amapá, University Campus Marco Zero do Equador, Rodovia Juscelino Kubitschek de Oliveira, Km 02, Bairro Zerão, 68902-280, Macapá, AP, Brazil.

[b]Federal University of Western Pará, Institute of Collective Health (Tapajós Unit), 68035-110 Santarém, PA, Brazil.

[c]Department of Physical Chemistry, Institute of Chemical of São Carlos, University of São Paulo. Av. João Dagnone, 1100, Ed. Prof. Douglas Wagner Franco, Santa Angelina, 13563–120, São Carlos, SP, Brazil.

[d]Drug Research Laboratory, Federal University of Amapá, University Campus Marco Zero do Equador, Rodovia Juscelino Kubitschek de Oliveira, Km 02, Bairro Zerão, 68902-280, Macapá, AP, Brazil.

[e]Drug Planning and Development Laboratory, Institute of Exact and Natural Sciences, Federal University of Pará, Belém, PA, Brazil.

[f]Artropod Laboratory, Federal University of Amapá, University Campus Marco Zero do Equador, Rodovia Juscelino Kubitschek de Oliveira, Km 02, Bairro Zerão, 68902-280, Macapá, AP, Brazil.

*Corresponding author: irlon.ferreira@gmail.com /Orcid.org/0000-0002-4517-0105

***C. guianensis* Oil**. FTIR ν_{max}(cm^{-1}) (pure) = 2926, 2855, 1748, 1466, 1165, 1022, 725.; ^{1}H NMR (500 MHz, $CDCl_3$) δ (ppm) = 5.38-5.24 (m, 3H), 4.29 (dd, *J* = 11.9, 4.3 Hz, 1H), 4.14 (dd, *J* = 11.9, 6.0 Hz, 2H), 2.38-2.27 (m, 5H), 2.07-1.97 (m, 6H), 1.61 (m, 5H), 1.38-1.20 (m, 49H), 0.91-0.85 (m, 7H).; ^{13}C NMR (126 MHz, $CDCl_3$) δ (ppm) = 173.5, 173.4, 173.0, 130.2, 129.9, 129.8, 128.2, 69.0, 62.2, 34.4, 34.2, 34.2, 32.1, 32.1, 29.9, 29.9, 29.9, 29.8, 29.8, 29.8, 29.7, 29.6, 29.5, 29.5, 29.4, 29.4, 29.33, 29.3, 29.27, 29.2, 29.2, 27.4, 27.3, 25.0, 25.0, 25.0, 22.8, 14.3.

***B. excelsa* Oil**. FTIR ν_{max}(cm^{-1}) (pure) = 2927, 2855, 1747, 1466, 1163, 1035, 724.; ^{1}H NMR (500 MHz, $CDCl_3$) δ (ppm) = 5.39-5.24 (m, 4H), 4.29 (dd, *J* = 11.9, 4.3 Hz, 1H), 4.14 (dd, *J* = 11.9, 6.0 Hz, 1H), 2.77 (t, *J* = 7.0 Hz, 1H), 2.31 (m, 4H), 2.07-1.98 (m, 5H), 1.61 (m, 5H), 1.37 – 1.23 (m, 19H), 0.88 (m, 5H).; ^{13}C NMR (126 MHz, $CDCl_3$) δ (ppm) = 173.7, 173.7, 173.7, 173.3, 173.2, 130.6, 130.4, 130.4, 130.4, 130.1, 130.1, 128.5, 128.5, 128.3, 128.3, 77.2, 69.3, 62.5, 34.6, 34.5, 34.4, 32.3, 32.3, 31.9, 30.2, 30.1, 30.1, 30.1, 30.1, 30.0, 30.0, 30.0, 29.9, 29.9, 29.9, 29.8, 29.8, 29.7, 29.7, 29.7, 29.7, 29.7, 29.6, 29.6, 29.6, 29.5, 29.5, 29.5, 29.5, 27.6, 27.6, 27.6, 26.0, 25.3, 25.3, 25.2, 23.1, 23.1, 23.0, 14.5, 14.5.

FABE-Cg. FTIR ν_{max}(cm^{-1}) (pure) = 2927, 2856, 1743, 1468, 1166, 1036, 724.; ^{1}H NMR (500 MHz, $CDCl_3$) δ (ppm) = 5.37-5.32 (m, 3H), 3.86 (d, *J* = 6.7 Hz, 6H), 2.38-2.29 (m, 8H), 2.08-1.99 (m, 12H), 1.93 (dt, *J* = 13.3, 6.7 Hz, 3H), 1.67-1.57 (m, 20H), 1.36-1.25 (m, 67H), 0.94 (d, *J* = 6.7 Hz, 18H), 0.89 (t, *J* = 7.0 Hz, 14H).; ^{13}C NMR (126 MHz, $CDCl_3$) δ (ppm) = 174.2, 130.2, 129.9, 70.5, 65.3, 63.5, 62.8, 34.6, 34.6, 32.1, 32.1, 29.9, 29.8, 29.8, 29.8, 29.8, 29.8, 29.7, 29.6, 29.5, 29.5, 29.4, 29.3, 29.3, 29.3, 29.3, 29.3, 29.2, 27.9, 27.4, 27.3, 25.2, 25.2, 22.8, 19.3, 14.3.

FABE-Be. FTIR ν_{max}(cm^{-1}) (pure) = 2927, 2857, 1743, 11467, 1164, 1036, 725.; ^{1}H NMR (400 MHz, $CDCl_3$) δ (ppm) = 5.38-5.30 (m, 3H), 3.85 (d, *J* = 6.7 Hz, 4H), 2.79-2.75 (m, 1H), 2.30 (t, *J* = 7.5 Hz, 3H), 2.07-1.98 (m, 5H), 1.92 (dt, *J* = 13.4, 6.7 Hz, 1H), 1.66 -1.58 (m, 5H), 1.36-1.22 (m, 29H), 0.92 (dd, *J* = 6.7, 3.0 Hz, 10H), 0.88 (td, *J* = 7.0, 4.1 Hz, 4H).; ^{13}C NMR (100 MHz, $CDCl_3$) δ (ppm) = 173.9, 173.9, 130.0, 129.9, 129.9, 129.8, 129.8, 129.6, 127.9, 127.7, 74.8, 70.2, 70.1, 65.0, 63.1, 62.3, 34.2, 34.2, 31.8, 31.7, 31.4, 29.6, 29.5, 29.5, 29.5, 29.5, 29.4, 29.4, 29.3, 29.2, 29.2, 29.2, 29.1, 29.0, 29.0, 28.9, 28.9, 27.5, 27.0, 27.0, 27.0, 27.0, 25.6, 25.0, 24.9, 22.5, 22.4, 18.9, 13.9, 13.9.

Figure S1. ^{1}H NMR (500 MHz, $CDCl_3$) of *C. guianensis* Oil.

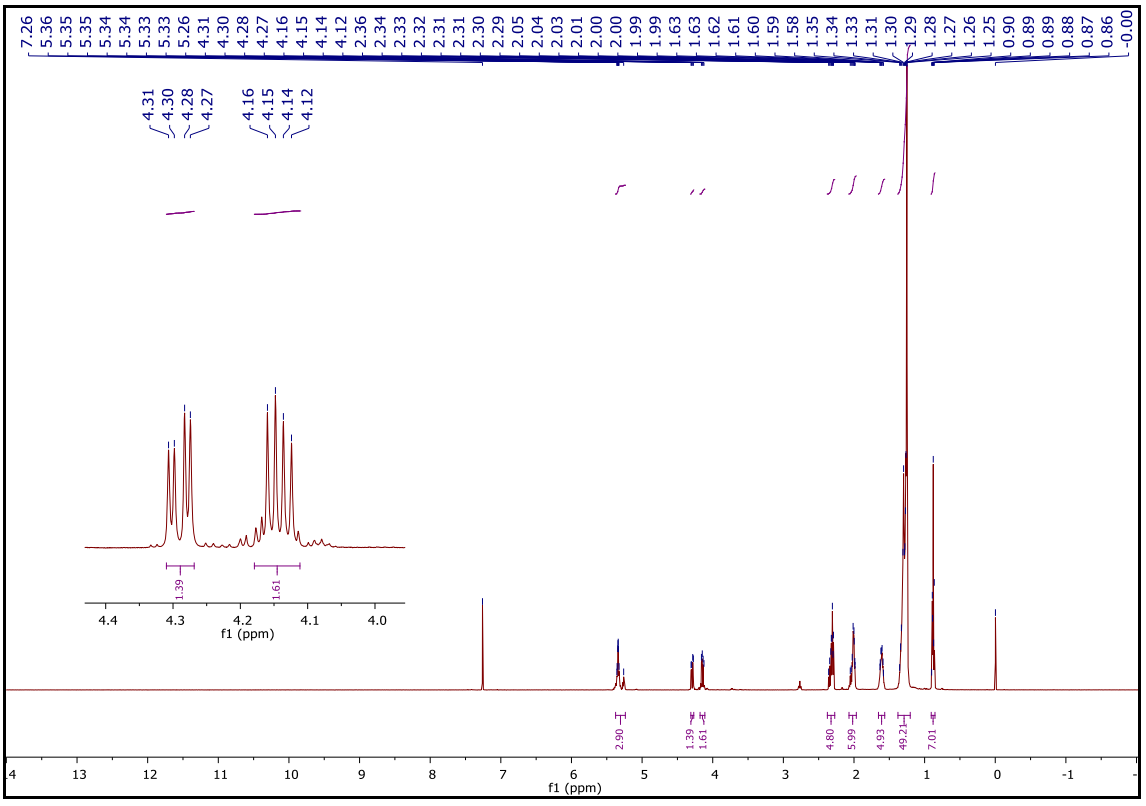

Figure S2. ^{13}C NMR (126 MHz, CDCl3) of *C. guianensis* Oil.

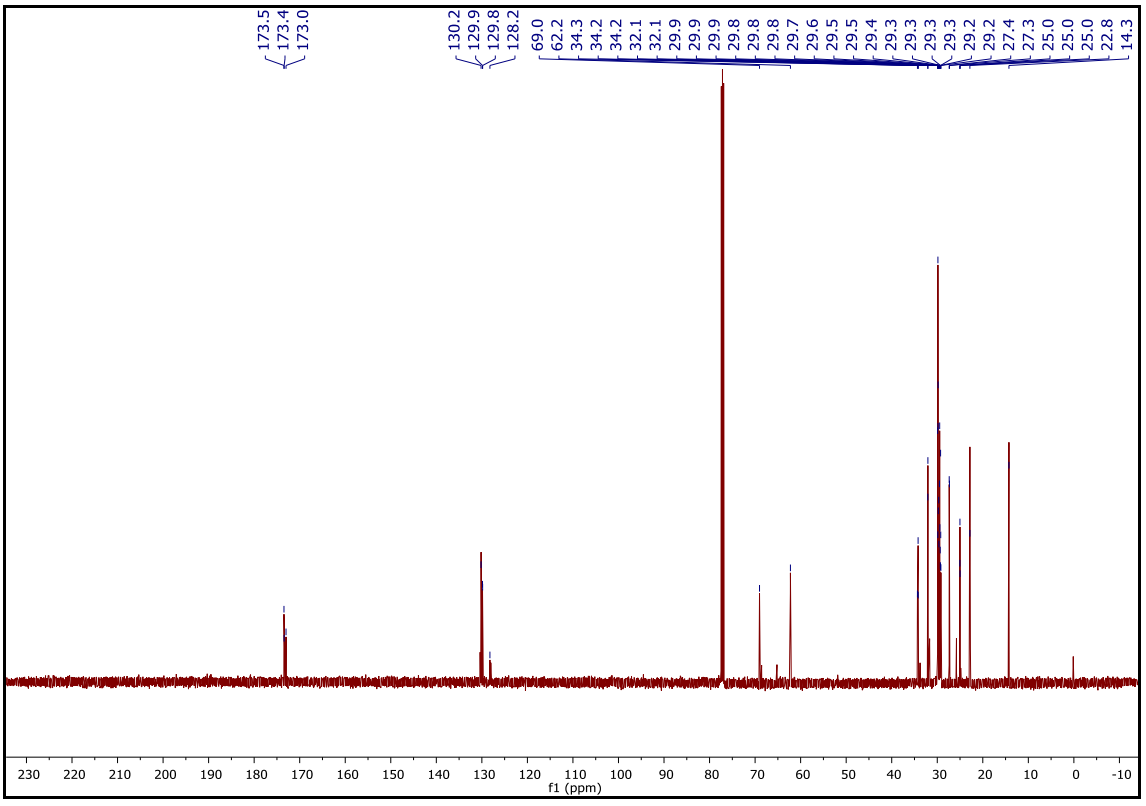

Figure S3. FT-IR of *C. guianensis* Oil.

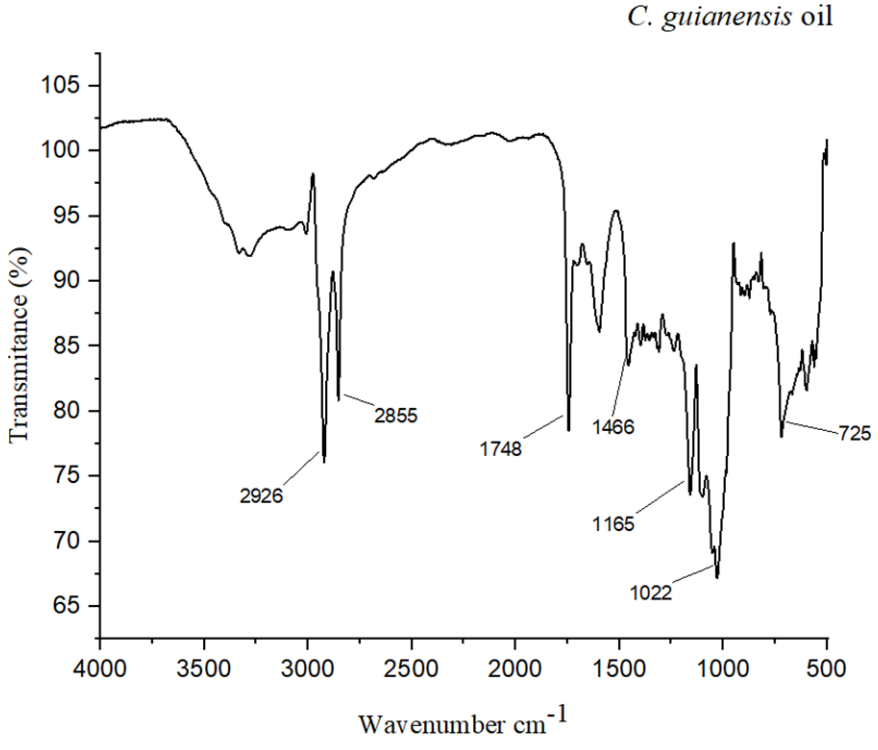

Figure S4. ^{1}H NMR (500 MHz, $CDCl_3$) of *B. excelsa* Oil.

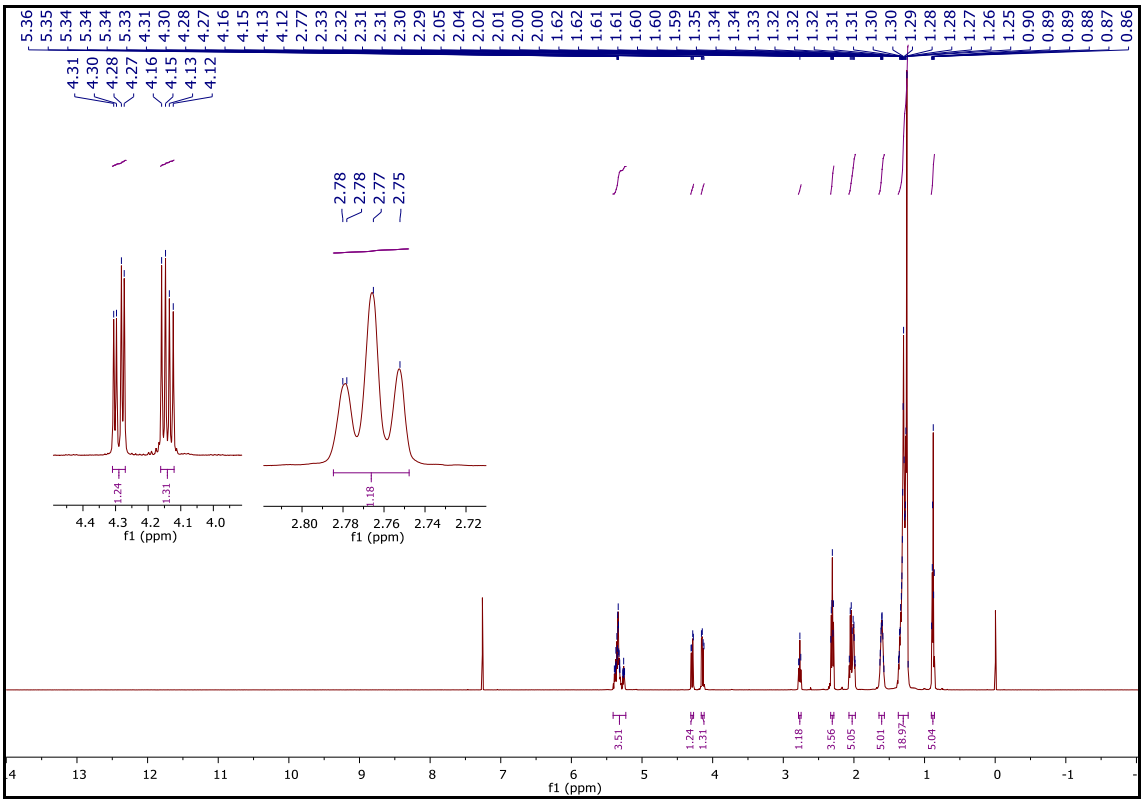

Figure S5. ^{13}C NMR (126 MHz, $CDCl_3$) of *B. excelsa* Oil.

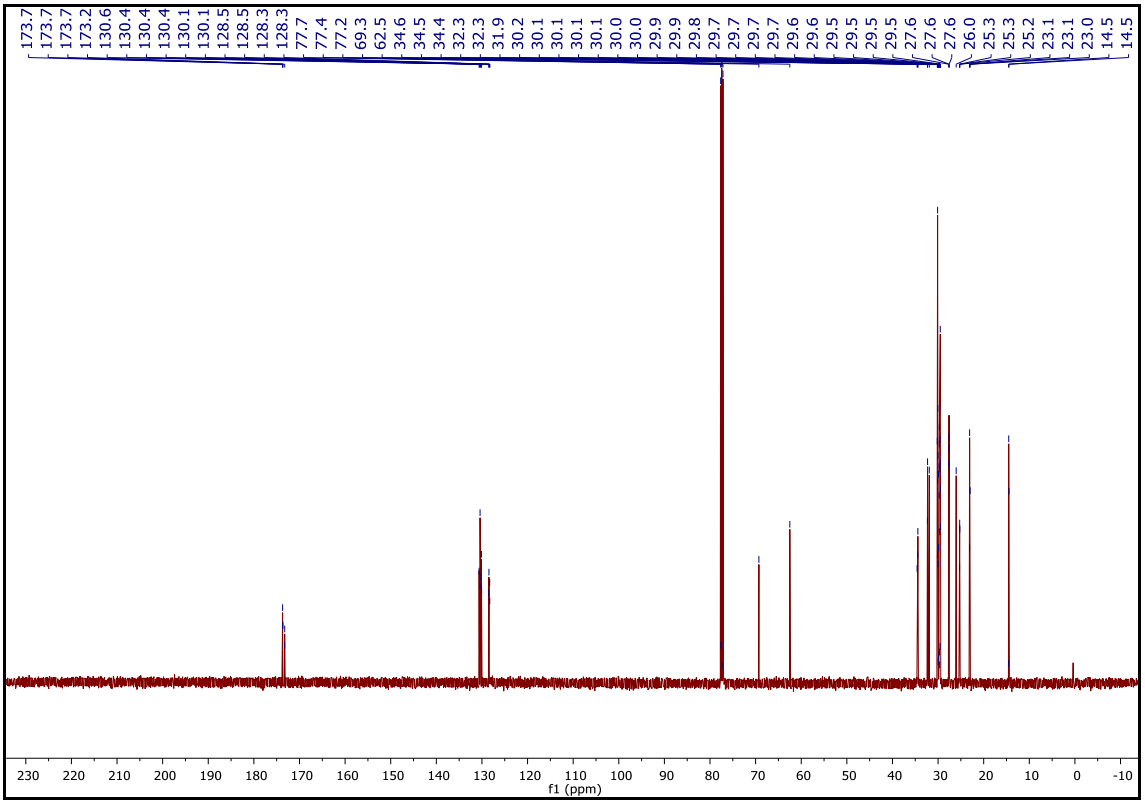

Figure S6. FT-IR of *B. excelsa* Oil.

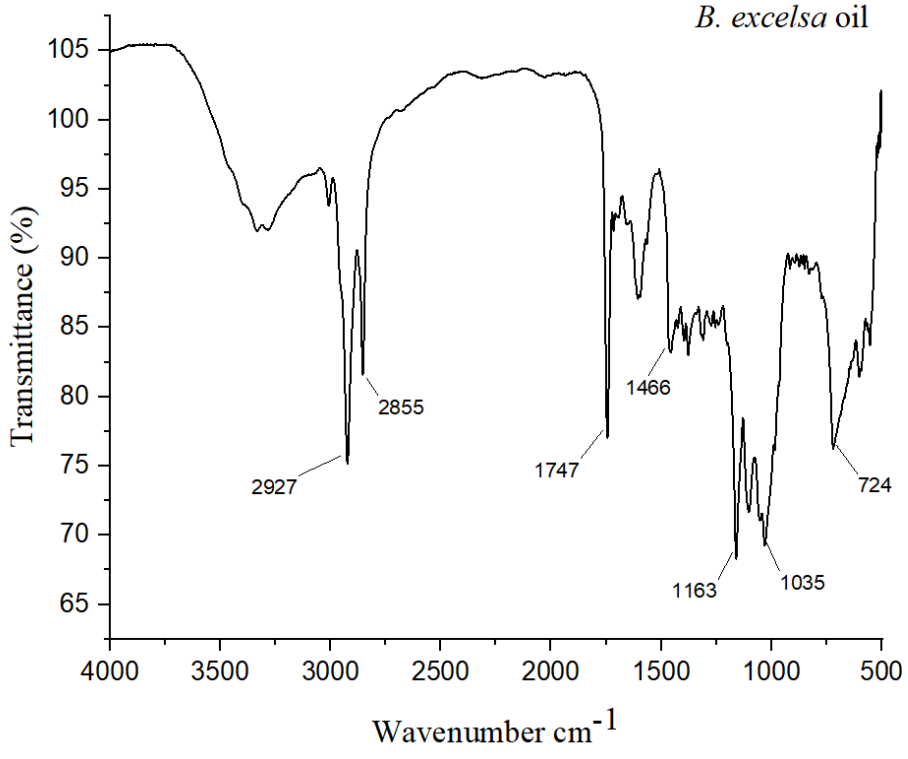

Figure S7. ^{1}H NMR (500 MHz, $CDCl_3$) of FABE-Cg.

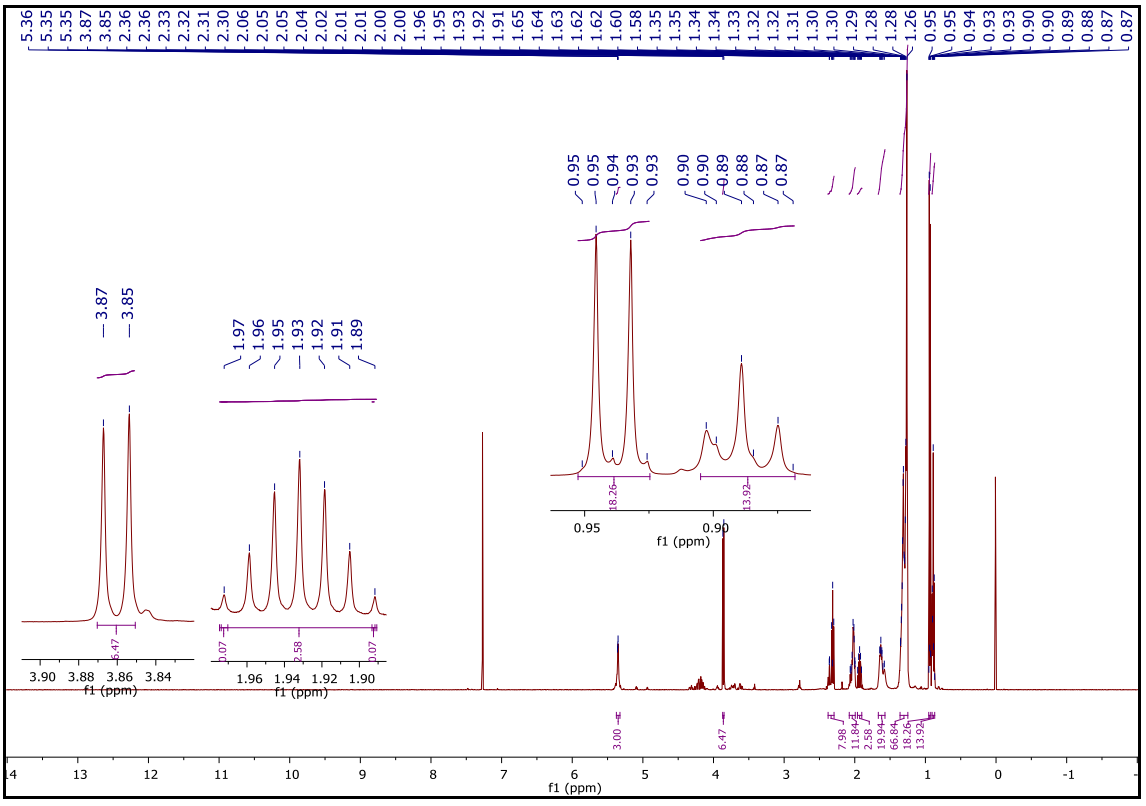

Figure S8. ^{13}C NMR (126 MHz, $CDCl_3$) of FABE-Cg.

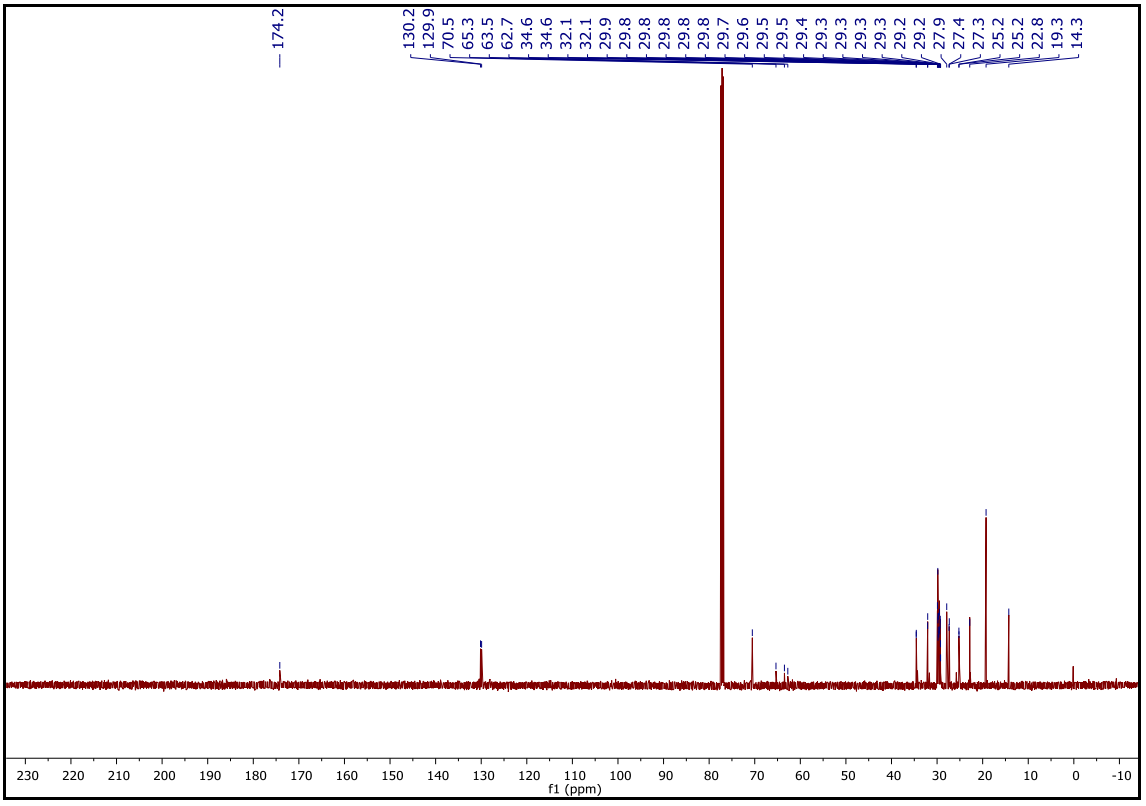

Figure S9. FT-IR of FABE-Cg.

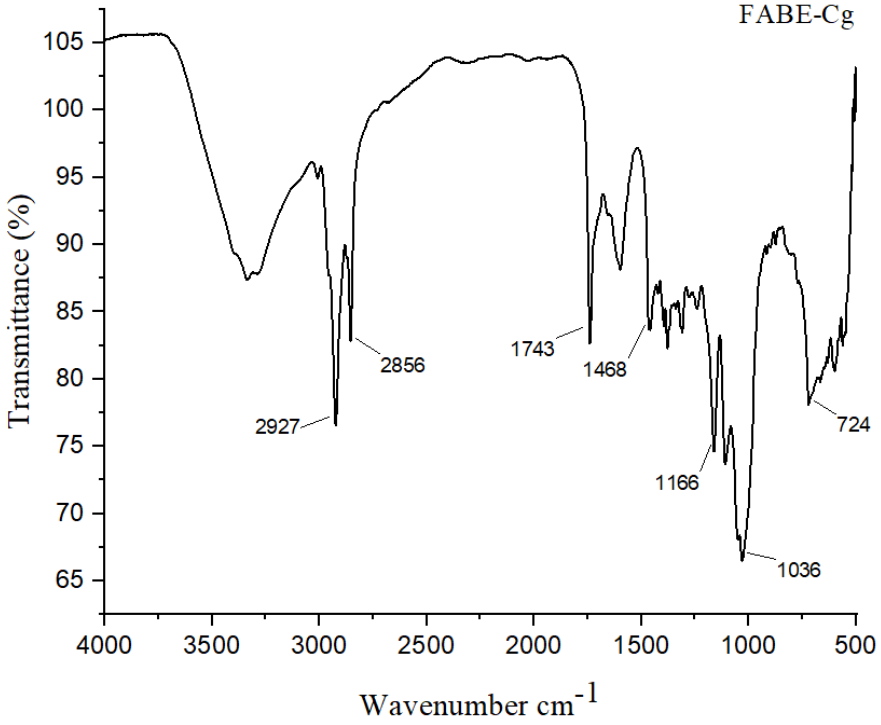

Figure S10. ^{1}H NMR (400 MHz, $CDCl_3$) of FABE-Be.

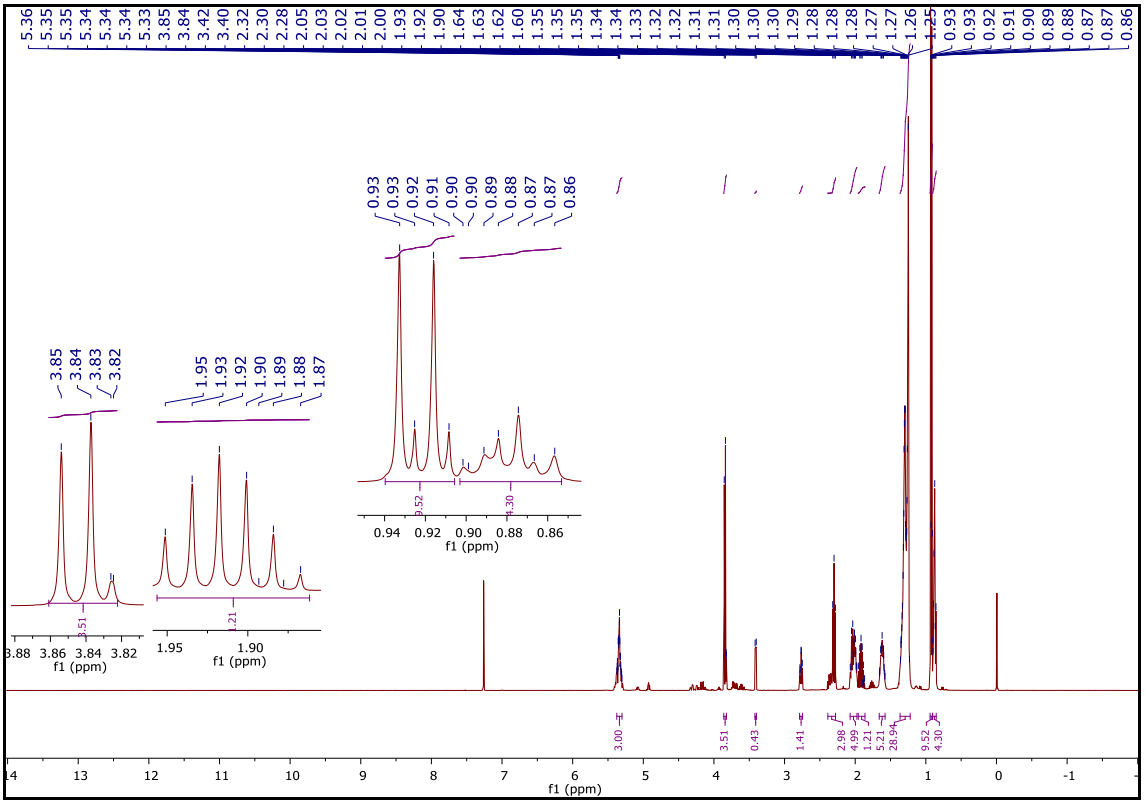

Figure S11. ^{13}C NMR (100 MHz, $CDCl_3$) of FABE-Be.

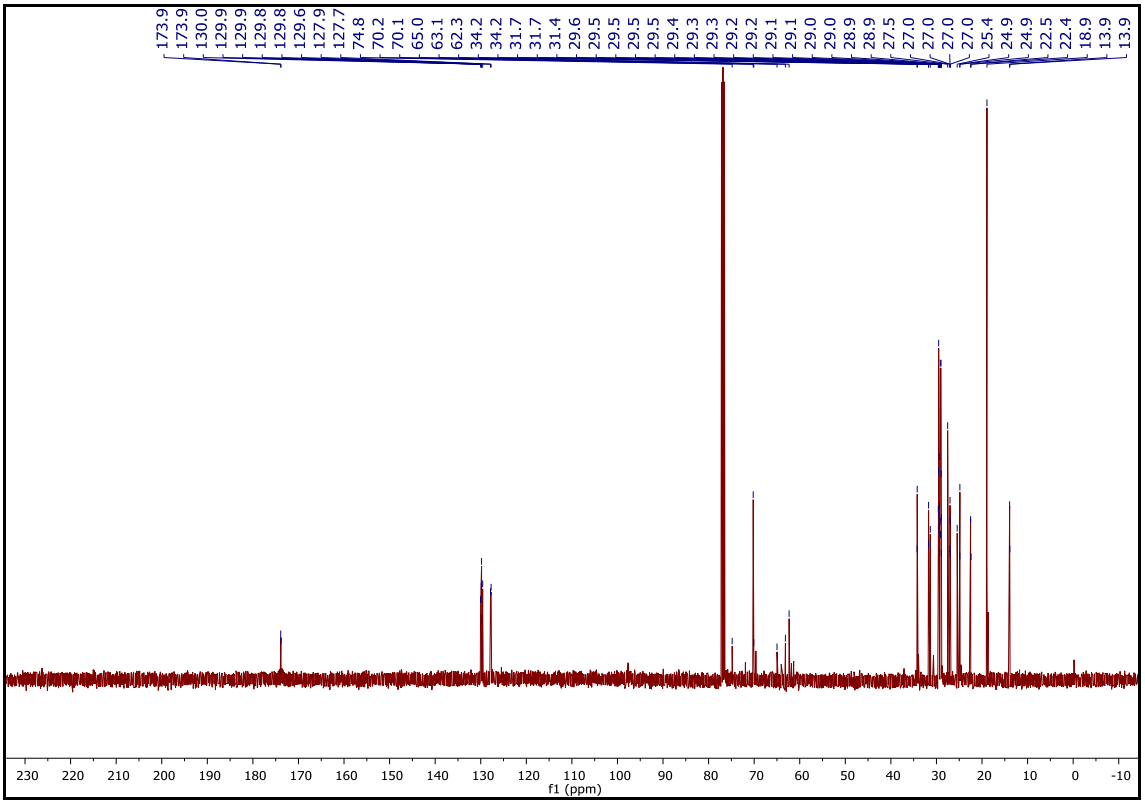

Figure S12. FT-IR of FABE-Be.

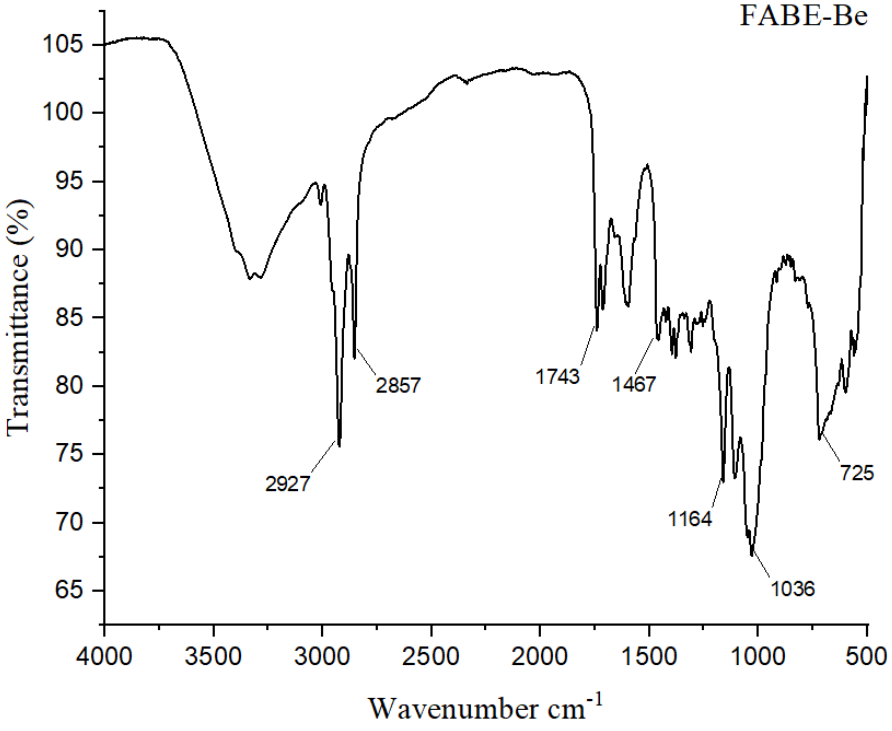

ANEXO 5

Material Suplementar

Potencial controle ecológico de nanopartículas de fibroína de seda e óleos amazônicos contra *Spodoptera frugiperda*

Victor H. S. Marinhoa, Donald Manigatb, Jéssica C. E. Vilhenac,d, Silvia M. M. Faustinoc, Raimundo N. P. Soutob, Irlon M. Ferreiraa,*

[a]Laboratório de Biocatálise e Síntese Orgânica Aplicada, Universidade Federal do Amapá, Campus Universitário Marco Zero do Equador, Rodovia Josmar Chaves Pinto, Km 02, Bairro Zerão, 68903-419, Macapá, AP, Brasil.

[b]Laboratório de Artrópodes, Universidade Federal do Amapá, Campus Universitário Marco Zero do Equador, Rodovia Josmar Chaves Pinto, Km 02, Bairro Zerão, 68903-419, Macapá, AP, Brasil.

[c]Laboratorio de Cultivo de Algas, Curso de Farmacia, Universidade Federal do Amapá, Campus Universitário Marco Zero do Equador, Rodovia Josmar Chaves Pinto, Km 02, Bairro Zerão, 68903-419, Macapá, AP, Brasil.

[d]Programa de Pós-Graduação em Ciências Ambientais, Universidade Federal do Amapá, Marco Zero do Equador, Rodovia Josmar Chaves Pinto, Km 02, Bairro Zerão, 68903-419, Macapá, AP, Brasil.

*Corresponding author: irlon.ferreira@gmail.com /Orcid.org/0000-0002-4517-0105

Tabela 1 (S1) Composição de ácidos graxos (%) da gordura de *A. Murumuru* determinada por análise de GC-MS.

Ácidos graxos	Picos	Tempo (min)	Concentração relativa (%)[c]
Capróico (C6:0)	1	3.63	1.73
Caprílico (C8:0)	2	6.54	2.40
Láurico (C12:0)	3	10.11	53.51
Mirístico (C14:0)	4	13.63	25.79
Palmítico (C16:0)	5	16.92	8.59
Linoléico (C18:2)	6	19.51	0.66
Oleico (C18:1)	7	19.59	3.88
Esteárico (C18:0)	8	19.96	3.45
Σ Saturado	-	-	95.47
Σ Monoinsaturado	-	-	3.88
Σ Poliinsaturado	-	-	0.66

Fig. 1 (S1). Composição de ácidos graxos da gordura de *A. murumuru*, determinada por análise de GC-MS. Ácidos Capróico (1); Caprílico (2); Láurico (3); Mirístico (4); Palmítico (5); Linoléico (6); Oleico (7); Esteárico (8).

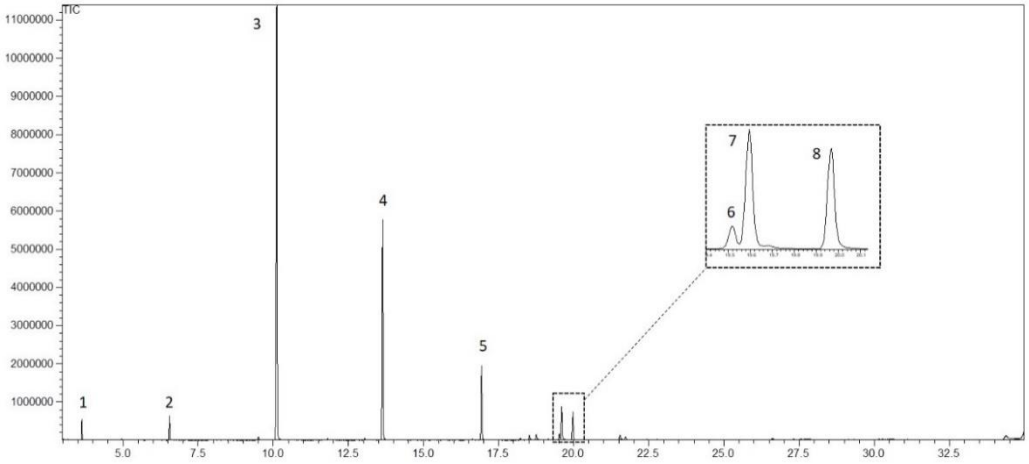

Tabela 2 (S2). Composição de ácidos graxos dos óleos de *C. guianensis* (andiroba) and *B. excelsa* (Brazil nut), determinada por análise de CG-MS.

Ácidos graxos[a]	**Concentração relativa (%)**[b] *C. guianensis*	**Concentração relativa (%)**[b] *B. excelsa*
Palmítico (C16:0)	40.5	19.0
Linoléico (C18:2, ω-6)	2.35	28.8
Oleico (C18:1, ω-9)	43.61	31.8
Vancênico (18:1, ω-7)	0.53	2.0
Esteárico (C18:0)	3.45	17.6
Não-identificado	1.95	-
Σ Saturado	43.95	36.6
Σ Monoinsaturado	44.14	33.8
Σ Poliinsaturado	2.35	28.8

Fig. 1 (S2). Perfil cromatográfico dos ácidos graxos dos óleos de *C. guianensis* (andiroba) e *B. excelsa* (castanha-da-Amazônia), conforme determinado pela análise CG-MS.